November 2020

The Utilization of Shared Energy Storage in Energy Systems: Design, Modeling and Optimization

Rui Dai
University of South Florida

The Utilization of Shared Energy Storage in Energy Systems: Design, Modeling and Optimization

by

Rui Dai

A dissertation submitted in partial fulfillment
of the requirements for the degree of
Doctor of Philosophy in Industrial Engineering
Department of Industrial and Management Systems Engineering
College of Engineering
University of South Florida

Major Professor: Hadi Charkhgard, Ph.D.
Tapas K. Das, Ph.D.
Changhyun Kwon, Ph.D.
Nasir Ghani, Ph.D.
He Zhang, Ph.D.

Date of Approval:
November 11, 2020

Keywords: Energy Storage Sharing, Multi-objective Optimization,
Integer Programming, Game Theory, Robust Optimization

Dedication

I dedicate this dissertation to my wife, my newborn daughter, my parents and to all who helped me along the way.

Acknowledgments

I would like to express my heartiest gratitude to my advisor, Dr. Hadi Charkhgard, for his invaluable support and professional guidance throughout my doctoral studies. His dynamism, vision, and sincerity have deeply inspired me. I really enjoyed working in the research environment he created that stimulates original thinking and innovative ideas. It was a great privilege and honor to work and study under his supervision.

I would like to acknowledge my sincere thanks to the members of my thesis committee, Dr. Tapas K. Das, Dr. Changhyun Kwon, Dr. Nasir Ghani, and Dr. He Zhang for their insightful suggestions for improving my thesis. I would also like to thank all my colleagues and friends at the University of South Florida who have helped me so much in my studies and daily life.

I am extremely grateful to my wife for her love, understanding, and continuing supports in my doctoral studies. I am very much thankful to my parents for their love, caring, and sacrifices for educating me for my future.

Table of Contents

List of Tables

List of Figures

Abstract

Energy storage (ES) plays a significant role in modern smart grids and energy systems. With the advances of ES technologies, efficiently applying ES to energy systems has become the bottleneck for achieving the benefits of ES. The traditional approach of utilizing ES is the so-called distributed framework in which there is a separate ES for each individual user. Due to the inherent limits in the distributed framework such as cost inefficiency and space limitations, many studies have promoted to utilize a shared ES in energy systems to further exploit the potentials of ES. However, current studies always focus on maximizing the benefits of utilizing the shared ES and neglect the importance of fairness in ES sharing. To build a successful ES sharing system, the challenge is to balance the conflict between efficiency and fairness in ES sharing. The efficiency means maximizing the overall economic benefits from ES sharing. The fairness is the regulation to ensure the fair energy exchange between the participants in ES sharing and fair distribution of benefits from ES sharing.

To bridge this gap, this thesis addresses the challenge of utilizing the shared ES in energy systems in terms of system design, operational strategy, and optimization algorithms. To the best of our knowledge, the first literature review for ES sharing has been completed in this thesis. This review determines the scope of ES sharing, classifies the architectures of ES sharing systems, and validates the research gaps for ES sharing.

This thesis proposes a balanced sharing strategy to achieve the tradeoff between efficiency and fairness in ES sharing. The strategy is developed based on multi-objective optimization to manage the ES sharing system with two users; It is extended to handle energy price uncertainty through robust optimization and operate the ES sharing system with multiple users by applying Game Theory concepts. The algorithm development work

in this thesis aims to advance the solutions to the balanced sharing strategy. It includes the improvement of the algorithms for multi-objective optimization, bi-linear optimization, and Game Theory.

Overall, this thesis presents an integral intellectual framework for ES sharing to address the key challenge of applying shared ES in energy systems.

Chapter 1: Introduction

1.1 Background and Motivation

In today's smart grids and energy systems, *Energy Storage* (ES) has been an indispensable facility to improve the efficiency and resilience of the systems. The users equipped with ES are able to create energy arbitrage by charging at off-peak price and discharging at peak price if the variant energy pricing plan is applied [1, 2, 3]. ES can also enhance the resilience of the energy systems when confronting the power outage due to disasters or systematic failures. Additionally, ES can ensure the stable generation of renewable energy, such as solar and wind power [4, 5, 6]. In the last decade, many household ES products appear in energy markets such as Tesla Powerwall, Alpha ESS SMILE5, and LG RESU (see Figure 1.1). Although ES has become prevalent in many energy sectors due to its benefits, the utilization of ES in future energy systems still faces many challenges at different levels such as designing the system framework and developing the management strategies.

(a) Tesla Powerwall (b) Alpha ESS SMILE5 (c) LG CHEM RESU

Figure 1.1 – Home energy storage products

The traditional framework to utilize ES in energy systems is the distributed framework [8, 7, 9, 10], i.e., a user owns and operates ES independently based on their own interests. There are some limits to the distributed ES systems. On one hand, the massive investment and maintenance cost[1] of ES make it cost-inefficient for the individual user, especially, the household. On the other hand, some ES technologies require huge space for installation and operation such as mechanical ES. The space limits of these types of ES restrict their applications for the distributed ES system. Hence, the shared ES is introduced as a novel architecture to utilize ES in energy systems to overcome the drawbacks of the distributed framework. The sharing framework can tackle the cost inefficiency through the cost sharing of all participants. It naturally matches the application of grid or utility-scale ES, since these ES are built to serve multiple users.

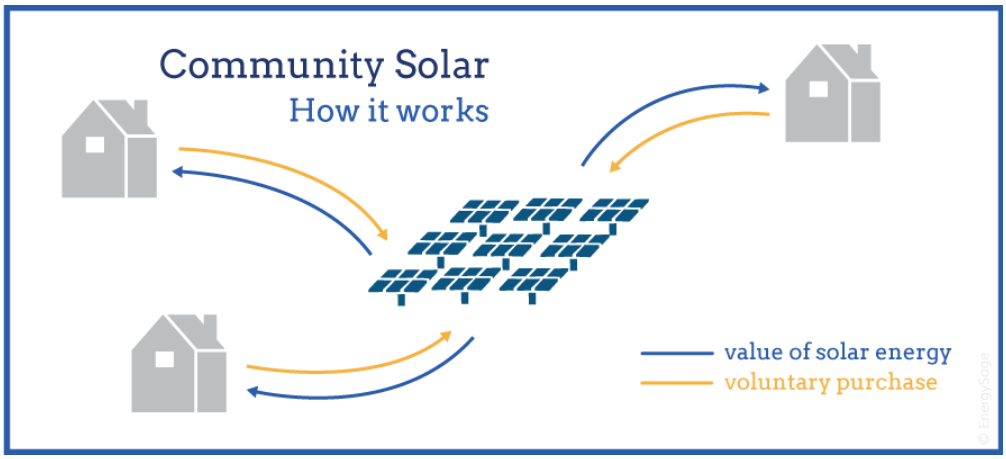

Figure 1.2 – EnergySage's Community Solar

To date, the successes of sharing business models in smart grids also motivate the researchers to explore the potentials of applying the sharing model to ES. Many studies published in last decade [11, 12, 13, 14] have advanced the design and optimization for the energy sharing or trading system. Additionally, the real-world energy sharing or trading projects have demonstrated its potentials and benefits. One of successful application in practice is the EnergySage's Community Solar project (see Figure 1.2). This project provides

[1] A 13.5 kWh Tesla Powerwall costs $11,000 (https://www.tesla.com/powerwall).

members of a community the opportunity to share the benefits of solar power even if they cannot or prefer not to install solar panels on their property. Interested readers are referred to the review papers for energy sharing [15, 16, 17] to learn the state-of-the-art of energy sharing.

Figure 1.3 – ShineHub: Big Battery based Virtual Power Plant project

In summary, due to the limits of distributed ES and the potential of energy sharing, shared ES has been a promising application of ES in future energy systems. Especially, the grid-scale or utility-scale ES such as Tesla Megapack[2] are designed for energy market or large scale energy community, in which ES sharing framework can better incentive the customers to participant in the ES projects. One of the shared ES practices is the "Big Battery" project provided by ShinHub (see Figure 1.3). This project allows the batteries of each household to interconnect with each other to form a "big battery" for sharing. The participating homes are assumed to be able to make money by supplying energy to the grid in peak times. Another shared ES program is provided by Tesla, which is called the Virtual Power Plant. In this program, the customers can enroll their Powerwall in the Connected Solutions. This program links batteries across the state to create a large supply of sustainable energy — a virtual power plant — to be used during peak demand. Note that the shared ES practice

[2]https://www.tesla.com/megapack

aims to create a large scale ES to serve a great number of customers and further explore the potentials of shared ES in energy markets.

With the advances of shared ES in energy systems/markets, many studies have been conducted to explore the design and management of the ES sharing system in the last decade. To build a successful ES sharing system, the main challenge is to ensure the efficiency and fairness of the ES sharing system. The *Efficiency* for ES sharing refers to an optimization model to maximize the benefits of sharing the energy and capacity of the shared ES. The criterion of efficiency appeals a computational efficient optimization framework for ES sharing. Note that in this dissertation, the term *Freedom* is equivalent to Efficiency that is used to evaluate the economic benefits of the ES sharing system, because giving more freedom to the users to share the ES can create more cost savings. *Fairness* is the regulation to the energy trading and sharing in ES sharing system. Guaranteeing fairness for ES sharing is the essence of the system to incentive the users to participate in the ES sharing. The core of achieving fairness is to develop a pricing or incentive based mechanism to ensure the users will be paid if they sell their energy or purchase the energy at an acceptable energy rate. Overall, in order to further promote the utilization of shared ES and explore the potentials of shared ES, it is worth studying how to design the ES sharing system and develop the corresponding operational strategy to achieve the tradeoff between efficiency and fairness for ES sharing.

1.2 Literature Review

In this section, a comprehensive literature review of the existing studies regarding ES sharing is presented. Note that the contents of the review originate from the preprint: Dai, R., Charkhgard, H., & Esmaeilbeigi, R. (2020). The utilization of shared energy storage in energy systems: a comprehensive review. In this review, we first identify the scope of ES sharing and introduce some concepts to help the readers to better understand the operation of the ES sharing system. The process of collecting the literature is also describes. We then

categorize the papers into four categories based on the architecture of the ES sharing system. Finally, the detailed review is presented to summarize the contributions of existing papers.

1.2.1 Scope of Energy Storage Sharing

In this section, we present the scope of ES sharing. We provide a brief explanation of some of the concepts relevant to ES sharing at the outset.

Users in an ES sharing system can represent different types of entities in energy systems. The user can be an end user of electricity that purchases energy from the (smart) power grid to satisfy its load, a microgrid that contains a group of energy loads and distributed energy resources, or a prosumer that can produce/purchase energy for self consumption and sell its energy surplus.

Capacity Sharing for shared ES indicates that the users trade their capacities of ES to other users temporarily. The purchaser of the capacity will operate the purchased block of ES independently. The seller cannot operate this block or use its stored energy until the capacity is returned. In other words, energy stored by the purchaser is totally managed by the purchaser and not the owner of the block.

Stored Energy Sharing for ES sharing specifies that the user can trade their stored energy in ES with other users for making a profit. This happens when the stored energy is a surplus to the user or there exists a price arbitrage opportunity.

Direct Implementation of a shared ES refers to the case in which a shared ES is installed for all users and each user can utilize the capacity of the shared ES for charging, discharging, or trading their stored energy. Two structures can be considered for such a shared ES network: installing an external ES which is connected to each user or interconnecting the internal ES of different users. Both structures allow capacity sharing as well as stored energy sharing since the users have access to each ES in the system.

Indirect Implementation of a shared ES refers to the case where a private ES is installed for each user, that is, each user only has access to their own ES. It follows that

capacity sharing cannot be adopted in this implementation. However, stored energy sharing is possible and it happens in the form of energy exchange between the users.

Comparing direct and indirect implementations of ES, we realize that the former is a preferred implementation approach since it allows a shared ES to achieve its full potential. This review mainly focuses on direct ES sharing and provides the detailed summary and comparison of the relevant studies. We will further discuss the direct and indirect implementation of the shared ES through the discussion of the architectures of ES sharing system.

The majority of the studies on ES sharing concern developing a sharing mechanism that maximizes the benefits of adopting a shared ES while maintaining cohesion among the users. When operating an ES sharing system, the main challenge is to ensure the capacity sharing and stored energy sharing are both efficient and fair. The efficiency in the context of a shared ES refers to maximizing the benefits of sharing the ES. Fairness, on the other hand, refers to the regulations/constraints imposed on capacity sharing and stored energy sharing to guarantee the fair distribution of benefits. It motivates users to participate in the ES sharing programs by establishing a pricing or incentive-based mechanism. In this paper, we investigate the reviewed studies for ES sharing in terms of the balance between efficiency and fairness. More precisely, we evaluate their sharing mechanism and analyze how they achieve efficiency and fairness.

1.2.2 Method of Identifying Relevant Articles

The relevant papers in this review have been collected through the following process. We used the Scopus database to search the papers related to the shared ES. We searched the papers by using the keywords “energy storage" and “share, shared, sharing, or trading" in Title, Abstract, and Keywords of the papers. We then refined the results to only English language and the last decade, *i.e.,* papers published within Jan 2009 to July 2020. A total of

6,380 conference/journal articles satisfied these conditions. We then briefly read the papers one by one to manually remove the ones that are not related to ES sharing.

From 6,380 papers, only 263 papers[3] were identified as related to ES sharing (both direct and indirect implementations). Table 1.1 presents the numbers of the papers published within the last decade, the papers reviewed in this paper, and the total citations of the reviewed papers. We can observe that the number of publications related to ES sharing has increased every year. The last 3 years account for the largest increase in the number of publications. This observation clearly justifies the need for a literature review to identify the pros and cons of the current studies regarding shared ES and clarify the research gaps for future study. Note that from a total of 263 papers, only 48 articles were related to direct ES sharing. So, we only reviewed them in this paper.

Table 1.1 – Statistics of the papers related to ES sharing

Year	#Paper	#Reviewed	#Total Citation
2009	0	0	0
2010	0	0	0
2011	2	0	0
2012	2	1	6
2013	9	1	181
2014	6	1	246
2015	10	2	42
2016	21	4	334
2017	38	5	229
2018	64	14	245
2019	82	11	87
2020	31	9	13
Total	263	48	1383

1.2.3 Architectures of Energy Storage Sharing

In this section, variants of ES sharing systems are reviewed. The existing body of the literature can be divided into four categories based on the ownership of ES. These

[3]The full list of the papers for ES sharing can be found in (https://github.com/ruidai-usf/EnergyStorageSharing).

categories can be illustrated through Figure 1.4 in which the interaction between different interconnected users in an ES sharing system is depicted. Figure 1.4b–1.4d illustrate variants of the direct ES sharing system which is the main focus of this paper. More precisely, ES sharing in this paper refers to an energy trading or sharing system in which the structure of the system allows for Capacity Sharing as well as Stored Energy Sharing. In the remainder of the paper, if we use the terms “ES Sharing" or “Shared ES" without specifying it as the indirect ES sharing, we mean the direct ES sharing.

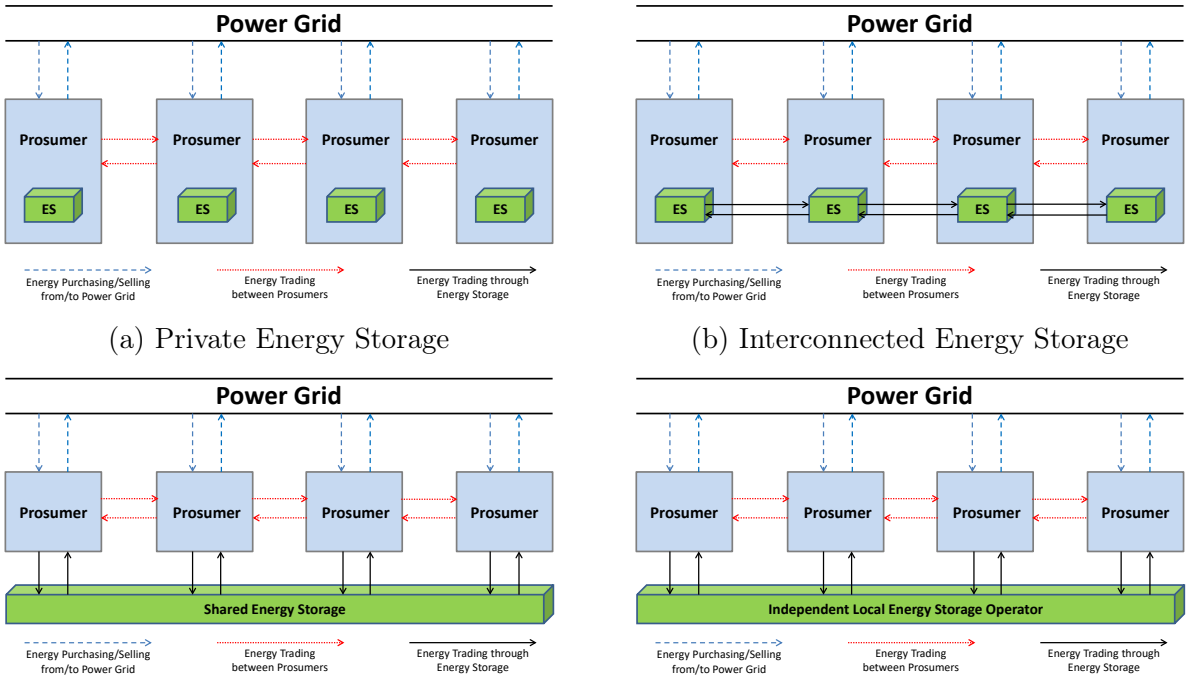

(a) Private Energy Storage

(b) Interconnected Energy Storage

(c) Co-owned Energy Storage

(d) Independent Energy Storage

Figure 1.4 – The architectures of ES sharing system

1.2.3.1 Private Energy Storage

Figure 1.4a presents the structure of an indirect ES sharing system in which ES is a private property for each user. Each user owns their ES and operates it independently. This structure is the mainstream framework to apply ES in energy systems, especially the energy trading and energy sharing systems. In this structure, ES is not the resource for sharing. It supports the energy exchange between the users as an internal energy facilities for the users.

The indirect ES sharing problem is usually solved as an energy trading problem by developing the operational strategy to coordinate the energy exchange. In [18], a cooperative game based incentive strategy is proposed for energy trading between interconnected microgrids in which an independent ES is installed for each microgrid. In [19], a bi-level distributed operation framework is developed to optimize the energy trading and maximize the revenue of the interconnected microgrids with uncertain renewable energy and load. In [20], a mixed integer linear programming model is applied to optimally control the households equipped with solar energy resources and individual ES in a peer-to-peer energy trading market. In [13], multiclass energy management is applied to the peer-to-peer energy trading framework to coordinate the energy exchange among the heterogeneous prosumers, which consist of ES, renewable energy resources, and/or energy load.

Installing ES for each user is inefficient because of investment cost, space requirement and maintenance expenses. Structure (a) also needs the user to determine the exact size of ES in the investment stage. However, it is challenging for the users to determine the size of ES for the long-term operation under the uncertain energy prices and demands. If the size is not decided properly, the users would waste the surplus of energy or leave some capacity unused. Therefore, Structure (a) is not generally a suitable framework to promote efficient utilization of ES in modern energy systems.

1.2.3.2 Interconnected Energy Storage

Capacity Sharing can handle the inefficient sizing for the individual ES since the users can adjust the capacity of ES they can access by trading the ES capacity with others. It can be realized by interconnecting the ES owned by each user, shown in Figure 1.4b. Structure (b) allows the users to share the capacity of their ES with others by creating a block of capacity in their ES for trading. The studies relevant to this structure usually focus on developing the incentive mechanism to promote the users to share their ES capacity. In [21], a noncooperative game theoretical framework is proposed to manage the interaction and

energy trading between a number of geographically distributed storage units by letting each unit decide the maximum amount of capacity to sell. In [22], a noncooperative Stackelberg game based auction approach is developed to determine how residential units share their ES capacity with the facility controllers of large buildings. Note that Structure (b) is still suffering the drawbacks of the distributed framework since ES is still installed for each user.

1.2.3.3 Co-owned Energy Storage

In Structure (c) one shared ES is installed for all users as can be seen in Figure 1.4c. This structure is the mainstream architecture of ES sharing systems. There are multiple strategies to operate the co-owned shared ES system. One of the common operational strategies is to determine the capacity allocation for each user first and then let the user operate its obtained block of ES independently. Stored Energy Sharing is not implemented in this strategy. Hence, this strategy considers ES sharing as a resource allocation problem [23, 24, 25]. Another strategy to operate the co-owned shared ES in the literature assumes that an aggregator controls the entire system and coordinates the capacity allocation and stored energy distribution to manage the shared ES [26]. The next subsection will present more details about the operational strategies for the co-owned shared ES.

1.2.3.4 Independent Energy Storage

A shared ES can be managed by an independent operator as shown in Figure 1.4d. The independent operator decides the price for purchasing/selling energy from/to the shared ES for the users and controls the shared ES based on the users' decisions on exchanging energy with the shared ES. Note that the aggregator of the shared ES in Structure (c) prices the capacity of ES to realize the capacity allocation, while the independent operator in Structure (d) prices the energy stored in ES to direct the users' charging/discharging behavior.

The authors in [27] propose a new market framework by taking the ES as a stand-alone operator in order to optimally sell options and trade energy in the market to resolve the imbalances of the system operator. A Stackelberg game-based energy trading strategy is developed in [28] to minimize energy cost for a neighborhood area with energy communications between interconnected users. This neighborhood area consists of an independent shared ES, users with non-dispatchable energy generation and an electricity retailer.

The advantage of Structure (d) is that the independent operator coordinates both Capacity Sharing and Stored Energy Sharing for the operation of the shared ES. However, the challenge is how to predetermine the price for energy trading between the independent ES operator and users and fairly allocating the stored energy to each user. Additionally, if the independent ES operator is a for-profit entity in the market, the design of the ES sharing market should properly balance the conflict between the ES operator and the users.

1.2.4 Review of Energy Storage Sharing

This section reviews the studies regarding ES sharing through multiple angles. We first discuss the possible scenarios for applying shared ES in the energy systems. We then review the decision frameworks such as business model, control strategy and optimization model developed for operating the ES sharing system. We also investigate the method(s) proposed to handle uncertainty in the shared ES system. Finally, we explore the possible ways that the shared ES could be integrated with other energy technologies.

1.2.4.1 Implementation and Operational Aspects

The main context for applying shared ES is a community or neighborhood area. In this scenario, ES is installed as a shared *Community ES* to provide the energy storage service to multiple households or buildings. Usually, the Community ES is assumed to be operated by an aggregator that collects the information from each household and decides the allocation

of capacity of Community ES and the incentive for the household to exchange the stored energy.

The authors in [29] employ a single-sided combinatorial auction model to coordinate the ES sharing among multiple households. In [30], the authors propose a profit maximization strategy to operate the shared ES designed for multi-unit apartment-type factory buildings. In [31], a welfare optimization model as well as a game theoretical (bi-level) model are developed to optimize the energy allocation and pricing of the shared energy resources in an apartment building considering objectives such as cost and emission reduction. In [32], the authors investigate several projects that provide shared ES for multiple households to validate the potential business models and barriers of the shared ES usage. In [14], an energy sharing scheme is proposed in which an aggregator takes advantage of shared distributed energy resources such as solar energy and ES for both energy sharing and peak shaving. This scheme applies a sharing contribution index to measure different users' contributions to energy sharing.

A shared ES may also be operated as a cloud. This application of shared ES adopts the cloud concept in computer science. The *cloud ES* combines multiple ES technologies such as electrochemical and mechanical ES to create an ES cloud that provides the storage service for a large number of customers in the energy market. Compared to the Community ES, the cloud ES is designed to serve the market. The business model for the cloud ES publishes the price of the capacity of the cloud ES first. Then the customers rent the appropriate capacity of cloud ES based on their own interests and the price of the capacity. These customers can independently operate the capacity they rented and need to return the capacity at the end of the planning horizon. In [23], the authors propose the concept of cloud ES. This cloud ES is constructed by centralized batteries and provides storage services for residential and small commercial users. A two-stage optimization model is developed in [24] for cloud ES sharing. In stage one, the aggregator determines the investment and pricing for the storage capacity. In stage two, each user decides the virtual capacity to purchase at the start of the planning

horizon and operate the storage capacity independently through the entire horizon. Note that the cloud ES sharing only implements Capacity Sharing since cloud ES just provides the ES capacity rent service to the market. The users cannot gain benefits from trading their stored energy in cloud ES sharing.

1.2.4.2 Decision Frameworks

The sharing economy, a business model that allows the users to profit from trading the access of their goods or services to others, has experienced rapid growth in the last decade. The success of sharing economy has motivated researchers to explore the potential of applying the sharing economy model to ES sharing. The sharing economy model can validate the economic benefits that ES sharing could provide as opposed to operating the ES independently. The authors in [33] explore sharing economy opportunities for a specific application in the future smart grids. In this application, a collection of firms invest in ES to arbitrage against variable energy prices and share the surplus of their stored energy. A sharing economy approach for ES sharing is presented in [34]. Their proposed approach has clarified that ES sharing is an economically attractive solution for the ES operators as well as ES potential investors. The authors in [35] demonstrate the potential of shared ES for a neighborhood area, in which residents are able to dynamically optimize the energy demand and the energy storage level to maximize their utility.

Some classical economy theories are applied to the ES sharing system such as Game Theory, Portfolio Theory and Auction. All these models are applied to balance the distribution of benefits from ES sharing in order to ensure the cohesion and sustainability of the ES sharing system. The authors in [36] explore sharing opportunities of ES among a group of consumers and apply the cooperative game theory model to the ES sharing system. They have demonstrated that the cooperation of ES sharing is beneficial for the users that either already have storage capacity or want to acquire it. In [37], the authors optimize the energy consumption schedule and the battery ES capacity for ES sharing among the interconnected

microgrids through non-cooperative and cooperative game models. In [38], a new portfolio theory-based model is proposed to optimize the ES capacity allocation for different service objectives such as increasing their expected profits and reducing risk. In [39], the authors propose a new ES sharing business model to address multiple revenue streams which can be attributed to different market activities and players. This auction-based ES sharing model allocates ES resources by assigning the rights of using stored energy and ES capacity to the users. In [40], a dispatch strategy is developed to optimally allocate the capacity of the shared ES for domestic customers and distribution network operators in order to maximize the overall savings on both energy costs and investment costs.

Some of the studies in the literature focus on the control strategy design for the ES sharing system. In [41], an online algorithm is developed for real-time energy management of the ES sharing system, in which the homes equipped with ES can buy storage capacities from each other to form the shared ES. The authors in [42] study the energy management problem for the ES sharing system including multiple users, renewable energy sources and a single shared ES and solve the problem by designing a central controller to jointly optimize the energy charged/discharged to/from the shared ES. In [43], a novel ES sharing system is proposed to study sharing ES capacity among transmission and distribution entities in the energy system. The study in [44] uses a reinforcement learning algorithm, the deep deterministic policy gradient algorithm, to continuously control the shared ES within building clusters for the optimal energy dispatch. In [45], a framework is proposed to integrate residential and community-level ES in an existing low voltage network, and a fast linear low voltage model was developed to ensure sufficient accuracy for network stabilization purposes.

To help the decision makers operate the shared ES when facing multiple conflicting objectives, multi-objective optimization based frameworks have been proposed. The authors in [46] propose a collaborative decision framework to return Pareto-optimal operational decisions for the energy sharing among building clusters where the buildings share energy generation and ES. In [47], a bi-objective mixed integer linear programming formulation is

proposed for an energy system with an ES shared between two buildings that can address the conflict between efficiency and fairness. In [48], a collaborative energy management technique in a microgrid is proposed. In this microgrid, the apartments collaborate with each other to decide resource allocation and energy scheduling in order to maximize the total net profit. The authors in [49] employ a multi-objective mixed integer liner program to minimize operational costs and carbon emissions of an aggregator operating a Community ES system under two scenarios with different Community ES ownerships. In [50], a new multi-objective optimization model is introduced for storage dispatch in a network of grid-connected microgrids with battery and renewable energy resources.

1.2.4.3 Incorporating Uncertainty

Uncertainty plays a crucial role in managing an ES sharing system. It should be considered since the management of an ES highly relies on the predetermined energy prices and policies as well as predictable energy loads and demands. Uncertainty comes in three different forms: stochastic, robust and fuzzy. To address these types of uncertainty, decision makers employ stochastic programming, robust optimization and fuzzy/uncertain programming, respectively. Stochastic programming is used when the probability distribution of the data (e.g., demand or price) is available. This is often the case in the presence of historical data. Robust optimization is generally applied to analyze worst-case performance of the system over data intervals (or uncertainty sets). Finally, fuzzy and uncertain programming are used when no historical data are available. In such cases, the data are modeled through a possibility or membership function which indicates the degree to which certain values could be plausible or believable. Interested readers are referred to [51] for further details.

In [52], a multi-stage stochastic program is developed to minimize the energy purchase cost of a shared community with multiple houses, solar energy resources and shared ES. In [53], the authors propose a robust framework for the day-ahead energy scheduling of interconnected smart homes with a shared ES system to take into account users' behavior

uncertainty. The authors in [54] propose a game theoretical framework to manage an ES sharing system by characterizing the messaging behaviors of users, where the users have privacy requirements and aim to maximize their own costs individually. An optimal sizing method for the shared ES is proposed in [55], where the demand of each customer is stochastic and it is satisfied through a combination of energy from the grid and shared ES. In [56], a robust biobjective mixed integer bilinear programming framework is developed to fairly and efficiently operate an ES sharing system with two users under energy price uncertainty.

1.2.4.4 Integration with Other Energy Technologies

Shared ES can be incorporated with many other energy technologies such as renewable energy, on-site generation and electric vehicles. In such integrated energy systems, the operational policy should decide how to optimally dispatch the energy generated from different energy resources for current use or storage for future use.

The authors in [57] study energy and financial flows in five Australian apartment buildings with solar energy and shared ES through the real apartment metered load profiles and simulated solar generation profiles. In [58], a new method is proposed to enable high penetration of solar energy in low voltage distribution networks by using shared ES and variable tariffs. To address the challenge of energy allocation and pricing of distributed energy resources, the authors in [59] develop a peer-to-peer energy sharing framework to promote the neighboring prosumers share the surplus of their distributed energy resources and control the aggregated shared ES. In [60], the authors propose a novel sizing method and economic evaluations for the shared ES coupled with charging stations. They evaluate using second-life battery modules as a potential approach to reuse the retired electric vehicle battery for cutting costs and implementing sustainable solutions. In [61], a two-stage planning model is developed to realize the optimal allocation of the energy resources such as distributed wind turbine and shared battery ES as well as the optimal dispatch of individual virtual

ES (aggregated controllable loads) in an energy system. Interested readers are referred to [62, 63] for the real-world shared solar and ES projects.

1.3 Contributions of the Dissertation

This dissertation presents a landscape of the topic, ES sharing, by studying this topic through aspects such as system design, operational strategy modeling, and optimization. The contributions of this dissertation are explained as follows:

- This dissertation conducts a comprehensive literature review for ES sharing, which is the first review work for this topic. In this review, the papers related to ES sharing are extracted to a dataset that can be employed by the researchers interested in ES sharing.

- Through the review, the architectures of applying shared ES in energy systems are identified and categorized. The pros and cons of different structures of ES sharing system are also explained.

- The main challenge of ES sharing, that is the conflict between efficiency and fairness, is validated in this dissertation. The qualitative measurements for these two criteria are defined in this dissertation to facilitate the evaluation of the performance of the sharing strategy for ES sharing.

- This dissertation proposes a balance sharing strategy for ES sharing that is demonstrated to balance the efficiency and fairness in ES sharing. This strategy is further extended to handle energy price uncertainty and manage the ES sharing system with multiple (over two) users.

- The dissertation also contributes to optimization algorithms. A two-stage method is developed to exactly solve the bi-objective pure integer linear programs by combining two of the fastest criterion space search algorithms. In addition, a novel formulation

for Piecewise McCormick Relaxation is proposed which is demonstrated to save 80% run time.

1.4 Outline of the Dissertation

The remaining content of this dissertation is organized as follows:

- In Chapter 2, the two-stage method for bi-objective pure integer linear programs is proposed. This method combines two criterion space search algorithms, the Balanced Box Method [64] and the ϵ-constraint method [65]. The experimental results show that the two-stage method outperforms these two algorithms.

- In Chapter 3, the balanced sharing strategy for managing the ES sharing system with two buildings is presented. This strategy is developed based on the bi-objective optimization and ensures the fair stored energy exchange through the compensation mechanism. This strategy is experimentally demonstrated to balance the efficiency and fairness of ES sharing.

- In Chapter 4, the balanced sharing strategy is extended to handle price uncertainty in the ES sharing system with two buildings. This strategy incorporates the robust optimization to guarantee the fairness of stored energy exchange even in the worst case scenario. Besides, the binary formulation for the Piecewise McCormick Relaxation is explained in this chapter. The efficacy of robust sharing strategy is validated through the experiments.

- In Chapter 5, a game theory-based approach for balancing the multi-prosumer energy storage sharing is proposed. This approach is originated from the sharing strategy proposed in Chapter 3 and improved by applying the cooperative Game Theory. The enhancement of the solution techniques for this approach facilitates this approach to solve the ES sharing system with many users, which is illustrated in the computational results.

- In Chapter 6, the conclusion of this dissertation is drawn and the future research directions are discussed.

Chapter 2: A Two-stage Approach for Bi-objective Integer Linear Programming

This chapter was previously published as [66]: Dai, R., & Charkhgard, H. (2018). A two-stage approach for bi-objective integer linear programming. Operations Research Letters, 46(1), 81-87. In this work, a two-stage approach is proposed to solve the bi-objective integer linear programs and return the exact nondominated frontier. This method combines two of the fastest (criterion space search) algorithms, the Balanced Box Method [64] and the ϵ-constraint method [65], by incorporating the advantages of these two methods. The experiment results demonstrate that our proposed method 1) is better than the Balanced Box Method and ϵ-constraint method in terms of solution time, and (2) needs to solve less single objective integer programs than the Balanced Box Method (similar to the ϵ-constraint method).

2.1 Bi-objective Integer Linear Programs

Many problems in different fields such as scheduling, transportation, and production planning can be formulated as an integer linear program. However, these problems often involve multiple objectives, and so due to conflicts between them, the feasible solution that simultaneously optimizes all of the objectives usually does not exist. Consequently, in practice, decision makers want to understand the trade off between the objectives for these problems before choosing a suitable solution. Thus, generating many or all efficient solutions, i.e., solutions in which it is impossible to improve the value of one objective without a deterioration in the value of at least one other objective, is the primary goal in multi-objective integer linear programming.

This work focuses on developing an exact algorithm for *Bi-Objective Integer Linear Programs* (BOILPs). First, we introduce some necessary notation and concepts related to BOILPs to facilitate presentation and discussion of other sections. Let $\boldsymbol{c}^1$ and $\boldsymbol{c}^2$ be n-vectors. $\boldsymbol{A}$ be an $m \times n$ matrix, and $\boldsymbol{b}$ be an m-vector, a BOILP can be stated as follows:

$$\min_{\boldsymbol{x} \in \mathcal{X}} \{z_1(\boldsymbol{x}), z_2(\boldsymbol{x})\}, \tag{2.1}$$

where $\mathcal{X} := \left\{\boldsymbol{x} \in \mathbb{Z}^n_+ : \boldsymbol{A}\boldsymbol{x} \leq \boldsymbol{b}\right\}$ represents the *feasible set in the decision space*, and $z_1(\boldsymbol{x}) := \boldsymbol{c}^1\boldsymbol{x}$ and $z_2(\boldsymbol{x}) := \boldsymbol{c}^2\boldsymbol{x}$ are two linear objective functions. Note that $\mathbb{Z}^n_+ := \{\boldsymbol{s} \in \mathbb{Z}^n : \boldsymbol{s} \geq \boldsymbol{0}\}$. The image $\mathcal{Y}$ of $\mathcal{X}$ under vector-valued function $\boldsymbol{z} = (z_1, z_2)$ represents the *feasible set in the objective/criterion space*, i.e., $\mathcal{Y} := z(\mathcal{X}) := \{\boldsymbol{y} \in \mathbb{R}^2 : \boldsymbol{y} = z(\boldsymbol{x})\}$. It is assumed that $\mathcal{X}$ is *bounded*, and all coefficients/parameters are integers, i.e., $\boldsymbol{A} \in \mathbb{Z}^{m \times n}$, $\boldsymbol{b} \in \mathbb{Z}^m$. and $\boldsymbol{c}^i \in \mathbb{Z}^n$ for $i = 1, 2$.

Definition 1. A feasible solution $\boldsymbol{x} \in \mathcal{X}$ is called *efficient* or *Pareto optimal*, if there is no other $\boldsymbol{x}' \in \mathcal{X}$ such that $z_k(\boldsymbol{x}') \leq z_k(\boldsymbol{x})$ for $k = 1, 2$ and $\boldsymbol{z}(\boldsymbol{x}') \neq \boldsymbol{z}(\boldsymbol{x})$. If $\boldsymbol{x}$ is efficient, then $\boldsymbol{z}(\boldsymbol{x})$ is called a *nondominated point*. The set of all efficient solutions $\boldsymbol{x}' \in \mathcal{X}$ is denoted by $\mathcal{X}_E$. The set of all nondominated points $\boldsymbol{z}(\boldsymbol{x})$ for some $\boldsymbol{x} \in \mathcal{X}_E$ is denoted by $\mathcal{Y}_N$ and referred to as the *nondominated frontier*.

Overall, multi-objective optimization is concerned with finding *all* nondominated points. Since by assumption $\mathcal{X}$ is bounded, the set of nondominated points of a BOILP, i.e., $\mathcal{Y}_N$, is finite.

2.2 Contributions of the Proposed Two Stage Method

The main contribution of our research is efficiently combining two of the fastest (criterion space search) algorithms, including the *Balanced Box Method* (BBM) developed by the authors in [64] and the *ϵ-constraint method* developed by the authors in [65], to take the main advantage of both of these algorithms, and hence solving BOILPs faster.

BBM is a recently developed algorithm which can be viewed as an extension of the *box algorithm* [67]. The authors in [64] have numerically shown that BBM can compute the nondominated frontier, i.e., the set of points in the criterion space corresponding to the efficient solutions, faster than many (if not all) of the existing methods such as the ϵ-constraint method, the augmented weighted Tchebycheff method [68, 69], and the perpendicular search method [70]. It is worth mentioning that if $\mathcal{Y}_N \neq \emptyset$ denotes the set of nondominated points of a BOILP, then BBM solves $3|\mathcal{Y}_N|$ (feasible) Single-Objective Integer Linear Programs (SOILPs).

On the other hand, the ϵ-constraint method is perhaps the most well-known algorithm for computing the (entire) nondominated frontier of BOILPs because of its simplicity and its long history. The authors in [64] have shown that this algorithm does not outperform BBM in terms of solution time mainly because in BBM high-quality feasible solutions are naturally available to be initialized in SOILPs. Note that in the ϵ-constraint method, this may be done by making additional computational efforts, e.g., developing a heuristic approach. However, the main advantage of the ϵ-constraint method is the fact that it solves only $2|\mathcal{Y}_N| + 1$ (feasible) SOILPs.

In light of the above, the main goal of this paper is to develop a combined approach that (1) is better than BBM and ϵ-constraint method in terms of solution time, and (2) needs to solve less SOILPs than BBM (similar to the ϵ-constraint method). To achieve these properties at the same time, the proposed approach starts by employing the BBM and at some point it switches to the ϵ-constraint method. Of course the switching time is critical because if we switch too early the solution time would probably not be much different from the ϵ-constraint method. Similarly, if it occurs too late, solving less SOILPs than BBM will not probably be achieved, and the solution time would probably not be much different from BBM. We develop a simple but effective mechanism for the switching that causes up to around 25% and 40% improvements in the solution time in comparison to the solution times of the original BBM and the ϵ-constraint method, respectively.

It is worth mentioning that the idea of combining multiple existing algorithms to obtain a more effective algorithm has been previously studied in the literature. For example, recently, the authors in [71] propose an algorithm entitled *Adaptive Search in Objective Space* (ASOS) which successfully combines the perpendicular search method [70] and the ϵ-constraint method. A key feature of ASOS is that it employs a *dynamic switch* meaning that it may switch between the perpendicular search method and the ϵ-constraint method multiple times during the course of algorithm. However, our two-stage approach uses a *fixed switch*.

In the computational study, we show that our two-stage approach is competitive with ASOS. Specifically, we show that ASOS outperforms our two-stage approach on bi-objective binary linear programs (note that ASOS is originally developed for solving such instances). However, our approach outperforms ASOS on (general) bi-objective integer linear programs (even if we transform such programs to bi-objective binary linear programs). We also numerically show that if we replace the fixed switch by the dynamic switch (used in ASOS) in our algorithm, then the generated two-stage approach does not work well.

2.3 The BBM and the ϵ-constraint Method

A high-level description of BBM, and the ϵ-constraint method is given in this section.

2.3.1 The Balanced Box Method

This algorithm maintains a priority queue of rectangles in the criterion space in non-increasing order of their areas. At the beginning, there is no rectangle in the priority queue. So, the algorithm first finds the endpoints of the nondominated frontier, denoted by $\boldsymbol{z}^T$ and $\boldsymbol{z}^B$. These two points result in defining a rectangle, denoted by $R(\boldsymbol{z}^T, \boldsymbol{z}^B)$, containing all not yet found nondominated points. Next, we explain the workings of the algorithm in an arbitrary iteration.

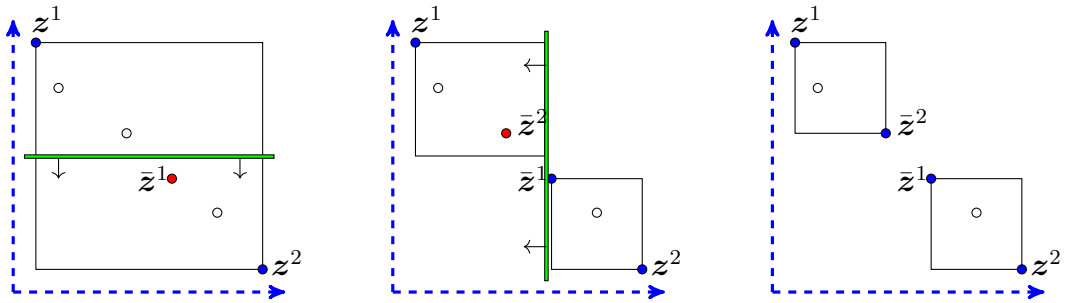

(a) Step 1 (b) Step 2 (c) Step 3

Figure 2.1 – The workings of BBM at each iteration

The algorithm pops out an element of the priority queue, denoted by $R(\boldsymbol{z}^1, \boldsymbol{z}^2)$ in which $\boldsymbol{z}^1$ and $\boldsymbol{z}^2$ with $z_1^1 < z_1^2$ and $z_2^1 > z_2^2$ are two already found nondominated points. The algorithm then splits the rectangle horizontally into two equal parts, i.e., it adds the cut $z_2(\boldsymbol{x}) \leq \frac{z_2^1 + z_2^2}{2}$ to the model. It first searches the bottom rectangle for the not-yet discovered local endpoint, which is denoted by $\bar{\boldsymbol{z}}^1$ in Figure 2.1a. Next, the algorithm adds the cut $z_1(x) < \bar{z}_1^1$ to the model to split the rectangle vertically. It then searches the left rectangle for the not-yet discovered local endpoint, which is denoted by $\bar{\boldsymbol{z}}^2$ in Figure 2.1b.

It can be shown that by finding these two local endpoints, $R(\boldsymbol{z}^1, \boldsymbol{z}^2)$ can be split into (at most) two independent rectangles, i.e., $R(\boldsymbol{z}^1, \bar{\boldsymbol{z}}^2)$ and $R(\bar{\boldsymbol{z}}^1, \boldsymbol{z}^2)$ containing all not yet found nondominated points in $R(\boldsymbol{z}^1, \boldsymbol{z}^2)$ as shown in Figure 2.1c. So, these two new rectangles should be added to the priority queue, before starting the next iteration. Note that BBM employs several enhancement techniques that interested readers can find them in [64]. All those enhancements are used in this research as well.

Proposition 2. BBM solves at most $3|\mathcal{Y}_N|$ SOILPs [64].

2.3.2 The ϵ-constraint Method

Similar to BBM, the ϵ-constraint method first finds the endpoints of the nondominated frontier, i.e., $\boldsymbol{z}^T$ and $\boldsymbol{z}^B$. These two nondominated points define a rectangle $R(\boldsymbol{z}^B, \boldsymbol{z}^T)$ containing all not yet found nondominated points. The algorithm then starts to generate

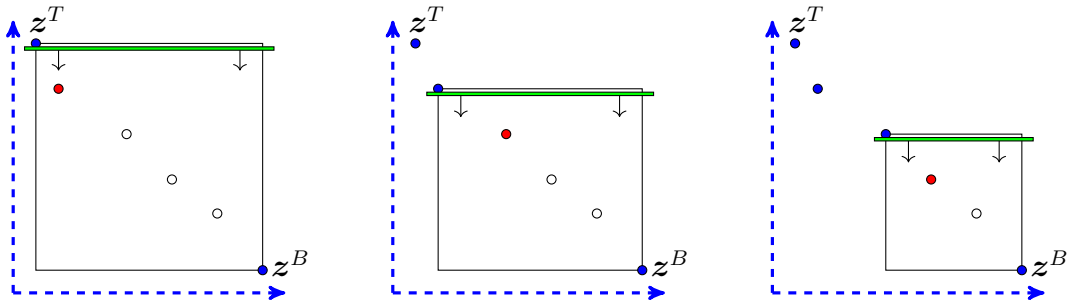

(a) Iteration 1 (b) Iteration 2 (c) Iteration 3

Figure 2.2 – An illustration of the workings of ϵ-constraint method

the nondominated points one by one from the direction starting at $\boldsymbol{z}^T$ and ending at $\boldsymbol{z}^B$. An illustration of the first three iterations of the algorithm can be found in Figure 2.2. Let $\boldsymbol{z}^{Last}$ be the nondominated point found in the last iteration, the new nondominated point (denoted by $\boldsymbol{z}^{New}$) can be produced by adding the cut $z_2(\boldsymbol{x}) < z_2^{Last}$ to the model and searching the corresponding rectangle.

Finally, as soon as it turns out that $\boldsymbol{z}^{New} = \boldsymbol{z}^B$, the algorithm terminates. Note that there are several enhancement techniques for the ϵ-constraint method that interested readers can find in [64]. All those enhancements are used in this research as well.

Proposition 3. The ϵ-constraint method solves at most $2|\mathcal{Y}_N| + 1$ SOILPs. [65]

2.4 The Two-stage Approach for BOILP

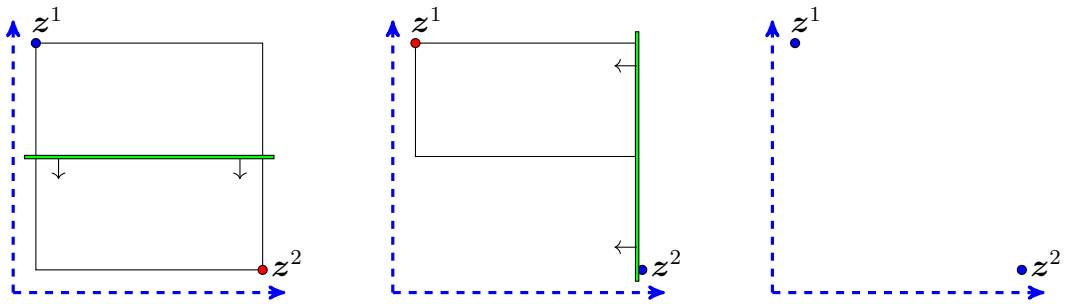

(a) Step 1 (b) Step 2 (c) Step 3

Figure 2.3 – The workings of BBM when $R(\boldsymbol{z}^1, \boldsymbol{z}^2)$ is empty

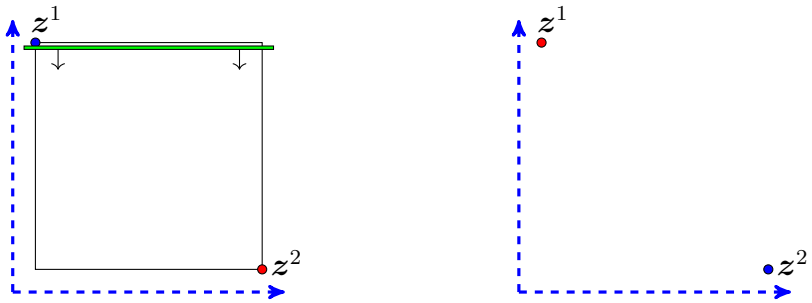

(a) Step 1 (b) Step 2

Figure 2.4 – Applying ϵ-constraint method to validate a empty rectangle

We first make an observation about BBM to show the main motivation of our research. From workings of BBM in Figure 2.3, we observe that when a rectangle is empty, two SOILPs have to be solved to prove that it is empty. Now suppose that whenever a rectangle is empty, we immediately switch to the ϵ-constraint method as shown in Figure 2.4. In this case, for each empty rectangle, only one SOILP has to be solved. So, we can conclude that if a given rectangle $R(\boldsymbol{z}^1, \boldsymbol{z}^2)$ is expected to be empty, then by switching to the ϵ-constraint method, hopefully we can avoid solving one redundant SOILP.

In light of the above, our proposed method solves a BOILP in two stages. In the first stage, it employs BBM in order to generate some nondominated points from different parts of the nondominated frontier, and so it quickly splits the search region into small rectangles (that are hopefully empty). In the second stage, the algorithm switches to the ϵ-constraint method to conduct the searching in the not yet explored rectangles.

Obviously, the mechanism for triggering the switch significantly influences the performance of the proposed method. If we trigger the switch too early, rectangles in the queue are probably not empty, and so the solution time may even increase. Similarly, if we trigger the switch too late, opportunities to save SOILPs while exploring empty rectangles will be eliminated, and so the solution time may not improve at all. The following definition and proposition are informative.

Definition 4. The *ideal switch* is defined as generating all nondominated points of a BOILP exactly once by BBM, and then switching to the ϵ-constraint method for exploring empty rectangles.

Proposition 5. The two-stage method with ideal switch solves at most $\lceil 2.5|\mathcal{Y}_N| \rceil$ SOILPs.

Proof. For computing a nondominated point for the first, two SOILPs have to be solved. Since in BBM, the rectangles are disjoint, after computing all nondominated points there are at most $\lceil 0.5|\mathcal{Y}_N| \rceil$ empty rectangles in the priority queue. For each empty rectangle, one SOILP has to be solved by the ϵ-constraint method to prove that it is empty. Therefore, the result follows. □

We note that in practice it is highly unlikely to realize the ideal switch and to push the proposed two-stage method to its theoretical maximum efficiency. This is because real-world BOILPs rarely have well-distributed nondominated frontiers, i.e., the distance between two adjacent nondominated points may vary significantly. In consequence, avoiding exploring empty rectangles in the first stage is likely to be impossible. However, since BBM explores rectangles in non-decreasing order of their areas, it is expected that empty rectangles to arise more often at the end of the search. This is because intuitively smaller rectangles are more likely to be empty. So, by considering this observation, we next introduce a simple switching technique that can potentially meet two goals including (1) reducing the solution time, and (2) saving SOILPs.

Let $\eta \in [0, 1]$ and $\theta \geq 1$ be two user-defined parameters. Furthermore, let β be the number of times that BBM was not able to find a new nondominated point in the last θ SOILPs that it has solved. We impose our proposed method to switch as soon as $\beta \geq \lceil \eta\theta \rceil$ holds. Intuitively, this condition measures how often we may face empty rectangles in the subsequent iterations of BBM.

2.5 A Computational Study

In this computational study, we first conduct a set of experiments to determine a reasonable value for θ and η, and then compare the performance of our proposed two-stage method with the performance of some other exact methods. We implement the ϵ-constraint method, BBM, ASOS, and the proposed two-stage approach in C++ and employ CPLEX 12.7 to solve SOILPs. All computational experiments are carried out on a Dell PowerEdge R630 with two Intel Xeon E5-2650 2.2 GHz 12-Core Processors (30MB), 128GB RAM, and the RedHat Enterprise Linux 6.8 operating system, and using a single thread.

2.5.1 Switch Threshold Selection

In order to conduct the experiments in this section, two large sets of instances with only binary decision variables are downloaded from `http://hdl.handle.net/1959.13/1036183`. Both sets contain four classes of instances which are used in some previous studies (see for instance [64]). The first set contains 20 instances of (bi-objective) 2-Dimensional Knapsack Problem (2DKP) with 375, 500, 625, and 750 binary variables. The second set contains 20 instances of (bi-objective) Assignment Problem (AP) with 200×200, and 300×300 binary variables.

We assume that $\theta \in \{7, 15, 31\}$ and $\eta \in \{0.1, 0.2, 0.4, 0.6\}$ and consider all possible combinations to find the best value for θ and η. It is worth mentioning that, regardless of value of η, we have computationally observed that (in practice) the proposed trigger will be activated naturally when at least θ rectangles are explored by BBM. Note that, we know that in BBM (1) after exploring a rectangle, the area of the two new rectangles are at most half of the original rectangle [64], and (2) the rectangles will be explored in non-decreasing order of their areas. So, exploring θ rectangles by BBM, implies that the sum of areas of not yet explored rectangles is at most $\frac{a(R(\boldsymbol{z}^T, \boldsymbol{z}^B))}{\theta+1}$, where $a(R(\boldsymbol{z}^T, \boldsymbol{z}^B))$ is the area of $R(\boldsymbol{z}^T, \boldsymbol{z}^B)$. This can be an indication that the proposed two-stage method will perform well even if the

goal is to compute high-quality approximations for the nondominated frontier when a limited computational time is available (of course this is because of using BBM in the first stage).

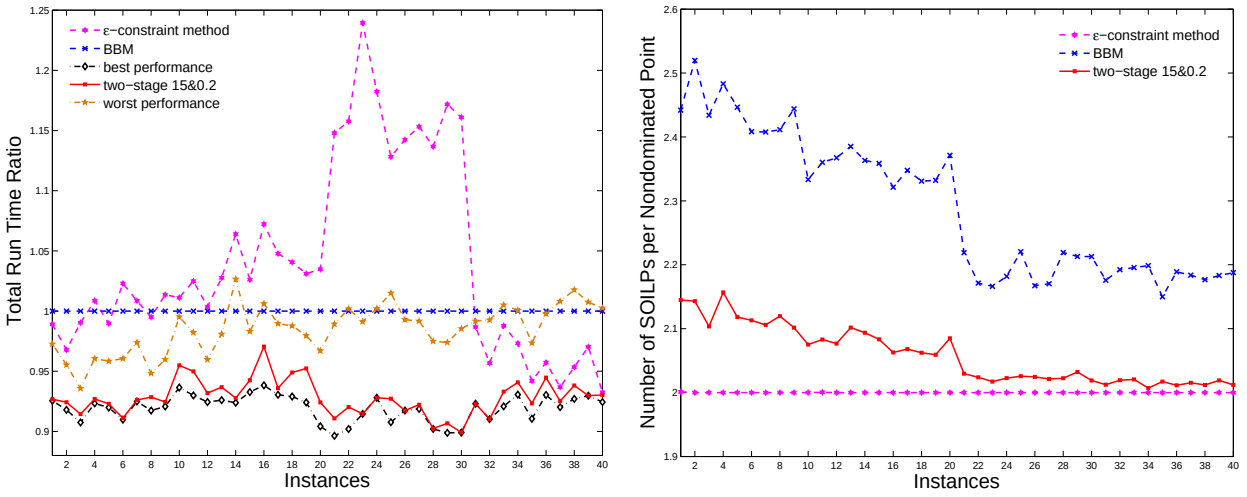

(a) Solution time

(b) Number of SOILPs

Figure 2.5 – Performance of the proposed threshold

Our proposed values for θ and η are 15 and 0.2, respectively. The performance of our proposed values can be observed from Figure 2.5a, in which the ratio of the solution time of each algorithm to the solution time of BBM are reported for each instance. The first 20 instances are 2DKP instance, and the others are AP instances. In this figure, the "best performance" and "worst performance" shows the performance of the best and worst combinations of $\theta \in \{7, 15, 31\}$ and $\eta \in \{0.1, 0.2, 0.4, 0.6\}$ for each individual instance that resulted the minimum and maximum solution time, respectively. For example, for Instance 1 the combination ($\theta = 7$, $\eta = 0.1$) may be the best one, but for Instance 2 the same combination may be the worse one. So, the overall performance of any combination lies within the best and worse performances. Observe that even the worse performance is better than both BBM and ϵ-constraint method in most instances. Observe too that the proposed combination performance is almost as good as the best performance, and the solution time of the proposed combination is always better than both BBM and the ϵ-constraint method. In fact the solution time of the proposed method is up to around 25% less than BBM and up to around 40% better than ϵ-constraint method. It is worth mentioning that, from Figure 2.5b,

we see that the average number of SOILPs per each nondominated point when using the proposed combination is significantly smaller than BBM and it is close to the ϵ-constraint method.

2.5.2 Performance Comparison

In this section, we compare the performance of the proposed two-stage method with the performance of BBM, ϵ-constraint method, ASOS, and a different version of our proposed two-stage method that employs a dynamic switch. Before we present the computational results, we briefly explain (a variant of) ASOS.

ASOS is a two-stage approach that employs a dynamic switch. This approach is developed for solving BOILPs with only binary variables. The underling idea of this algorithm is to effectively combine the perpendicular search method with the ϵ-constraint method. The main weakness of the perpendicular search method is that it may solve many infeasible SOILPs during its search. Consequently, ASOS attempts to heuristically find some interior feasible points in a rectangle before exploring it. If it fails then it searches the rectangle using the ϵ-constraint method. Otherwise, it searches the rectangle using the perpendicular search method.

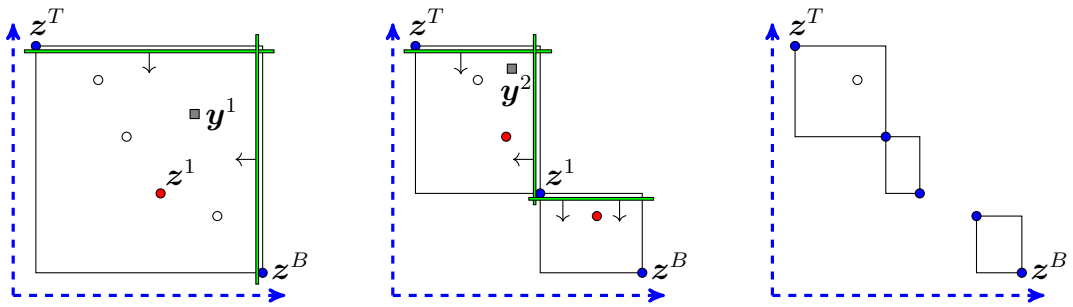

(a) Iteration 1 (b) Iteration 2 (c) Iteration 3

Figure 2.6 – An illustration of the workings of ASOS

Figure 2.6 illustrates the main operations of ASOS. In Figure 2.6a, we assume that a feasible point $\boldsymbol{y}^1$ is known for $R(\boldsymbol{z}^T, \boldsymbol{z}^B)$, and so it should be explored by the perpendicular

search method. In other words, ASOS simply adds two cuts $z_1(\boldsymbol{x}) < z_1^B$ and $z_2(\boldsymbol{x}) < z_2^T$ to the model and searches for a new nondominated point using $\boldsymbol{y}^1$. Note that the new nondominated point can be any nondominated point and here we simply denote it by $\boldsymbol{z}^1$. After finding $\boldsymbol{z}^1$, $R(\boldsymbol{z}^T, \boldsymbol{z}^B)$ should be split into two rectangles $R(\boldsymbol{z}^T, \boldsymbol{z}^1)$ and $R(\boldsymbol{z}^1, \boldsymbol{z}^B)$ as shown in Figure 2.6b. For $R(\boldsymbol{z}^T, \boldsymbol{z}^1)$ again we assume that a feasible point denoted by $\boldsymbol{y}^2$ is known and so it should be explored by the perpendicular search method. However, for $R(\boldsymbol{z}^1, \boldsymbol{z}^B)$, we assume that no feasible point is known and so the ϵ-constraint method should be used to explore it. This implies that only the cut $z_1(\boldsymbol{x}) < z_2^1$ should be added to model to explore the rectangle for finding the closest nondominated point to $\boldsymbol{z}^1$. The new rectangles after exploring $R(\boldsymbol{z}^T, \boldsymbol{z}^1)$ and $R(\boldsymbol{z}^1, \boldsymbol{z}^B)$ are shown in Figure 2.6c.

Note that an effective and simple heuristic for finding a feasible solution in a rectangle proposed by the authors in [71] is called *Boundary solution Induced Neighborhood Search* (BINS). This heuristic simply fix the value of any decision variable of the problem to zero (or one) if the value of such a decision variable is zero (or one) in both solutions corresponding to top and bottom endpoints of the rectangle (that ASOS has stored in memory previously). The reduced integer linear program is most likely easier to solve and so we can see whether it can result in finding a feasible point within the rectangle.

Note too that the idea of BINS can be applied to our proposed two-stage approach as well. This implies that instead of having a fixed switch, we can have a dynamic switch. Basically, when exploring a rectangle we apply the BINS. If it succeeds then we use BBM, otherwise we apply the ϵ-constraint method. We denote by DTS our proposed two-stage method with the dynamic switch. Table 2.1 shows the performance of different algorithms on all instances of AP and 2DKP. In this table, 'T(Sec.)' shows the solution time in seconds and '#IP' shows the number of SOILPs solved for our proposed two-stage method (with fixed switch). We provide the results of other exact methods as the percentage of increase in the solution time and the number of SOILPs in comparison with the results of the two-stage method. We observe that the solution time of the proposed two-stage approach is better than

Table 2.1 – Performance of different algorithms on binary integer instances

Problem		Two-stage		%Increase							
				BBM		ϵ-constraint		DTS		ASOS	
Class	**Instance**	**T(Sec.)**	**#IP**	**T**	**IP**	**T**	**IP**	**T**	**IP**	**T**	**IP**
2DKP:A	1	1,008.7	1,791	8.8	13.8	6.9	-6.7	5.0	38.5	-4.3	36.3
	2	1,089.2	1,963	9.0	17.6	4.0	-6.7	1.8	39.5	-5.4	40.0
	3	1,977.9	2,438	8.9	15.7	7.6	-4.9	4.6	40.9	-1.5	39.6
	4	1,027.8	2,161	7.0	15.1	7.8	-7.3	4.4	37.2	1.8	35.8
	5	1,549.6	2,044	7.1	15.5	6.7	-5.6	4.6	39.3	-3.2	37.4
2DKP:B	6	2,563.5	2,992	8.1	14.0	10.4	-5.3	6.4	38.7	-3.5	34.1
	7	4,628.3	3,776	8.1	14.3	8.6	-5.0	7.4	39.4	-3.9	35.8
	8	3,742.4	3,262	6.6	13.8	7.6	-5.6	3.1	39.3	-5.1	34.9
	9	2,487.4	2,812	7.0	16.3	8.0	-4.8	2.5	41.1	-5.6	39.5
	10	2,688.0	3,343	6.5	12.4	7.2	-3.6	4.6	40.1	-3.7	32.9
2DKP:C	11	5,905.0	4,793	5.2	13.3	7.9	-4.0	3.6	40.5	-3.9	33.2
	12	6,294.0	4,438	6.3	14.0	8.0	-3.7	2.7	41.0	-3.2	35.7
	13	6,856.3	4,731	6.5	13.5	11.0	-4.8	5.3	39.5	-3.1	31.1
	14	4,585.8	4,807	7.2	12.9	13.4	-4.5	7.0	39.5	-4.5	30.0
	15	4,631.2	3,950	5.9	13.2	9.1	-4.0	5.5	40.9	-0.6	34.2
2DKP:D	16	8,952.5	6,250	3.8	12.5	11.0	-3.0	7.2	41.1	-4.8	30.9
	17	9,386.2	5,865	6.2	13.5	11.6	-3.3	5.4	40.0	-4.8	30.6
	18	8,713.6	6,022	3.9	13.0	9.0	-3.0	4.2	40.7	-4.9	30.5
	19	8,827.8	5,531	2.6	13.3	6.3	-2.9	3.2	41.0	-2.8	28.5
	20	7,225.2	5,185	1.1	13.7	1.8	-4.1	0.8	40.3	-3.9	32.1
Avg.		**4,707.0**	**3,908**	**6.3**	**14.1**	**8.2**	**-4.6**	**4.5**	**39.9**	**-3.5**	**34.2**
AP:A	21	1,215.4	1,372	9.0	9.3	25.4	-1.5	12.0	38.0	-11.5	14.4
	22	1,241.0	1,441	7.8	7.3	24.5	-1.2	12.3	38.3	-12.2	14.0
	23	1,278.7	1,408	5.2	7.4	28.8	-0.9	10.2	38.1	-18.5	15.9
	24	1,321.3	1,523	6.6	7.9	27.5	-1.1	13.8	37.4	-17.9	13.7
	25	1,298.7	1,424	5.9	9.6	20.9	-1.3	10.1	39.8	-15.7	18.3
AP:B	26	3,053.8	3,053	5.1	7.0	24.6	-1.2	10.9	41.0	-7.7	22.4
	27	2,723.1	2,753	6.2	7.4	23.1	-1.1	9.4	39.3	-9.0	17.3
	28	2,770.3	2,797	8.8	9.7	27.3	-1.1	12.1	40.5	-6.7	19.0
	29	3,036.7	2,959	8.0	8.9	27.6	-1.6	11.3	39.3	-9.2	20.4
	30	2,781.8	2,770	7.4	9.6	28.8	-0.9	10.0	40.1	-15.3	20.7
AP:C	31	3,236.8	1,636	4.9	8.1	3.2	-0.6	12.6	38.5	-16.9	12.7
	32	3,189.6	1,670	7.8	8.6	3.8	-1.0	13.5	37.4	-14.5	12.3
	33	3,216.6	1,663	4.1	8.7	0.3	-1.0	11.9	37.3	-18.0	11.7
	34	3,301.8	1,688	5.4	9.5	3.8	-0.4	13.9	39.3	-9.4	13.6
	35	3,024.6	1,642	5.8	6.6	2.9	-0.9	14.8	37.2	-12.9	10.9
AP:D	36	7,710.4	3,512	8.4	8.8	2.6	-0.6	13.2	40.3	-12.9	17.0
	37	8,336.2	3,807	7.8	8.4	4.1	-0.8	13.3	38.6	-14.3	16.8
	38	8,045.0	3,690	8.1	8.2	2.9	-0.6	13.7	39.8	-13.7	15.3
	39	8,154.3	3,713	7.9	8.1	3.1	-0.9	12.0	38.4	-12.5	17.9
	40	8,206.8	3,676	8.8	8.7	1.2	-0.6	9.4	40.1	-12.6	17.1
Avg.		**3,857.1**	**2,410**	**6.9**	**8.4**	**14.3**	**-1.0**	**12.0**	**38.9**	**-13.1**	**16.1**

the ϵ-constraint method, BBM, and DTS, but not as good as ASOS. Note that ASOS solves more SOILPs since it needs to solve some additional SOILPs because of BINS. However, if BINS finds a solution then ASOS uses it to warm-start the perpendicular search method and so overall ASOS solution time is smaller.

Table 2.2 – Performance of different algorithms on general integer instances

Problem		**Two-stage**		**%Increase**									
				BBM		**ϵ-constraint**		**DTS**		**ASOS**		**ASOS-U**	
Class	**Instance**	**T(Sec.)**	**#IP**	**T**	**IP**	**T**	**IP**	**T**	**IP**	**T**	**IP**	**T**	**IP**
A	1	1,163.7	1,003	14.8	25.1	4.2	-8.8	3.3	36.8	2.6	37.5	34.1	59.4
	2	1,700.5	2,771	21.8	24.5	3.2	-9.4	6.6	35.9	5.9	36.6	33.9	49.2
	3	2,730.4	1,985	20.1	24.8	21.1	-8.7	23.1	37.0	23.2	37.3	34.6	52.8
B	4	2,230.5	1,539	18.2	24.6	15.7	-10.8	14.2	33.8	13.8	34.4	37.9	59.0
	5	397.9	1,046	24.6	27.8	2.8	-9.8	4.5	35.2	4.1	36.0	55.4	58.2
	6	434.1	1,257	20.5	25.0	16.2	-9.5	15.1	35.9	17.5	37.0	76.9	58.5
C	7	396.0	654	20.2	25.8	8.3	-9.0	5.3	36.2	6.8	37.8	41.6	56.9
	8	2,782.6	878	19.7	23.7	7.8	-9.7	8.8	35.5	5.1	35.3	13.9	52.1
	9	217.5	1,168	17.3	22.7	6.2	-10.7	7.5	34.1	6.0	36.6	79.3	56.6
D	10	1,024.2	3,873	24.1	26.8	1.5	-9.3	3.2	36.0	4.2	42.3	115.6	52.6
	11	383.1	2,217	25.5	28.4	6.5	-8.9	12.8	36.6	7.2	37.3	207.0	60.7
	12	468.9	2,389	24.7	30.6	4.1	-7.6	1.5	38.6	3.3	39.1	154.3	63.0
E	13	3,770.9	1,531	19.6	30.3	4.4	-5.5	4.1	41.7	5.7	42.1	31.9	63.2
	14	2,764.5	2,621	17.3	25.6	3.8	-8.9	3.6	36.8	2.6	37.9	46.9	59.4
	15	858.6	1,930	18.2	26.4	1.3	-9.2	3.1	36.2	4.2	36.6	39.9	52.4
F	16	1,202.9	565	12.2	23.5	47.8	-9.9	49.1	34.9	47.3	36.6	41.1	57.9
	17	2,049.2	1,301	18.3	26.5	8.2	-8.9	13.6	36.4	6.4	37.0	21.5	55.3
	18	1,031.8	1,358	21.3	29.2	3.0	-9.2	3.9	36.0	5.0	36.7	54.7	59.6
G	19	567.5	1,186	22.5	31.2	5.7	-7.2	5.7	39.1	8.3	39.6	107.9	60.3
	20	2,167.5	3,497	23.1	27.5	2.3	-8.4	4.2	37.4	3.1	37.5	103.0	56.7
	21	447.5	1,767	16.3	22.2	2.5	-10.8	6.9	33.8	6.4	35.1	167.5	52.9
H	22	1,794.4	1,509	18.5	19.3	10.4	-9.0	8.9	36.5	11.5	42.7	56.7	54.4
	23	751.8	364	8.9	22.8	58.1	-12.4	57.9	31.0	68.0	33.8	60.9	61.3
	24	3,390.1	2,983	17.0	26.0	7.5	-9.3	6.1	36.2	8.8	40.6	38.0	56.6
I	25	991.0	2,044	25.5	28.8	4.7	-9.3	1.1	36.0	6.1	39.5	116.8	58.8
	26	4,421.1	1,348	21.8	27.3	5.9	-9.4	5.7	35.8	6.0	36.5	26.6	56.6
	27	3,072.5	2,334	21.6	28.2	3.8	-9.0	5.4	36.5	4.7	41.7	35.6	59.9
Avg.		**1,600.4**	**1,745.1**	**19.8**	**26.1**	**9.9**	**-9.2**	**10.6**	**36.1**	**10.9**	**37.8**	**67.9**	**57.2**

Since ASOS is better than the proposed two-stage method, a natural question is whether the proposed two-stage method can be of interest at all? In order to show this, we generated 9 classes of random integer linear programs and each with three instances. These classes differ in the number of variables, i.e., n, and constraints, i.e., m, since we assume that $n \in \{400, 500, 600\}$ and $m \in \{6, 8, 10\}$. Class A denotes the smallest set of instances with $n = 400$ and $m = 6$ and Class I denotes the largest set of instances with $n = 600$ and $m = 10$. To construct each instance, we randomly draw the components of the vectors $\boldsymbol{c}^1$ and $\boldsymbol{c}^2$ from the discrete uniform distribution from the interval $[-100, -1]$. We also randomly draw the entries of A from the discrete uniform distribution from the interval

$[1, 100]$. Finally, we randomly select the component $i \in \{1, \ldots, m\}$ of vector $\boldsymbol{b}$ from the discrete uniform distribution from the interval $[100, \sum_{j=1}^{n} a_{ij}]$.

Table 2.2 shows the results of different algorithms on the generated 27 random instances. We note that BINS can be easily generalized to be used for any integer linear program. Moreover, all instances can be transformed to BOILPs with only binary decision variables. For example, a general integer variable $x_j \in [0, U]$ where $j \in \{1, \ldots, n\}$ can be replaced by $x_j = \sum_{q=0}^{U} q x'_{jq}$ where $x'_{jq} \in \{0, 1\}$ for $q \in \{0, \ldots, U\}$ and $\sum_{q=0}^{U} x'_{jq} = 1$. This is called the *unary transformation* and we denote by ASOS-U when the unary transformation is used and solved by ASOS. Note that we can also replace x_j where $j \in \{1, \ldots, n\}$ by $x_j = \sum_{q=0}^{\lfloor \log_2 U \rfloor} 2^q x'_{jq}$where $x'_{jq} \in \{0, 1\}$ for $q \in \{0, \ldots, \lfloor \log_2 U \rfloor\}$. This is called the *binary transformation*. However, since ASOS with the unary transformation performs significantly better than binary transformation for our test instances, we do not report the results of binary transformation.

From Table 2.2, we observe that the proposed two-stage method outperforms all other methods. Specifically, on average, it is around 11% faster than ASOS and 68% than ASOS-U. This is mainly because for our test instances with general integer decision variables, (the extended version of) BINS always fails for ASOS. So, the performance of ASOS cannot be better than the ϵ-constraint method. For ASOS-U, BINS often works but the size of ASOS-U is the main reason for its poor performance.

2.6 Conclusion

We presented a simple but effective two-stage approach for solving BOILPs. This method combines BBM and the ϵ-constraint method to remedy their weakness. The proposed method is faster, and solves less SOILPs. We hope that its simplicity, versatility, and performance encourages (more) researchers to consider studying combined methods for BOILPs.

Chapter 3: Bi-objective Optimization Approach for Managing Building Clusters with a Shared Energy Storage

This chapter was previously published as [47]: Dai, R., & Charkhgard, H. (2018). Bi-objective mixed integer linear programming for managing building clusters with a shared electrical energy storage. Computers & Operations Research, 96, 173-187. In this work, a contract balanced strategy is proposed to manage the building clusters with the shared energy storage to address the conflict between fairness and efficiency in the energy storage sharing. This strategy is modeled as a bi-objective mixed integer nonlinear program, and some linearization techniques are applied to facilitate the solution. The case study demonstrates that the proposed strategy can maximize the economic benefits of energy storage sharing with the fairness guaranteed.

3.1 Overview

Emerging smart grid infrastructures are allowing buildings to connect to components in other buildings and utilize them in different ways. Clearly, these interconnected building clusters provide new opportunities for building operators to collaborate and help reduce their operational costs over a planning horizon. Nevertheless, since each building can be treated as an independent decision maker here, related fairness concerns have to be addressed in these collaborative environments. We address these issues on building clusters when a single electrical energy storage is shared between two buildings with deterministic demand.

We note that in general sharing (electrical) energy storage facilities between buildings introduces two further considerations, i.e., *fairness* and *freedom*. Now the term “fairness" is difficult to define, but one can reasonably assume that it means that the amount of energy

a building charges into an energy storage should be equal to the amount of energy that it discharges (uses). Similarly, the term “freedom" refers to how freely a building can discharge energy from an energy storage. Now obviously these two aims are conflicting and hence one can pursue a trade-off here. For example, increased freedom may save more costs for buildings, but at the same time may result in a completely unfair system (potentially leading to a breakdown of collaboration agreements between buildings). Hence implementing trade-offs between fairness and freedom here is not obvious. To the best of our knowledge, we are the first exploring the tradeoff between fairness and freedom in the context of building clusters with a shared energy storage. However, it is worth mentioning that there exist studies about similar topics in other fields. For example, in a recent study in the field of computer science, [72] explore fairness and freedom in tiered storage systems in computer networks.

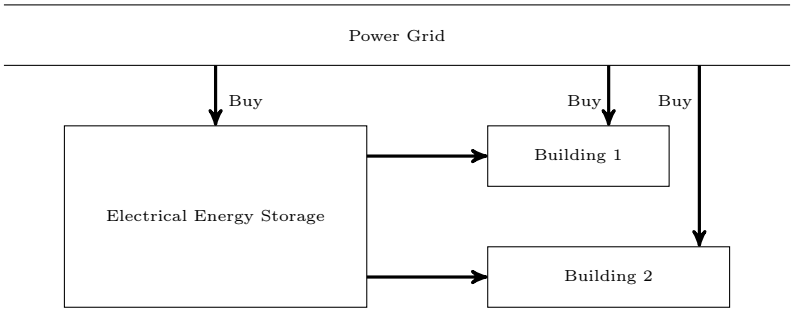

Figure 3.1 – Energy flow for two buildings sharing an electrical storage

We develop three energy storage sharing strategies including *extreme free strategy*, *extreme fair strategy*, and *contract balance strategy*. We present a novel bi-objective mixed integer linear programming formulation for the configuration shown in Figure 3.1 under each of these energy storage sharing strategies. It is worth mentioning that the contract balance strategy simply penalizes a building if it discharges more energy from the storage than what it actually charged into the storage (in entire planning horizon). The penalty is basically the cost that it has to be paid to the other building. To best of our knowledge, there is no study that has explored the consequences of the contract balance strategy in this context.

We develop a novel technique to measure the degree of fairness and freedom of our proposed contract balance strategy. By conducting a comprehensive computational study, we show that the contract balance strategy is not only significantly better than the extreme free strategy in terms of fairness, but also it is significantly better than extreme fair strategy in terms of cost savings.

It is worth mentioning that the proposed contract balance strategy yields bi-linear terms in the mathematical formulation. As a result, properly handling these nonlinear terms and efficiently linearizing them is a key challenge in itself. So, another contribution of our research is showing how piecewise McCormick relaxation can be efficiently used for linearizing bi-linear terms with high level of precision.

3.2 Preliminaries

In this section, we introduce some necessary notations and concepts related to *multi-objective mixed integer linear programs* (MOMILPs) to facilitate presentation and discussion of other sections. Foremost, a MOMILP can be stated as follows:

$$\min_{(x,y)\in\mathcal{F}} \{z_1(x,y),\ldots,z_p(x,y)\}, \tag{3.1}$$

where $\mathcal{F} := \left\{(x,y) \in \mathbb{Z}_+^{n_1} \times \mathbb{R}_+^{n_2} : Ax + \bar{A}y \leq b\right\}$ represents the *feasible set in the decision space*, and $z_i(x,y) = c^i x + \bar{c}^i y$ for each $i = 1,\ldots,p$ represents a linear objective function.The image $\mathcal{O}$ of $\mathcal{F}$ under vector-valued function $z = \{z_1,\ldots,z_p\}$ represents the *feasible set in the objective/criterion space*, i.e., $\mathcal{O} := z(\mathcal{F}) := \{o \in \mathbb{R}^p : o = z(x,y) \text{ for some } (x,y) \in \mathcal{F}\}$. It is assumed that $\mathcal{F}$ is *bounded*, and all coefficients/parameters are rational, i.e., $A \in \mathbb{Q}^{m\times n_1}$, $\bar{A} \in \mathbb{Q}^{m\times n_2}$, and $c^i, \bar{c}^i \in \mathbb{Q}^{n_1+n_2}$ for all $i = 1,\ldots,p$. Note that the term *multi-objective linear program* (MOLP) is also used sometimes if $n_1 = 0$, and the term *multi-objective integer linear program* (MOILP) if $n_2 = 0$.

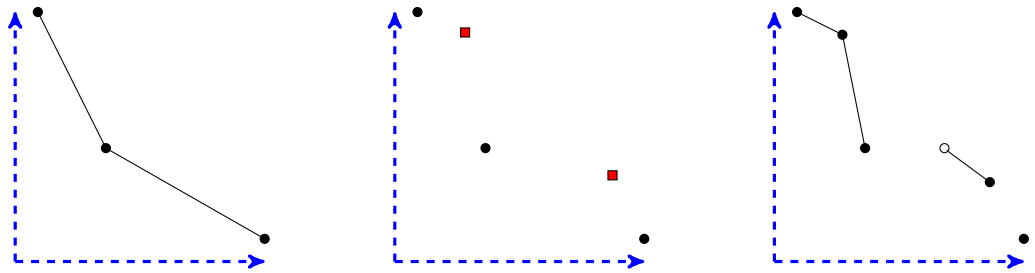

(a) MOLP. (b) MOILP. (c) MOMILP.

Figure 3.2 – An illustration of the nondominated frontier with two objectives

Definition 6. A feasible solution $(x', y') \in \mathcal{F}$ is called *efficient* or *Pareto optimal*, if there is no other $(x, y) \in \mathcal{F}$ such that $z_k(x, y) \leq z_k(x', y')$ for $k = 1, \ldots, p$ and $z(x, y) \neq z(x', y')$. If (x', y') is efficient, then $z(x', y')$ is called a *nondominated point*. The set of all efficient solutions $(x', y') \in \mathcal{F}$ is denoted by $\mathcal{F}_E$. The set of all nondominated points $z(x', y') \in \mathcal{O}$ for some $(x', y') \in \mathcal{F}_E$ is denoted by $\mathcal{O}_N$ and referred to as the *nondominated frontier* or the *efficient frontier*.

Definition 7. Let $(x', y') \in \mathcal{F}_E$. If there is a $\lambda \in \mathbb{R}^p_>$ such that (x', y') is an optimal solution to $\min_{(x,y)\in\mathcal{F}} \lambda^T z(x, y)$, then (x', y') is called a *supported efficient solution* and $z(x', y')$ is called a *supported nondominated point*.

Definition 8. Let $\mathcal{O}^e$ be the set of extreme points of the convex hull of $\mathcal{O}$. A point $z(x', y') \in \mathcal{O}$ is called an *extreme supported nondominated point* if $z(x', y')$ is a supported nondominated point and $z(x', y') \in \mathcal{O}^e$.

Overall, multi-objective optimization is concerned with finding *all* nondominated points, i.e., supported as well as unsupported nondominated points. Specifically, $\min_{(x,y)\in\mathcal{F}} z(x, y)$ is defined to be precisely $\mathcal{O}_N$. Now it is well-known that both the set of efficient solutions $\mathcal{F}_E$ and the set of nondominated points $\mathcal{O}_N$ of a MOLP are supported and connected, i.e., between any pair of nondominated points there exists a sequence of nondominated points with the property that all points on the line segment between consecutive points in the sequence are also nondominated [73]. Consequently, for a MOLP to describe all nondominated points, it suffices to find all extreme supported nondominated points. An illustration of the

nondominated frontier of a MOLP when $p = 2$ is shown in Figure 3.2a, i.e., where the horizontal line shows the first objective value and the vertical line shows the second objective value.

Now the set of nondominated points of a MOILP is finite (since by assumption $\mathcal{F}$ is bounded). However, unfortunately, due to the existence of unsupported nondominated points, finding all nondominated points of a MOILP is much more challenging. Along these lines, the nondominated frontier of a MOILP when $p = 2$ is also shown in Figure 3.2b where the red rectangles are unsupported. Finding all nondominated points of a MOMILP is even more challenging. Namely, if at most one of the objective functions contains continuous decision variables, then the set of nondominated points is finite and existing MOILP solution approaches can be applied to solve a MOMILP. However, in all other cases the efficient frontier of a MOMILP may contain connected parts as well as supported and unsupported nondominated points. Therefore, in these cases, the set of nondominated points is not finite and existing algorithms for solving a MOILP cannot be used. An illustration of the nondominated frontier of a MOMILP when $p = 2$ is shown in Figure 3.2c as well, i.e., where even half-open (or open) line segments may exist in the nondominated frontier. Interested readers are referred to [74, 75, 76, 77, 78] for further details on algorithms for MOILPs and MOMILPs.

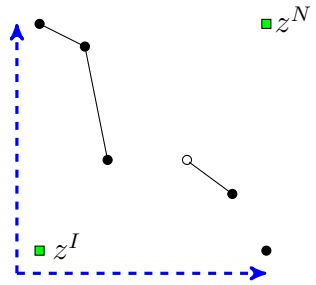

Figure 3.3 – The ideal and nadir points of a MOMILP with $p = 2$

The following concepts are also helpful. A representation of these concepts is given in Figure 3.3.

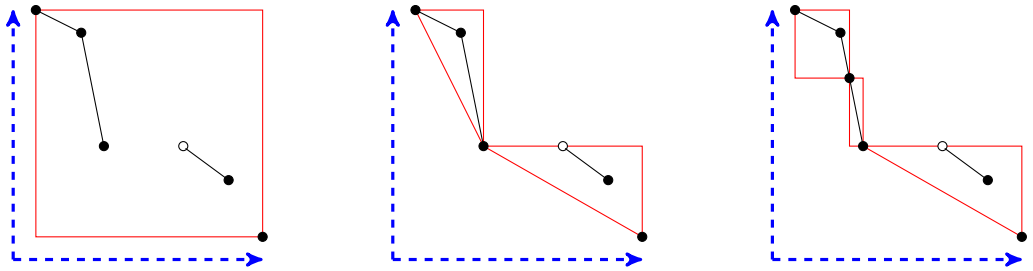

(a) Iteration 0 (b) Iteration 1 (c) Iteration 2

Figure 3.4 – Progression of TSM to discover nondominated points

Definition 9. The point $z^I \in \mathbb{R}^p$ is the *ideal point* if $z_i^I = \min_{(x,y)\in\mathcal{F}_E} z_i(x,y)$ for all $i \in \{1,\ldots,p\}$.

Definition 10. The point $z^N \in \mathbb{R}^p$ is the *nadir point* if $z_i^N = \max_{(x,y)\in\mathcal{F}_E} z_i(x,y)$ for all $i \in \{1,\ldots,p\}$.

It is also worth mentioning that the proposed formulations in this study are all bi-objective mixed integer linear programs, i.e., MOMILPs with $p = 2$. There are a few algorithms that can solve a bi-objective mixed integer linear program. In this study, we use the *triangle slitting method* (TSM), which is one of the most efficient algorithms [79]. We next present a high-level description of the algorithm.

TSM maintains a list of rectangles and right-angled triangles (in the criterion space) that need to be explored. At the beginning, this list is empty. So, TSM works by first computing the endpoints of the nondominated frontier. These two points are then used to define the first rectangle containing all the "not yet found" nondominated points, as shown in Figure 3.4a. The algorithm explores a rectangle by finding the locally extreme supported nondominated points within the rectangle. Now it can be shown that by finding these points, the rectangle can be split into a set of right-angled triangles containing all "not yet found" nondominated points, as shown further in Figure 3.4b. The algorithm explores a triangle by first checking whether its hypotenuse is part of the nondominated frontier. If that is the case, then the triangle is removed from the list, otherwise it is split into at most two other rectangles. This operation is further illustrated in Figure 3.4c, where the hypotenuse of the

top triangle in Figure 3.4b is not part of the nondominated frontier so it is split into two new rectangles. The algorithm repeats these procedures until finding a full representation of the nondominated frontier, i.e., the list of rectangles and triangles becomes empty.

3.3 The Basic Mathematical Model for Energy Storage Sharing

In this section, we develop a basic bi-objective mixed integer linear programming formulation for computing optimal operational strategies in building clusters when a single electrical energy storage is shared between two buildings with deterministic demand (see Figure 3.1). For simplicity, we assume that the electricity flow is at steady state, and cables are incapable of losing energy. However, we assume that some amount of energy may be lost while charging and discharging the electrical energy storage. Furthermore, we assume that the electrical energy storage cannot be at charging and discharging states at the same time. The main parameters and decision variables used in the basic formulation are given Tables 3.1 and 3.2.

Table 3.1 – Parameters of the basic model for energy storage sharing

$\mathcal{T}$	The index set of time periods of equal length.
$\mathcal{N}$	The index set of buildings, i.e., $\mathcal{N} := \{1, 2\}$.
L_t^i	The electricity (load) demand of Building $i \in N$ at time period $t \in \mathcal{T}$.
$\bar{E}$	The capacity of the prower grid. The total amount of energy that can be purchased from the power grid at each time period cannot be more than $\bar{E}$.
$\bar{B}$	The capacity of the electrical energy storage. The total amount of energy available at the electrical energy storage cannot be more than $\bar{B}$ at each time period.
$\underline{B}$	The buffer of the electrical energy storage. The total amount of energy available at the electrical energy storage cannot be less than $\underline{B}$ at each time period.
$\bar{C}$	The maximum amount of energy that can be charged into the electrical energy storage at a given time period if the storage is at charging state.
$\underline{C}$	The minimum amount of energy that should be charged into the electrical energy storage at a given time period if the storage is at charging state.
$\bar{D}$	The maximum amount of energy that can be discharged from the electrical energy storage at a given time period if the storage is at discharging state.
$\underline{D}$	The minimum amount of energy that should be discharged from the electrical energy storage at a given time period if the storage is at discharging state.
η^c	The charging efficiency coefficient of the electrical energy storage, i.e., $\eta^c \in (0, 1]$.
η^d	The discharging efficiency coefficient of the electrical energy storage, i.e., $\eta^d \in (0, 1]$.

Table 3.2 – Decision variables of the basic model for energy storage sharing

e_t^i	A non-negative continuous decision variable that captures the amount of electricity reaching Building $i \in \mathcal{N}$ from the power grid at time period $t \in \mathcal{T}$.
b_t^i	A non-negative continuous decision variable that captures the amount of energy that Building $i \in \mathcal{N}$ has purchased from the power grid at time period $t \in \mathcal{T}$ to be sent to the electrical energy storage. Note that $b_t^i \times \eta^c$ is the real amount of energy that will be stored in the electrical energy storage at time period $t \in \mathcal{T}$ by Building $i \in \mathcal{N}$.
d_t^i	A non-negative continuous decision variable that captures the amount of electricity reaching Building $i \in \mathcal{N}$ from the electrical energy storage at time period $t \in \mathcal{T}$. Note that $\frac{d_t^i}{\eta^d}$ is the real amount of energy discharged from the electrical energy storage by Building $i \in \mathcal{N}$ at time period $t \in \mathcal{T}$.
m_t	A non-negative continuous decision variable that captures the amount of electricity available in the electrical energy storage at time period $t \in \mathcal{T}$.
s_t^c	A binary decision variable that takes the value of one if the electrical energy storage is charging at time period $t \in \mathcal{T}$, and 0 otherwise.
s_t^d	A binary decision variable that takes the value of one if the electrical energy storage is discharging at time period $t \in \mathcal{T}$, and 0 otherwise.

The basic bi-objective mixed integer linear programming formulation can be written as,

$$\min \{z_1, z_2\} \tag{3.2}$$

$$\text{s.t.} \sum_{i \in \mathcal{N}} (e_t^i + b_t^i) \leq \bar{E} \qquad \forall t \in \mathcal{T} \tag{3.3}$$

$$e_t^i + d_t^i = L_t^i \qquad \forall i \in \mathcal{N}, \forall t \in \mathcal{T} \tag{3.4}$$

$$s_t^c + s_t^d \leq 1 \qquad \forall t \in \mathcal{T} \tag{3.5}$$

$$\underline{C} s_t^c \leq \sum_{i \in \mathcal{N}} b_t^i \eta^c \leq \bar{C} s_t^c \qquad \forall t \in \mathcal{T} \tag{3.6}$$

$$\underline{D} s_t^d \leq \sum_{i \in \mathcal{N}} \frac{d_t^i}{\eta^d} \leq \bar{D} s_t^d \qquad \forall t \in \mathcal{T} \tag{3.7}$$

$$\sum_{i \in \mathcal{N}} b_t^i \eta^c - \sum_{i \in \mathcal{N}} \frac{d_t^i}{\eta^d} = m_t - m_{t-1} \qquad \forall t \in \mathcal{T} \tag{3.8}$$

$$\underline{B} \leq m_t \leq \bar{B} \qquad \forall t \in \mathcal{T} \tag{3.9}$$

$$e_t^i, b_t^i, d_t^i, m_t \geq 0 \qquad i \in \mathcal{N}, t \in \mathcal{T} \tag{3.10}$$

$$s_t^c, s_t^d \in \{0, 1\} \qquad t \in \mathcal{T}, \tag{3.11}$$

where z_1 is the objective function of the first building and z_2 is the objective function of the second building. We will discuss about these functions in Section 3.4. Constraints (3.3) ensure that the amount of electricity purchased from the power gird is restricted by the

capacity of the power grid at each time period. Constraints (3.4) guarantee that the total amount of electricity purchased from the power grid and also discharged from the electrical energy storage will cover the total electricity load of each building at each time period. Constraints (3.5) ensure that the state of the electrical energy storage cannot be charging and discharging at the same time. Constraints (3.6) and (3.7) ensure that the amount of energy charged and/or discharged from the electrical energy storage is within the allowed range at any time period. Constraints (3.8) impose the energy conservation in the electrical energy storage at any time period. Finally, Constraints (3.9) ensure that the amount of energy available at the electrical energy storage is within the allowed range at any time period. Note that, for simplicity, we assume that

$$m_0 = m_{|T|} = \underline{B}. \tag{3.12}$$

So, this should also be added to the formulation.

3.4 The Trade-off Between Fairness and Freedom

As it is mentioned in the introduction, we assume that each building is an independent decision maker that wants to minimize its own total cost. However, the shared electrical energy storage introduces two further considerations, i.e., fairness and freedom. Three different energy storage sharing strategies are introduced in this section to deal with the trade-off between fairness and freedom. We show how the basic formulation presented in Section 3.3 can be customized for each of these strategies.

For the sake of clarification, we note that in this study, we sometimes use the terms such as "balance", "steady" and "stable" that are well-defined in other fields, in particular Game Theory. However, in this study, only informal interpretations of these terms are considered. In particular, “balance" is used for a strategy which is between extreme free and

extreme fair strategies. “Steady" and "stable" are used for strategies or solutions that are expected to last for a long period of time.

3.4.1 Extreme Free Strategy

In this strategy, there is no restriction on using the electrical energy storage for any building at any time. So, the bi-objective formulation corresponding to this strategy is precisely the basic formulation defined by (3.2)-(3.12). Also, in this strategy, the objective function of Building $i \in \mathcal{N}$ (which is its total operational cost) can be defined as,

$$z_i := \sum_{t \in \mathcal{T}} r_t^i (e_t^i + b_t^i), \tag{3.13}$$

where r_t^i is the unit price of buying electricity from the power grid at time period $t \in T$ for building $i \in \mathcal{N}$. It is evident that the nondominated frontier of this bi-objective optimization problem is appealing for both buildings in term of cost savings. However, it is not interesting in terms of fairness since each building can use the electrical energy storage without taking into account that maybe the other building has paid the cost of available energy in the storage. So, any collaboration under this strategy does not seem to be stable.

3.4.2 Extreme Fair Strategy

In this strategy, each building discharges exactly the same amount of energy that it charges into the electrical energy storage in the entire planning horizon. The bi-objective formulation corresponding to this strategy is similar to the extreme free strategy but for each building $i \in \mathcal{N}$ the following additional constraint should be added,

$$\sum_{t \in \mathcal{T}} b_t^i \eta^c = \sum_{t \in \mathcal{T}} \frac{d_t^i}{\eta^d}. \tag{3.14}$$

It is evident that the nondominated frontier of this bi-objective optimization problem is appealing for both buildings in term of fairness. So, any collaboration under this strat-

egy seems to be quite stable. However, we observe that buildings (significantly) lose their flexibility in using the electrical energy storage under this strategy. So, we can expect that the nondominated frontier of this bi-objective optimization problem to be significantly less attractive in terms of cost savings for buildings. Note that the nondominated frontier of this strategy is not necessarily a single point since buildings still have the opportunity to take advantage of the energy storage to reduce their costs.

3.4.3 Contract Balance Strategy

For each building $i \in \mathcal{N}$, we define

$$g^i = \sum_{t \in \mathcal{T}} b_t^i - \frac{d_t^i}{\eta^c \eta^d}. \tag{3.15}$$

Observe that $g^i = 0$ is basically the additional constraint that we added to the model for Building i in the extreme fair strategy. So, by using this observation, g^i is simply the amount of energy that Building $i \in \mathcal{N}$ has purchased from the power grid in the entire planning horizon to charge the electrical energy storage, but was not able to use it. Note that we have assumed that $m_0 = m_{|T|} = \underline{B}$. Therefore, if a building charges some amount of energy into the storage and does not use it (in the entire planning horizon) then it must have been used by the other building. Observe too that since there are only two buildings, we must have that $g^1 = -g^2$.

By using this definition, in this strategy, if $g^i > 0$ for Building $i \in \mathcal{N}$ then the other building will be penalized. The penalty is basically the cost that has to be paid to Building i by Building $i' \in N \backslash \{i\}$. We assume that the penalty is equal to $\bar{r}^i g^i$ where

$$\sum_{t \in \mathcal{T}} r_t^i b_t^i = \bar{r}^i \sum_{t \in \mathcal{T}} b_t^i. \tag{3.16}$$

So, $\bar{r}^i$ is basically the average unit price of electricity that Building i has purchased from the power grid to charge the electrical energy storage in the entire planning horizon.

So, $\bar{r}^i g^i$ can be interpreted as the refund to Building i for the amount of energy that it has purchased but was not able to use. Consequently, the bi-objective formulation of the contract balance strategy is as follows,

$$\min\ z_1 := \sum_{t\in\mathcal{T}} r_t^1(e_t^1 + b_t^1) - \max\{\bar{r}^1 g^1, 0\} + \max\{\bar{r}^2 g^2, 0\} \tag{3.17}$$

$$\min\ z_2 := \sum_{t\in\mathcal{T}} r_t^2(e_t^2 + b_t^2) - \max\{\bar{r}^2 g^2, 0\} + \max\{\bar{r}^1 g^1, 0\} \tag{3.18}$$

$$\text{s.t. } (3.3) - (3.12), (3.15), (3.16)$$

$$g^1, g^2 \in \mathbb{R} \tag{3.19}$$

$$\bar{r}^1, \bar{r}^2 \geq 0. \tag{3.20}$$

Note that this formulation contains some nonlinear terms in the objective functions and Constraints (3.16).

3.5 Linearizing the Formulation of Contract Balance Strategy

Note that to best of our knowledge, there is no exact solver for bi-objective mixed integer non-linear programs. Consequently, to be able to use the power of TSM, we next explain how the bi-objective formulation of the contract balance strategy can be efficiently linearized (with high level of precision).

3.5.1 Removing the Max Functions in the Objective Functions

In the objective functions, there are two max functions. Removing these functions can be done easily by introducing two new non-negative continuous variables, i.e., $\hat{g}^1$, $\hat{g}^2$, one binary variable, i.e., $\bar{y} \in \{0, 1\}$, and a few additional constraints. So, objective functions (3.17) and (3.18) should be replaced by

$$\min\ z_1 := \sum_{t\in\mathcal{T}} r_t^1(e_t^1 + b_t^1) - \bar{r}^1 \hat{g}^1 + \bar{r}^2 \hat{g}^2 \tag{3.21}$$

$$\min\ z_2 := \sum_{t\in\mathcal{T}} r_t^2(e_t^2 + b_t^2) - \bar{r}^2\hat{g}^2 + \bar{r}^1\hat{g}^1 \tag{3.22}$$

$$\text{s.t. } g^1 \le \hat{g}^1 \tag{3.23}$$

$$\hat{g}^1 \le M\bar{y} \tag{3.24}$$

$$\hat{g}^1 \le g^1 + M(1-\bar{y}) \tag{3.25}$$

$$g^2 \le \hat{g}^2 \tag{3.26}$$

$$\hat{g}^2 \le M(1-\bar{y}) \tag{3.27}$$

$$\hat{g}^2 \le g^2 + M\bar{y} \tag{3.28}$$

$$\hat{g}^1, \hat{g}^2 \ge 0 \tag{3.29}$$

$$\bar{y} \in \{0,1\}, \tag{3.30}$$

where M is a sufficiently large value. The additional constraints ensure that $\hat{g}^1 = \max\{0, g^1\}$ and $\hat{g}^2 = \max\{0, g^2\}$. Furthermore, we know that $g^1 = -g^2$. Hence, either $\hat{g}^1 = 0$ or $\hat{g}^2 = 0$ (or both). This observation is captured by introducing the new binary decision variable, i.e., $\bar{y}$. Observe that if $\bar{y} = 0$ then $\hat{g}^1 = 0$ (and $\hat{g}^2 = g^2$), and also if $\bar{y} = 1$ then $\hat{g}^2 = 0$ (and $\hat{g}^1 = g^1$).

3.5.2 Linearizing Bi-linear Terms

Although we were able to remove the max functions in both objective functions, there are still multiple bi-linear terms in both objective functions (3.21) and (3.22), and Constraints (3.16) including $\bar{r}^i\hat{g}^i$ for each $i \in \mathcal{N}$, and $\bar{r}^i b_t^i$ for each $i \in \mathcal{N}$ and $t \in \mathcal{T}$.

A widely used approach to linearize (continuous) bi-linear terms when a lower bound and an upper bound are known for each variable in the bi-linear term is McCormick relaxation [80]. Suppose that we would like to linearize the bi-linear term x_1x_2 where we know that $x_1^L \le x_1 \le x_1^U$ and $x_2^L \le x_2 \le x_2^U$. In McCormick relaxation, any instance of x_1x_2 will be replaced by a new variable, denoted by w, and the following additional linear constraints

(sometimes referred to as McCormick envelopes) should be added to the model,

$$
\begin{aligned}
& w \geq x_1^L x_2 + x_1 x_2^L - x_1^L x_2^L \\
& w \geq x_1^U x_2 + x_1 x_2^U - x_1^U x_2^U \\
& w \leq x_1^U x_2 + x_1 x_2^L - x_1^U x_2^L \\
& w \leq x_1^L x_2 + x_1 x_2^U - x_1^L x_2^U \\
& w \in \mathbb{R}.
\end{aligned}
$$

To increase the accuracy of the standard McCormick relaxation, we can partition the domain of the variables to obtain a tighter relaxation. In this case, a new set of binary variables should be introduced to make sure that only one of the generated search regions is active at any time. This is known as piecewise McCormick relaxation [81]. For example, by partitioning the domain of x_1 into 3 pieces, and the domain of x_2 into 4 pieces a total of $3 \times 4 = 12$ search regions will be constructed. Consequently, 12 sets of McCormick envelopes should be added to the formulation. Also, 12 new binary variables should be introduced, and we need to make sure that only one of these 12 search regions is active at anytime. So, we observe that piecewise McCormick relaxation can significantly increase the size of the formulation. Figure 3.5 shows the co-occurrence graph for bi-linear terms

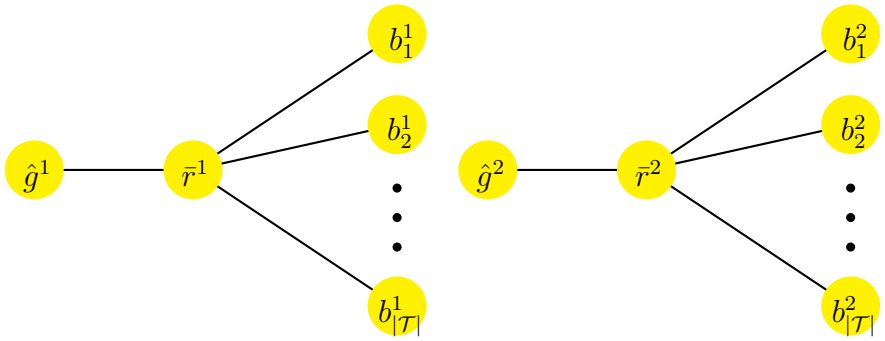

Figure 3.5 – Co-occurrence graph for bi-linear terms

in the (revised) formulation of the contract balance strategy. In this graph nodes represent decision variables, and links represent the existence of corresponding bi-linear terms in the

formulation. We observe that in all bi-linear terms either $\bar{r}^1$ or $\bar{r}^2$ exist. That implies that to obtain tighter relaxations, we may only partition the domain of these two variables. By considering this observation, we next linearize all bi-linear terms of the formulation by using piecewise McCormick relaxation.

We first note that:

- $b_t^i \in [\underline{A}, \bar{A}]$ for all $i \in \mathcal{N}$ and $t \in \mathcal{T}$ where $\underline{A} := 0$ and $\bar{A} := \frac{\bar{C}}{\eta^c}$. This is obtained from the fact that if $s_t^c = 0$ then $b_t^i = 0$ and if $s_t^c = 1$ then $b_t^i \in [\frac{\underline{C}}{\eta^c}, \frac{\bar{C}}{\eta^c}]$.
- $\bar{r}^i \in [\underline{R}, \bar{R}]$ for all $i \in \mathcal{N}$ where $\underline{R} := \min\{r_t^i : i \in \mathcal{N}, t \in \mathcal{T}\}$ and $\bar{R} := \max\{r_t^i : i \in \mathcal{N}, t \in \mathcal{T}\}$.
- $\hat{g}^i \in [\underline{G}, \bar{G}]$ for all $i \in \mathcal{N}$ where $\underline{G} := 0$ and $\bar{G} := \frac{|\mathcal{T}| \max\{\frac{\bar{C}}{\eta^c}, \frac{\bar{D}}{\eta^c}\}}{2}$. The latter, i.e., the upper bound, can be obtained by assuming that one building only charges the electrical energy storage and the other only discharges. So, given that the storage cannot be at the charging and discharging states at the same time, the result follows.

We assume that the domain of $\bar{r}^1$ and $\bar{r}^2$, i.e., $[\underline{R}, \bar{R}]$, has to be partitioned into K equal pieces. Consequently, for each $k = 1, \ldots, K$, we define

$$\underline{R}_k^i := \underline{R}^i + \frac{(\bar{R}^i - \underline{R}^i)(k-1)}{K} \qquad \forall i \in \mathcal{N}$$
$$\bar{R}_k^i := \underline{R}^i + \frac{(\bar{R}^i - \underline{R}^i)k}{K} \qquad \forall i \in \mathcal{N}.$$

By using theses parameters, and applying piecewise McCormick relaxation, the bi-objective mixed integer linear programming formulation of the proposed contract balance strategy is as follows,

$$\min \; z_1 := \sum_{t \in \mathcal{T}} r_t^1 (e_t^1 + b_t^1) - v^1 + v^2 \tag{3.31}$$

$$\min \; z_2 := \sum_{t \in \mathcal{T}} r_t^2 (e_t^2 + b_t^2) - v^2 + v^1 \tag{3.32}$$

s.t. $(3.3)-(3.12), (3.15), (3.19), (3.23)-(3.30)$

$$\sum_{t\in\mathcal{T}} r_t^i b_t^i = \sum_{t\in\mathcal{T}} w_t^i \qquad \forall i \in \mathcal{N} \tag{3.33}$$

$$\hat{g}^i = \sum_{k=1}^{K} \hat{g}_k^i \qquad \forall i \in \mathcal{N} \tag{3.34}$$

$$b_t^i = \sum_{k=1}^{K} b_{tk}^i \qquad \forall i \in \mathcal{N}, \forall t \in \mathcal{T} \tag{3.35}$$

$$\sum_{k=1}^{K} y_k^i = 1 \qquad \forall i \in \mathcal{N} \tag{3.36}$$

$$y_k^i \underline{R}_k^i \leq \bar{r}_k^i \leq y_k^i \bar{R}_k^i \qquad \forall i \in \mathcal{N}, \forall k \in \{1,\ldots,K\} \tag{3.37}$$

$$y_k^i \underline{G} \leq \hat{g}_k^i \leq y_k^i \bar{G} \qquad \forall i \in \mathcal{N}, \forall k \in \{1,\ldots,K\} \tag{3.38}$$

$$y_k^i \frac{\underline{C}}{\eta^c} \leq b_{tk}^i \leq y_k^i \frac{\bar{C}}{\eta^c} \qquad \forall i \in \mathcal{N}, \forall t \in \mathcal{T}, \forall k \in \{1,\ldots,K\} \tag{3.39}$$

$$v^i \geq \sum_{k=1}^{K} (\underline{R}_k^i \hat{g}_k^i + \bar{r}_k^i \underline{G} - y_k^i \underline{R}_k^i \underline{G}) \qquad \forall i \in \mathcal{N} \tag{3.40}$$

$$v^i \geq \sum_{k=1}^{K} (\bar{R}_k^i \hat{g}_k^i + \bar{r}_k^i \bar{G} - y_k^i \bar{R}_k^i \bar{G}) \qquad \forall i \in \mathcal{N} \tag{3.41}$$

$$v^i \leq \sum_{k=1}^{K} (\bar{R}_k^i \hat{g}_k^i + \bar{r}_k^i \underline{G} - y_k^i \bar{R}_k^i \underline{G}) \qquad \forall i \in \mathcal{N} \tag{3.42}$$

$$v^i \leq \sum_{k=1}^{K} (\underline{R}_k^i \hat{g}_k^i + \bar{r}_k^i \bar{G} - y_k^i \underline{R}_k^i \bar{G}) \qquad \forall i \in \mathcal{N} \tag{3.43}$$

$$w_t^i \geq \sum_{k=1}^{K} (\underline{R}_k^i b_{tk}^i + \bar{r}_k^i \underline{A} - y_k^i \underline{R}_k^i \underline{A}) \qquad \forall i \in \mathcal{N}, \forall t \in \mathcal{T} \tag{3.44}$$

$$w_t^i \geq \sum_{k=1}^{K} (\bar{R}_k^i b_{tk}^i + \bar{r}_k^i \bar{A} - y_k^i \bar{R}_k^i \bar{A}) \qquad \forall i \in \mathcal{N}, \forall t \in \mathcal{T} \tag{3.45}$$

$$w_t^i \leq \sum_{k=1}^{K} (\bar{R}_k^i b_{tk}^i + \bar{r}_k^i \underline{A} - y_k^i \bar{R}_k^i \underline{A}) \qquad \forall i \in \mathcal{N}, \forall t \in \mathcal{T} \tag{3.46}$$

$$w_t^i \leq \sum_{k=1}^{K} (\underline{R}_k^i b_{tk}^i + \bar{r}_k^i \bar{A} - y_k^i \underline{R}_k^i \bar{A}) \qquad \forall i \in \mathcal{N}, \forall t \in \mathcal{T} \tag{3.47}$$

$$v^i, w^i_t, \hat{g}^i_k, \bar{r}^i_k, b^i_{tk} \geq 0 \qquad \forall i \in \mathcal{N}, \forall t \in \mathcal{T}, \forall k \in \{1, \ldots, K\} \tag{3.48}$$

$$y^i_k \in \{0, 1\} \qquad \forall i \in \mathcal{N}, \forall k \in \{1, \ldots, K\}, \tag{3.49}$$

where v^1 and v^2 are non-negative continuous variables to (approximately) capture the value of $\hat{r}^1\hat{g}^1$ and $\hat{r}^1\hat{g}^2$ respectively. Also, w^i_t for each $i \in \mathcal{N}$ and $t \in \mathcal{T}$ is a non-negative continuous variable to approximately capture the value of $\bar{r}^i b^i_t$. Constraints (3.33) are replacements of Constraints (3.16). Note that the domain of $\bar{r}^1$ and $\bar{r}^2$ are partitioned into K pieces. So, we also split the decision variables $\bar{r}^i$, $\hat{g}^i$, and b^i_t for each $i \in \mathcal{N}$ and $t \in \mathcal{T}$ into K new pieces by introducing three sets of non-negative continuous variables. Constraints (3.34) and Constraints (3.35) ensure that the value of $\hat{g}^i$ and/or b^i_t for each $i \in \mathcal{N}$ and $t \in \mathcal{T}$ can be obtained by adding up values of the corresponding K new decision variables. Note that there is no need to add any constraint of the form $\bar{r}^i = \sum_{k=1}^{K} \bar{r}^i_k$ since $\bar{r}^i$ is not used in this formulation. Again since the domain of $\bar{r}^i$ where $t \in \mathcal{N}$ is partitioned into K pieces, we introduce K binary variables, denoted by $y^i_1, \ldots, y^i_K$, for activating/deactivating the search regions/pieces. In particular, Constraints (3.36) to (3.39) ensure that exactly one piece is active at anytime. They also guarantee that if $y^i_k = 1$ for some $i \in \mathcal{N}$ and $k \in \{1, \ldots, K\}$, then we must have that $\bar{r}^i_{k'} = \hat{g}^i_{k'} = b^i_{tk'} = 0$ for all $k' \neq k$. Finally, Constraints (3.40) to (3.47) are simply McCormick envelopes to capture the value of v^i and w^i_t for each $i \in \mathcal{N}$ and $t \in \mathcal{T}$. Note that we know that the total operational cost of Building $i \in \mathcal{N}$ cannot be smaller than $\sum_{t \in \mathcal{T}} \underline{R}L^i_t$. Consequently, to improve the formulation, we suggest to add the following valid inequalities as well,

$$\sum_{t \in \mathcal{T}} r^1_t (e^1_t + b^1_t) - v^1 + v^2 \geq \sum_{t \in \mathcal{T}} \underline{R}L^1_t \tag{3.50}$$

$$\sum_{t \in \mathcal{T}} r^2_t (e^2_t + b^2_t) - v^2 + v^1 \geq \sum_{t \in \mathcal{T}} \underline{R}L^2_t. \tag{3.51}$$

3.6 Computational Results

To evaluate the performance of the extreme free, extreme fair, and contract balance strategies, we conducted a comprehensive computational study. We used C++ to implement all formulations, and employed TSM to exactly solve each instance. In this computational study, TSM uses CPLEX 12.7 as the single-objective integer programming solver. All computational experiments have been carried out on a Dell PowerEdge R630 with two Intel Xeon E5-2650 2.2 GHz 12-Core Processors (30MB), 128GB RAM, and the RedHat Enterprise Linux 6.8 operating system, and using a single thread.

We assumed that each time period represents one hour, and the entire planning horizon contains 24 hours, i.e., $|\mathcal{T}| = 24$. Based on this assumption, we generated 100 instances by randomly drawing r_t^i and L_t^i for each $i \in \mathcal{N}$ and $T \in \mathcal{T}$ from a discrete uniform distribution on the interval $[1, 20]$. Obviously, in this case, the demand load of each building at any time cannot be more than 20. So, since there are two buildings, we simply assume that $\bar{B} = 2 \times 20 = 40$, and $\underline{B} = 1$ for each instance. Furthermore, we assume that $\bar{C} = \bar{D} = 0.2 \times \bar{B}$ and $\underline{C} = \underline{D} = 0.05 \times \bar{B}$. It is also worth mentioning that the value of M can be safely set to $\bar{G} + 1$ (by definition).

This computational study has three sections to achieve the following three goals:

- Demonstrating the performance of the proposed piecewise McCormick relaxation (for the contract balance strategy) and choosing a proper value for the number of pieces, i.e., K.

- Comparing the extreme free, extreme fair strategy, and contract balance strategies in terms of fairness and freedom.

- Showing the performance of the proposed formulation for the contract balance strategy when the goal is to compute an approximate nondominated frontier.

3.6.1 Performance of the Piecewise McCormick Relaxation

We first note that after computing any feasible solution for the proposed piecewise McCormick relaxation, it is easy to compute the precise value of $\bar{r}^1$, $\bar{r}^2$. It is evident that, if the value of $\bar{r}^i\hat{g}^i$ is close to v^i for each $i \in \mathcal{N}$, then the quality of the (approximate) solution is good. So, by using this observation, for any feasible solution of the proposed piecewise McCormick relaxation, the following formula measures its quality,

$$\max\{|\frac{100(\bar{r}^i\hat{g}^i - v^i)}{\bar{r}^i\hat{g}^i + 0.001}| : i \in \mathcal{N}\}.$$

Note that we are only interested in efficient solutions, but there may be an infinite number of efficient solutions corresponding to the proposed piecewise McCormick relaxation. So, we cannot compute the proposed quality gap for all efficient solutions. So, instead, we compute the proposed gap for only two feasible solutions including:

- Solution 1: The optimal solution obtained by minimizing only the first objective function in the proposed piecewise McCormick relaxation.
- Solution 2: The optimal solution obtained by minimizing only the second objective function in the proposed piecewise McCormick relaxation.

In Figure 3.6, we have reported the worst quality gap obtained among these two solutions for all instances and for different values of K. Observe that the proposed quality gap decreases dramatically by increasing the value of K. For example, the quality gap of Instance 30 is decreased from around 300% to 50% by increasing the value of K from 1 to only 16.

In Figure 3.7, the average quality gap of Solution 1 and its average computing time among all instances for different values of K are given. Not surprisingly, the cost of computing better approximation is a dramatic increase in the solution time. We also observe that

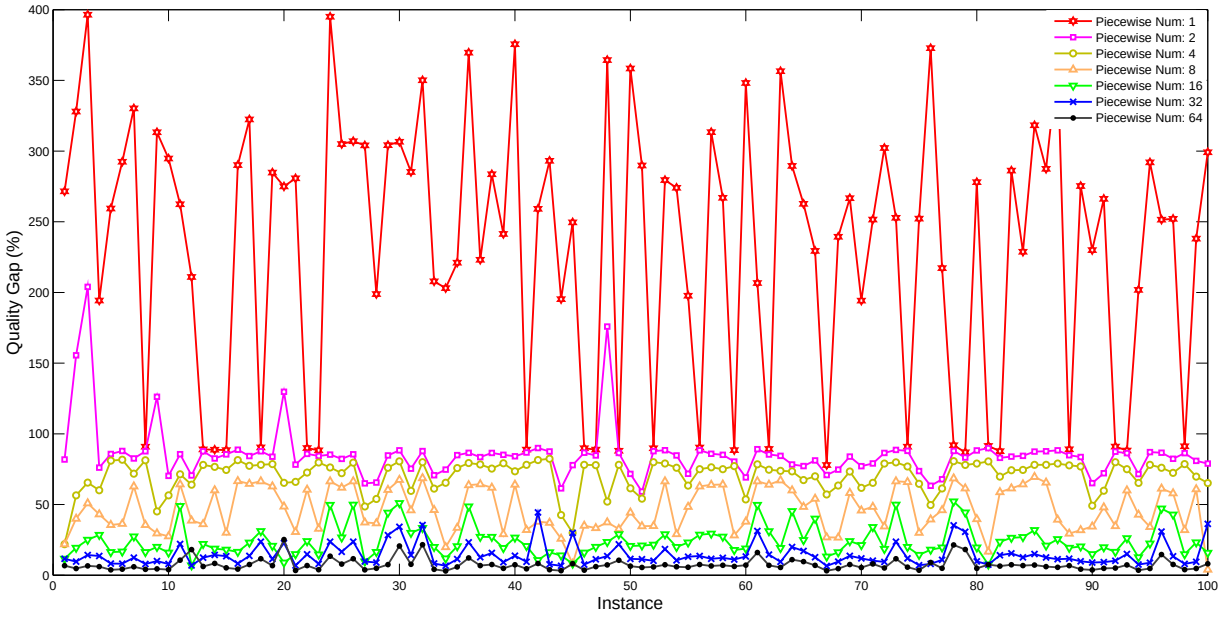

Figure 3.6 – Quality gap of each instance for different values of K

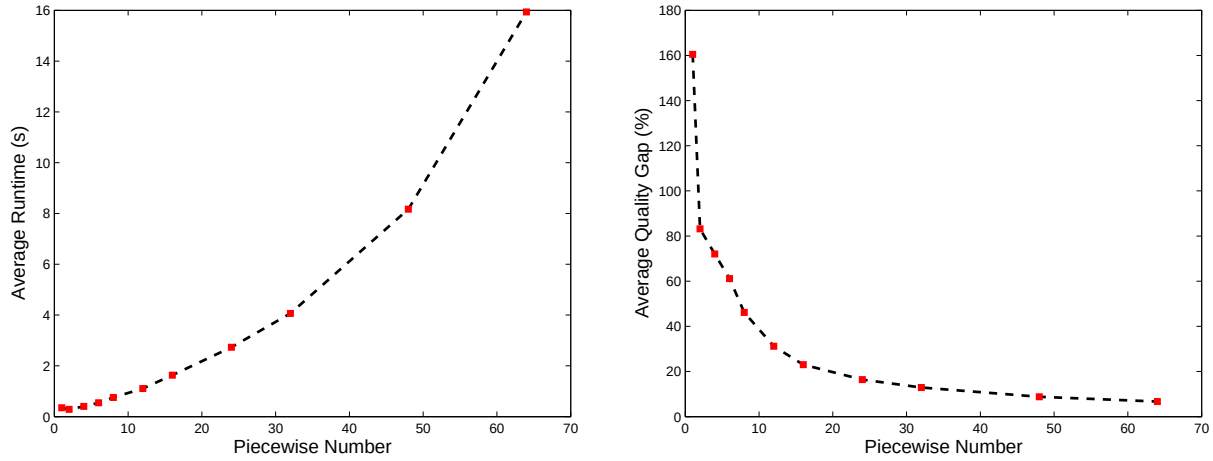

(a) Run time

(b) Quality gap

Figure 3.7 – Piecewise McCormick relaxation using different values of K

$K = 32$ seems to have a reasonable balance between solution time and the quality gap. So, for most of our experiments we will set $K = 32$.

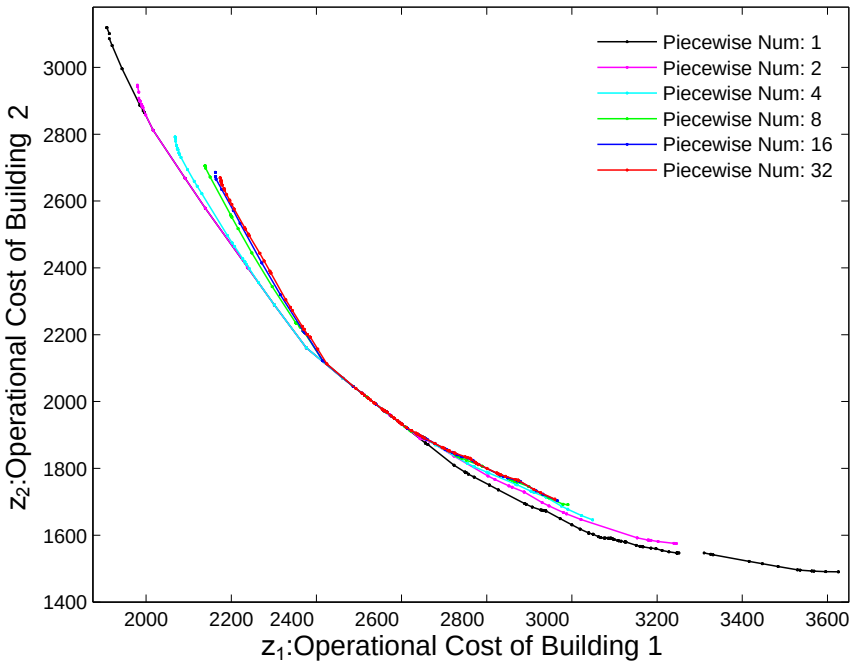

Figure 3.8 – The nondominated frontier for different values of K

The nondominated frontier of the proposed piecewise McCormick relaxation for different values of K on one of the instances are shown in Figure 3.8. Not surprisingly, increasing the value of K is causing a shift in the nondominated frontier toward increasing both objective values, i.e., the frontier is moved away from the origin. This is mainly because by increasing the value of K, a tighter relaxation will be obtained. Consequently, the top endpoint of the nondominated frontier may be shifted since the minimum possible cost of Building 1 cannot decrease using a tighter relaxation. Similarly the bottom endpoint of nondominated frontier may be shifted since the minimum possible cost of Building 2 cannot decrease using a tighter relaxation. We also observe that the nondominated frontier has almost reached to its steady state for $K = 32$, i.e., not much has changed between $K = 16$ and $K = 32$.

3.6.2 Fairness vs Freedom

In this section, we develop a technique to evaluate the freedom and fairness of an energy storage sharing strategy. We then demonstrate the effectiveness of the proposed contract balance strategy in contrast to the extreme free and fair strategies. The following Theorem and its corollary are helpful.

Theorem 11. Let $z^{1T}, z^{1B} \in \mathbb{R}^2$, $z^{2T}, z^{2B} \in \mathbb{R}^2$, and $z^{3T}, z^{3B} \in \mathbb{R}^2$ be the top and bottom endpoints of the nondominated frontier of the extreme free, contract balance, and extreme fair strategies, respectively. If $z_1^{2T} \neq z_1^{3T}$ and $z_2^{2B} \neq z_2^{3B}$ then

(i) $z_1^{1T} \leq z_1^{2T} \leq z_1^{3T}$ and $z_2^{1T} \geq z_2^{2T} \geq z_2^{3T}$;

(ii) $z_1^{1B} \geq z_1^{2B} \geq z_1^{3B}$ and $z_2^{1B} \leq z_2^{2B} \leq z_2^{3B}$.

The correctness of (i) in Theorem 11 can be obtained from the following two propositions.

Proposition 12. $z_1^{1T} \leq z_1^{2T}$ and $z_2^{1T} \geq z_2^{2T}$.

Proof. Let x^{2T} be a feasible solution corresponding to z^{2T} in the contract balance strategy. Evidently, by construction, x^{2T} must be feasible for the extreme free strategy. So, we must have $z_1^{1T} \leq z_1^{2T}$ because of two reasons. (1) By definition, the top endpoint of a nondominated frontier has the minimum possible cost for Building 1; (2) In the extreme free strategy, Building 1 does not pay for the (extra) energy arbitrage that Building 2 can provide to it. Therefore, in the rest of the proof, we only need to show that $z_2^{1T} \geq z_2^{2T}$. We prove this part by contradiction. Hence, suppose that $z_2^{1T} < z_2^{2T}$. This immediately implies that Building 1 has provided (extra) energy arbitrage to Building 2 (in the extreme free strategy). However, in the extreme free strategy, Building 2 does not pay to the other building. Consequently, Building 1 has only increased its costs by helping Building 2 and consequently, this contradicts the fact that the top endpoint of the nondominated frontier of the extreme free strategy should have the minimum possible cost for Building 1 (for that strategy). □

Proposition 13. If $z_1^{2T} \neq z_1^{3T}$ then $z_1^{2T} \leq z_1^{3T}$ and $z_2^{2T} \geq z_2^{3T}$.

Proof. Let x^{3T} be a feasible solution corresponding to z^{3T} in the extreme fair strategy. Evidently, by construction, x^{3T} must be feasible for the contract balance strategy. So, we must have $z_1^{2T} \leq z_1^{3T}$ because of two reasons. (1) By definition, the top endpoint of a nondominated frontier has the minimum possible cost for Building 1; (2) In the contract balance strategy, Building 2 can sell (extra) energy arbitrage (without making any profit or loss) to Building 1, and so Building 1 can take advantage of this opportunity if it is financially worth it. Therefore, in the rest of the proof, we only need to show that $z_2^{2T} \geq z_2^{3T}$. We prove this part by contradiction. Hence, suppose that $z_2^{2T} < z_2^{3T}$. This immediately implies that Building 1 has sold (extra) energy arbitrage (without making any profit or loss) to Building 2 (in the contract balance strategy), i.e., $v_1 > 0$ and so we must have $v_2 = 0$. Consequently, since Building 1 has not made any profit or loss by selling energy arbitrage to Building 2, we must have $z_1^{2T} = z_1^{3T}$ (a contradiction). □

The correctness of (ii) in Theorem 11 can be obtained from the following two propositions.

Proposition 14. $z_2^{1B} \leq z_2^{2B}$ and $z_1^{1B} \geq z_1^{2B}$.

Proof. Similar to the proof of Proposition 12. □

Proposition 15. If $z_2^{2B} \neq z_2^{3B}$ then $z_2^{2B} \leq z_2^{3B}$ and $z_1^{2B} \geq z_1^{3B}$.

Proof. Similar to the proof of Proposition 13. □

Corollary 16. If $z_1^{2T} \neq z_1^{3T}$ and $z_2^{2B} \neq z_2^{3B}$ then

- The ideal point of the nondominated frontier corresponding to the extreme free strategy provides a lower bound for the ideal points of other strategies;
- The nadir point of the nondominated frontier corresponding to the extreme free strategy provides an upper bound for the nadir points of other strategies;

- The nadir point of the nondominated frontier corresponding to the extreme fair strategy provides a lower bound for the nadir points of other strategies;
- The ideal point of the nondominated frontier corresponding to the extreme fair strategy provides an upper bound for the nadir points of other strategies.

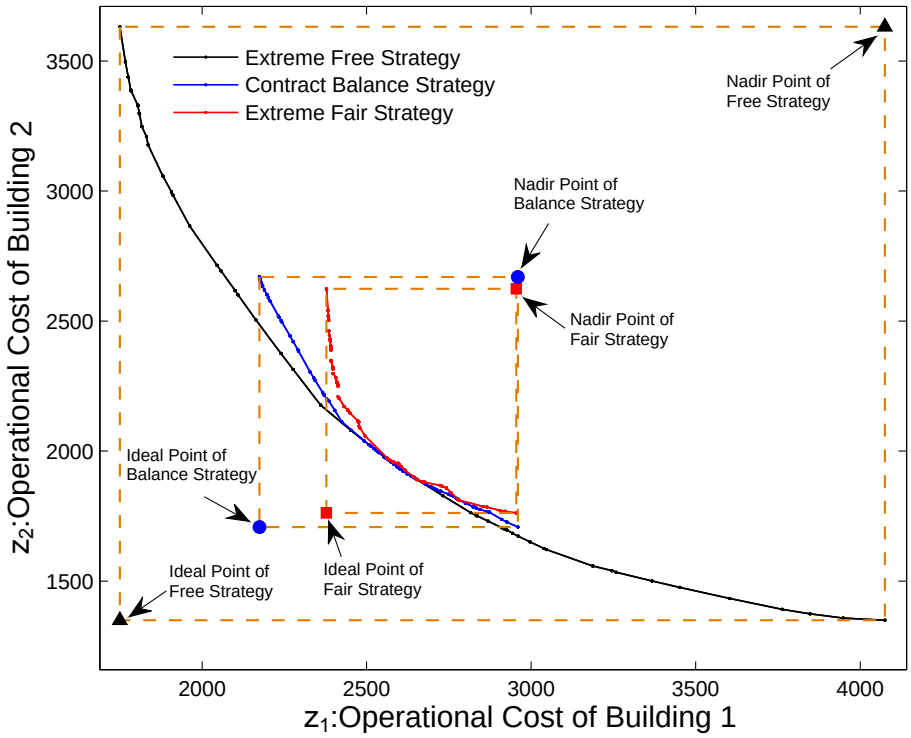

Figure 3.9 – Nondominated frontiers of different strategies

Figure 3.9 shows the nondominated frontier of all three strategies for one of the instances. The correctness of this theorem and its corollary can be clearly seen in this figure.

It is worth mentioning that for all our test instances, we observed that $z_1^{2T} \neq z_1^{3T}$ and $z_2^{2B} \neq z_2^{3B}$. So, in the rest of this section, we assume that $z_1^{2T} \neq z_1^{3T}$ and $z_2^{2B} \neq z_2^{3B}$. By using Corollary 16, the *degree of freedom* of an energy storage sharing strategy can be defined as the Euclidean distance between the ideal point of its nondominated frontier and the ideal point of the nondominated frontier of the extreme free strategy. Note that smaller distances imply higher freedom (i.e., more cost savings). Similarly, the *degree of fairness* of an energy

storage sharing strategy can be defined as the Euclidean distance between the nadir point of its nondominated frontier and the nadir point of the nondominated frontier of the extreme fair strategy. Note that again smaller distances imply higher fairness.

Let s^1, s^2, and s^3 represent the extreme free, cost balance, and extreme fair strategies, respectively. Also, let $I(s)$ and $N(s)$ be the degree of freedom and the degree of fairness of strategy s, respectively. It is worth mentioning that by Theorem 11, we assure that $I(s^3)$ to be larger than $I(s^2)$. Note that $I(s^1) = 0$. Also, by Theorem 11, we assure that $N(s^1)$ to be larger than $N(s^2)$. Note that $N(s^3) = 0$. So, we define

$$G^I(s^2) = \frac{100\big(I(s^3) - I(s^2)\big)}{I(s^3)},$$

and

$$G^N(s^2) = \frac{100\big(N(s^1) - N(s^2)\big)}{N(s^1)}.$$

By these definitions, $G^I(s^2)$ indicates the improvement percentage of the contract balance strategy in terms of freedom compared to the extreme fair strategy. Similarly, $G^N(s^2)$ indicates the improvement percentage of the contract balance strategy in terms of fairness compared to the extreme free strategy.

In Tables 3.3 and 3.4, we compare the proposed contract balance strategy with the extreme free and fair strategies for all instances. Observe that the contract balance strategy is around 24% better than the extreme fair strategy in terms of freedom on average. Also, it is around 92% better than the extreme free strategy in terms of fairness. So, the contract balance strategy is almost as fair as the extreme fair strategy. This implies that any collaboration based on this strategy should be quite stable too. Furthermore, compared to the extreme fair strategy, buildings can expect to save more costs because the contract balance strategy is significantly better in terms of freedom.

Table 3.3 – Strategies comparison (Instances 1-50)

Instance	Extreme Free		Extreme Fair		Contract Balance					
					$K = 16$			$K = 32$		
	Time(s.)	$N(s^1)$	Time(s)	$I(s^3)$	Time(s.)	$G^N(s^2)$	$G^I(s^2)$	Time(s.)	$G^N(s^2)$	$G^I(s^2)$
1	4.3	1,367.1	4.4	835.2	208.3	97.7%	32.2%	758.8	97.9%	31.9%
2	3.4	1,549.1	4.2	811.5	266.4	90.9%	40.2%	1,067.0	92.3%	38.4%
3	3.2	1,573.3	7.7	887.5	263.8	86.5%	43.6%	1,595.6	87.9%	42.8%
4	3.9	1,524.1	5.5	881.1	164.6	95.1%	24.9%	806.3	96.0%	23.0%
5	4.2	1,204.7	8.3	640.9	285.8	94.0%	14.5%	1,930.2	92.6%	11.7%
6	4.7	1,351.2	8.7	759.2	209.0	97.7%	26.1%	981.6	98.8%	23.3%
7	3.2	1,287.1	4.6	555.5	226.6	94.2%	28.8%	1,221.6	95.5%	25.6%
8	2.7	1,995.5	3.1	1,007.1	306.7	90.2%	19.4%	1,635.0	91.2%	17.5%
9	3.7	1,406.8	4.4	988.0	163.2	94.5%	34.3%	1,086.0	95.5%	32.9%
10	4.2	1,582.8	2.7	963.4	133.2	94.2%	28.6%	530.7	95.2%	26.9%
11	5.1	1,482.6	7.5	609.0	221.4	96.8%	26.2%	807.3	97.0%	24.0%
12	4.5	1,490.4	2.7	930.7	382.9	92.3%	20.9%	2,340.1	93.3%	19.5%
13	5.5	1,481.1	3.6	903.3	98.4	86.4%	26.8%	637.2	87.3%	25.1%
14	4.9	1,535.6	4.6	659.0	356.9	82.9%	32.9%	2,026.6	82.9%	30.4%
15	4.8	1,608.9	5.5	755.2	245.5	89.6%	19.6%	1,130.8	91.0%	18.0%
16	4.2	1,868.8	6.6	715.9	291.4	95.7%	18.2%	1,533.7	96.5%	15.4%
17	4.3	1,020.4	2.8	489.1	116.0	82.4%	24.0%	641.5	91.2%	21.1%
18	4.8	1,624.3	5.9	933.0	155.9	89.7%	24.1%	1,157.2	91.0%	22.4%
19	3.2	1,256.9	3.7	540.8	165.5	88.5%	22.9%	596.3	90.1%	20.5%
20	10.8	1,425.6	9.2	755.3	461.5	97.9%	17.7%	2,122.8	98.9%	17.1%
21	3.3	1,698.0	9.0	808.7	260.9	87.2%	26.4%	1,285.6	88.0%	24.9%
22	4.2	1,449.3	7.0	679.0	212.4	98.3%	18.0%	1,046.5	97.1%	15.9%
23	2.8	1,381.2	4.3	751.9	158.9	83.5%	30.3%	873.0	85.1%	28.0%
24	2.7	1,212.2	2.6	639.9	290.6	77.4%	52.7%	1,551.3	78.4%	50.6%
25	4.0	1,099.4	6.2	597.1	215.8	91.0%	34.8%	1,293.5	92.9%	31.7%
26	3.7	1,370.1	6.8	637.3	237.5	85.6%	27.3%	1,160.4	87.1%	24.3%
27	3.0	1,034.2	3.4	538.2	120.0	95.1%	27.8%	471.0	96.5%	27.3%
28	7.7	1,553.6	8.3	891.4	355.4	90.8%	21.0%	1,656.8	91.5%	19.2%
29	4.7	1,277.0	4.2	514.5	186.6	93.8%	28.9%	1,023.4	95.3%	26.6%
30	8.0	1,475.9	5.5	714.9	465.2	96.8%	21.5%	2,915.4	96.7%	19.7%
31	5.0	1,440.5	3.8	683.0	244.5	91.6%	29.1%	728.7	92.6%	25.9%
32	5.9	1,557.7	4.1	519.2	332.6	90.2%	32.6%	999.9	91.4%	30.2%
33	4.0	1,321.4	2.8	669.8	105.3	92.4%	23.8%	240.8	97.9%	21.7%
34	7.6	1,420.1	5.8	727.4	487.8	96.0%	10.7%	4,622.7	94.3%	8.5%
35	4.2	1,454.0	7.3	664.0	178.2	99.0%	23.3%	777.8	98.1%	20.8%
36	5.8	1,186.5	7.8	462.5	320.5	88.4%	33.7%	1,256.1	89.7%	30.5%
37	2.0	1,219.9	2.7	640.9	198.7	79.7%	32.0%	1,113.8	81.1%	29.5%
38	3.1	1,452.5	4.6	640.7	168.5	81.4%	29.1%	922.1	82.7%	26.6%
39	2.9	1,202.1	5.8	602.8	246.2	94.5%	16.2%	1,438.1	95.5%	12.6%
40	3.7	918.9	3.8	478.6	370.2	80.4%	27.6%	2,373.2	82.8%	23.2%
41	5.0	1,442.3	5.8	715.0	207.2	92.0%	25.2%	1,101.6	92.9%	23.0%
42	8.0	1,427.0	4.3	741.2	435.7	91.2%	22.4%	4,060.0	90.3%	20.8%
43	3.9	1,198.2	3.5	648.2	128.7	91.3%	24.5%	396.1	91.4%	23.3%
44	5.1	1,780.7	8.4	1,032.4	288.8	95.1%	25.5%	2,182.8	94.7%	23.9%
45	2.4	1,524.1	5.5	785.8	108.2	99.7%	26.9%	299.9	99.3%	25.3%
46	4.0	1,519.0	3.5	852.6	229.9	95.2%	19.9%	850.9	94.4%	17.5%
47	1.5	1,220.2	2.4	668.1	141.5	87.1%	29.8%	566.5	88.9%	27.3%
48	3.0	1,552.6	2.8	857.3	61.8	83.6%	46.6%	329.0	84.2%	45.4%
49	3.2	1,547.1	5.5	945.7	167.9	90.6%	27.1%	2,065.7	91.3%	25.1%
50	4.0	1,603.9	3.9	673.1	205.2	96.3%	22.1%	1,221.8	96.8%	20.5%

Table 3.4 – Strategies Comparison (Instances 51-100)

Index	Extreme Free		Extreme Fair		Contract Balance					
					$K = 16$			$K = 32$		
	Time(s)	$N(s^1)$	Time(s.)	$I(s^3)$	Time(s.)	$G^N(s^2)$	$G^I(s^2)$	Time(s.)	$G^N(s^2)$	$G^I(s^2)$
51	7.5	1,559.2	6.6	688.9	256.2	97.6%	16.2%	1,361.5	98.9%	14.0%
52	2.9	1,739.1	4.0	713.7	113.4	94.7%	28.7%	617.7	95.4%	25.9%
53	5.7	1,330.1	5.9	643.6	264.4	95.0%	31.3%	2,558.9	96.3%	28.2%
54	6.0	1,167.4	5.7	591.7	121.6	97.4%	22.6%	996.9	96.3%	19.2%
55	5.2	1,392.3	3.0	739.6	192.8	91.8%	26.2%	927.7	93.1%	23.7%
56	5.9	1,735.2	6.6	769.3	262.5	91.3%	26.4%	1,336.5	92.4%	23.5%
57	9.9	1,165.2	3.9	623.7	193.0	89.9%	21.3%	704.9	88.1%	18.7%
58	6.4	1,551.0	8.9	675.9	299.9	87.3%	28.8%	1,340.7	88.3%	26.1%
59	4.2	1,477.9	4.1	752.9	386.0	93.0%	27.9%	1,458.6	94.1%	25.6%
60	5.8	1,612.6	1.6	1,037.8	55.6	85.1%	45.5%	511.3	85.8%	44.8%
61	5.8	1,703.8	4.2	944.2	324.9	86.7%	36.8%	2,276.4	87.6%	35.0%
62	4.4	1,340.2	6.8	658.5	248.8	95.3%	23.7%	1,560.4	97.0%	20.7%
63	1.9	1,137.8	2.6	607.2	240.2	92.6%	32.7%	824.0	93.1%	31.4%
64	2.6	874.9	3.3	498.3	340.6	80.4%	25.5%	2,030.1	82.7%	21.0%
65	5.3	1,236.6	3.2	707.3	272.4	92.5%	20.9%	1,334.1	96.8%	18.8%
66	3.1	1,332.6	5.4	585.7	227.6	97.9%	24.8%	1,349.0	98.8%	22.9%
67	4.6	1,351.9	5.7	669.5	258.0	91.2%	19.4%	1,735.9	92.4%	17.2%
68	3.9	1,761.5	7.1	841.5	185.7	91.7%	25.0%	1,040.2	92.8%	23.4%
69	4.3	1,403.0	6.4	585.9	272.2	85.7%	24.9%	1,539.9	87.0%	22.3%
70	6.2	1,718.8	10.2	802.6	146.6	96.3%	16.4%	665.4	96.6%	14.1%
71	4.9	1,680.4	5.2	875.3	421.1	93.2%	25.6%	2,452.2	94.1%	24.1%
72	4.9	1,462.0	5.0	621.8	338.5	87.8%	25.4%	1,894.1	88.8%	23.0%
73	4.8	1,711.2	4.0	1,022.3	158.7	89.8%	39.4%	835.9	90.7%	37.9%
74	7.2	1,450.0	6.0	702.1	309.9	95.3%	19.7%	1,638.1	94.7%	17.4%
75	3.7	1,339.2	7.5	704.9	163.7	91.9%	16.8%	618.5	90.8%	14.2%
76	3.7	1,309.1	4.5	688.5	439.7	93.8%	25.7%	1,975.6	95.1%	23.7%
77	2.2	1,416.8	2.6	706.9	274.8	89.4%	24.2%	1,681.1	90.6%	21.8%
78	3.0	1,506.6	5.8	751.1	217.0	95.8%	27.6%	1,180.4	97.0%	26.1%
79	2.2	1,352.0	3.3	641.6	175.3	90.6%	36.4%	991.8	92.2%	33.8%
80	10.7	1,460.0	4.9	752.2	236.8	93.9%	29.0%	842.0	94.1%	26.7%
81	7.2	1,545.9	8.8	775.5	581.4	86.2%	25.3%	4,229.3	87.3%	23.9%
82	4.8	1,342.0	5.5	691.2	157.4	95.6%	27.9%	661.2	94.3%	25.5%
83	7.8	1,313.0	5.1	553.9	144.9	92.1%	32.1%	610.4	93.8%	29.1%
84	6.8	1,570.1	7.3	650.0	247.7	91.8%	33.2%	1,107.7	92.7%	30.4%
85	7.1	1,305.7	7.6	560.8	247.1	95.0%	25.4%	1,471.1	94.6%	22.6%
86	3.6	1,586.2	5.4	630.7	153.0	87.7%	27.2%	631.9	88.7%	25.3%
87	9.7	1,613.0	5.0	694.9	366.0	87.6%	26.6%	1,482.4	88.8%	23.8%
88	4.4	1,631.4	3.8	751.4	359.9	90.8%	20.3%	1,777.2	91.9%	17.8%
89	3.6	1,471.7	3.5	774.0	215.2	88.4%	30.2%	950.2	89.5%	27.6%
90	3.5	1,476.9	2.4	829.7	218.8	84.1%	23.4%	773.5	85.1%	20.8%
91	6.6	1,503.5	11.0	619.9	396.0	92.3%	15.6%	1,729.4	92.2%	12.4%
92	4.0	1,742.3	5.3	895.7	194.2	88.6%	27.1%	1,214.0	89.8%	24.9%
93	6.0	1,590.5	6.5	800.8	170.3	90.1%	31.7%	750.2	90.8%	30.1%
94	3.7	1,438.6	8.6	742.5	145.9	86.4%	22.7%	1,138.2	87.6%	20.3%
95	3.9	1,257.5	6.4	579.0	223.0	86.9%	28.8%	746.3	88.2%	26.2%
96	5.4	1,513.4	5.6	666.0	234.6	88.9%	32.2%	1,106.0	89.5%	30.6%
97	5.3	1,305.3	5.7	622.3	153.8	96.9%	22.1%	976.9	98.3%	19.4%
98	4.1	1,520.9	3.8	852.6	182.4	94.3%	21.9%	843.9	94.8%	19.8%
99	3.9	1,459.2	6.2	644.3	145.6	92.9%	26.5%	480.1	94.1%	23.6%
100	4.1	1,505.2	7.7	604.8	513.3	97.4%	5.1%	2,670.1	98.2%	3.3%
Avg	**4.7**	**1,441.5**	**5.3**	**719.5**	**243.0**	**91.2%**	**26.4%**	**1,310.6**	**92.1%**	**24.2%**

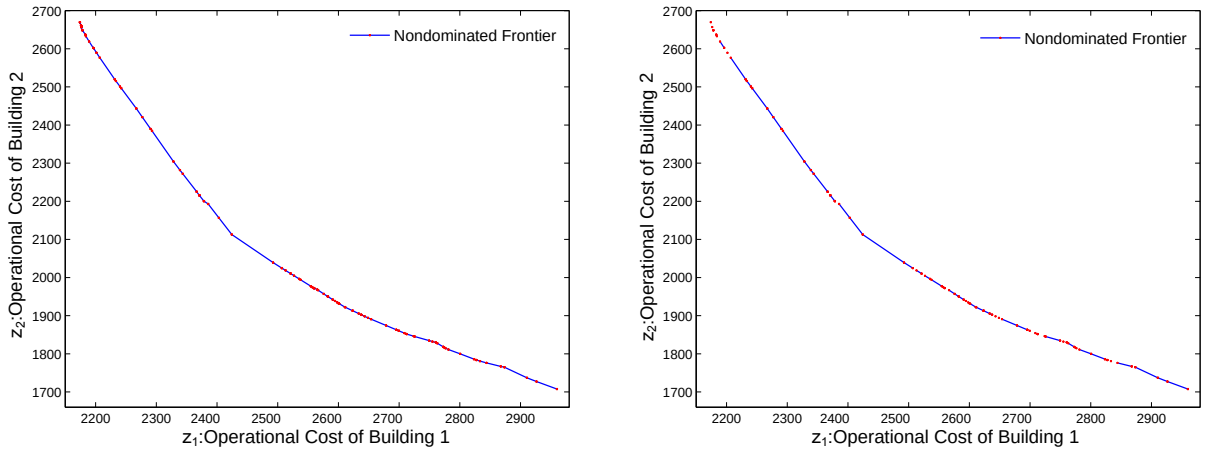

(a) Hypervolume gap of 0%

(b) Hypervolume gap of 0.1%

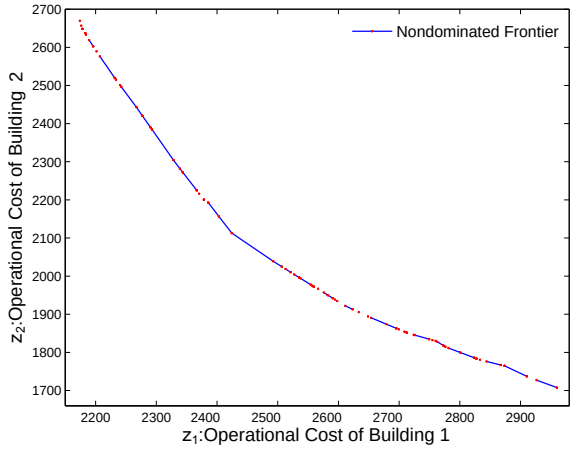

(c) Hypervolume gap of 0.2%

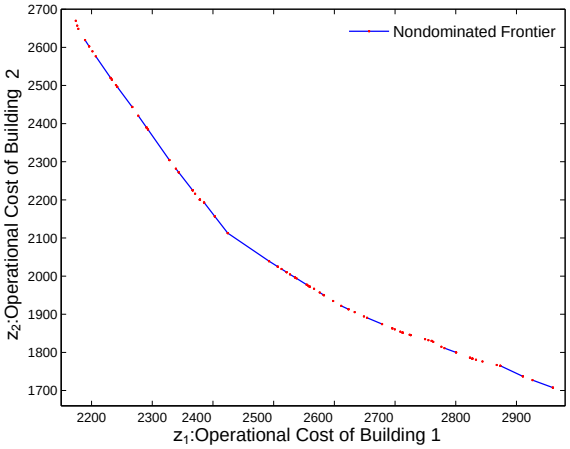

(d) Hypervolume gap of 0.4%

Figure 3.10 – Nondominated frontiers for different hypervolume gaps

3.6.3 Approximate Nondominated Frontier

In this section, we study the performance of the TSM in computing approximate nondominated frontiers for the contract balance strategy. Note that from a practical perspective, approximations are important since it will be too time-consuming to compute the exact efficient frontier for large values of $|\mathcal{T}|$ or if we incorporate further details in the model. Obviously, a key concern for any approximation scheme is how to measure its quality. To date various measures have been considered to gauge the quality of different approximate nondominated frontiers. One of the best examples here is the *hypervolume indicator* (or the S-metric) introduced by [82, 83]. Namely, if $\tilde{\mathcal{O}}_N$ is an approximate efficient frontier, then hypervolume $H(\tilde{\mathcal{O}}_N)$ measures the area of the dominated parts of the criterion space determined by $\tilde{\mathcal{O}}_N$ with respect to a *reference point*. Now a good choice for the reference point here is the nadir point. An approximate efficient frontier with a higher hypervolume is considered a better approximate efficient frontier because $H(\tilde{\mathcal{O}}_N) \leq H(\mathcal{O}_N)$, i.e., the hypervolume of an approximate efficient frontier cannot be larger than the hypervolume of the true efficient frontier. It is worth mentioning that [79] have shown that it is possible to find dual bounds (upper bounds) for the hypervolume, i.e., $H(\mathcal{O}_N) \leq \textsc{UpperBound}$. Hence the hypervolume gap can be defined as,

$$\frac{\big(\textsc{UpperBound} - H(\tilde{\mathcal{O}}_N)\big) \times 100}{\textsc{UpperBound}},$$

and this can provide a measure of the quality of an approximate frontier.

In this section, we consider four different hypervolume gaps including, 0%, 0.1%, 0.2% and 0.4%. Note that the result of hypervolume gap of 0% is the true nondominated frontier. Figure 3.10 shows the nondominated frontier of one of the instances for different hypervolume gaps. Clearly many of the line segments in the true nondominated frontier are not discovered for the hypervolume gap of 0.4%.

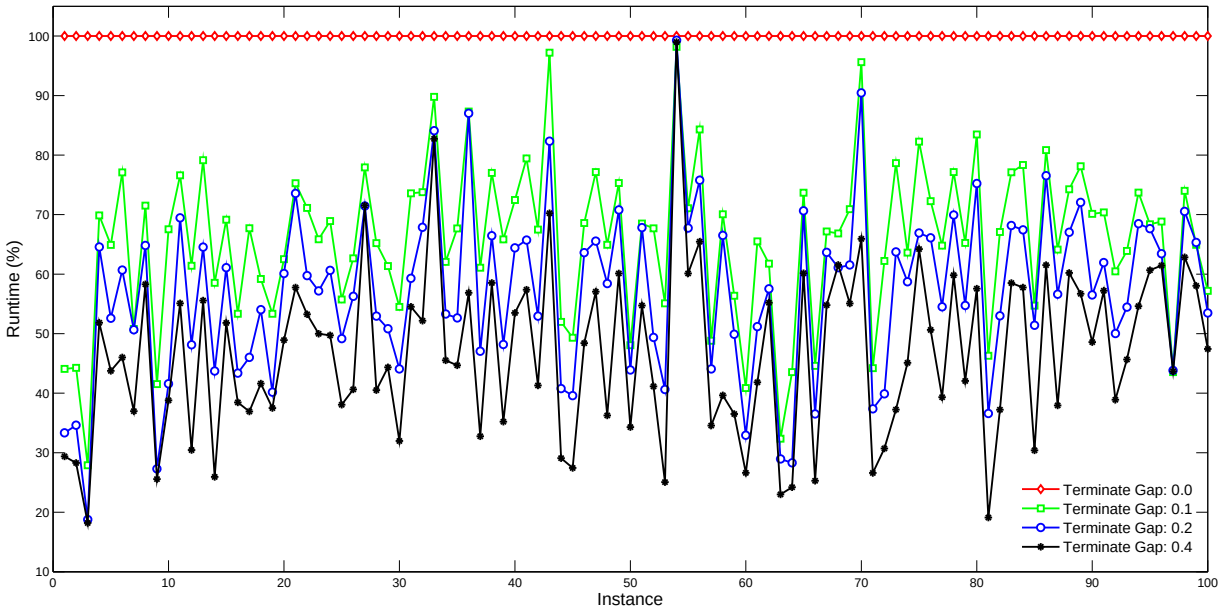

Figure 3.11 – Run time comparison of TSM for different hypervolume gaps

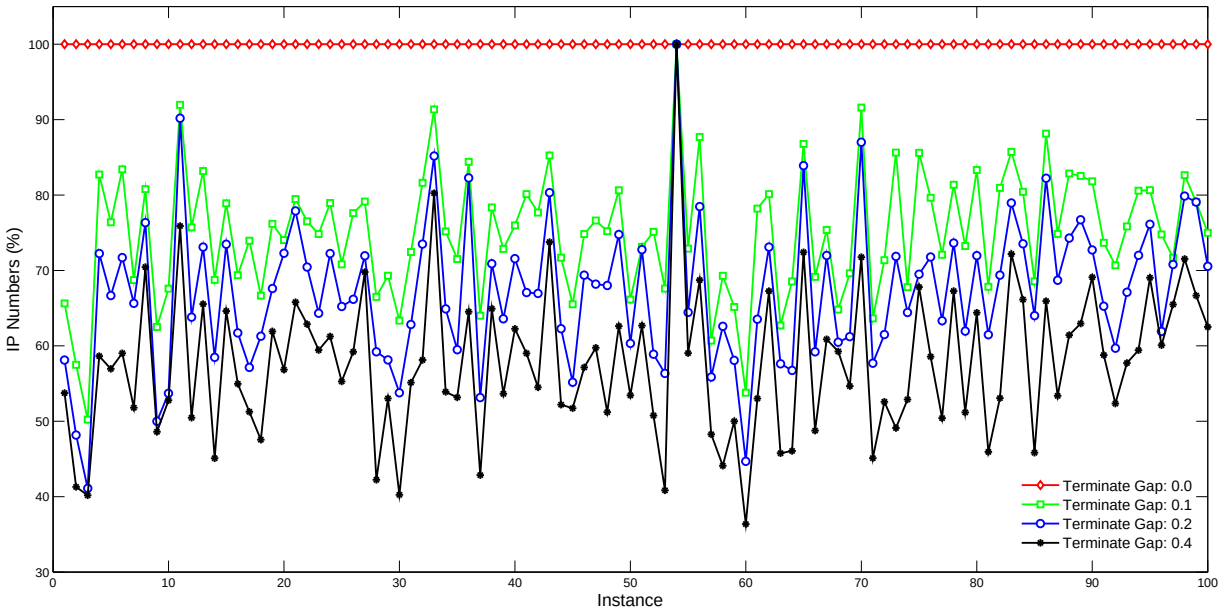

Figure 3.12 – IP comparison of TSM for different hypervolume gaps

Figure 3.11 shows the percentage of run time of TSM for different hypervolume gaps with respect to the run time of TSM to reach the hypervolume gap of 0%. Similarly, Figure 3.12 shows the percentage of the number of single-objective (mixed) integer programs (IPs) solved by TSM for different hypervolume gaps with respect to the number of IPs solved by TSM to reach the hypervolume gap of 0%. Observe that the slight increase in the hypervolume gap can significantly decrease the run time and the number of IPs solved by TSM. For example, for the optimality gap of 0.4%, the run time is reduced by a factor of around 2 on average.

3.7 Conclusion

Fairness and freedom are two important considerations that need to be taken into account during operational planning of any shared facility among independent agents/players. On one hand, imposing no limitation on using the facility may eventually cause the break of collaboration agreement between agents. On the other hand, imposing strict restrictions for using the facility may destroy opportunities for taking advantage of the facility. In this study, we addressed this issue in the context of building clusters with shared electrical energy storage and two buildings. We introduced three energy storage sharing strategies including extreme free, extreme fair, and contract balance strategies. By using bi-objective mixed integer programming techniques, we numerically showed that the contract balance strategy is almost as fair as the extreme fair strategy but it is significantly better than the extreme fair strategy, in terms of freedom.

We note that in practice the contract balance strategy can be implemented in different ways. So, further studies are required to determine the best way of doing so. One possible way is to consider a centralized agent that has full information about the status of the energy storage, electricity load and the unit price of buying electricity from the power grid at each time period for each building. The agent computes the exact or approximate nondominated frontier corresponding to the contract balance strategy, and decides which nondominated

point should be chosen. We note that selecting a desirable nondominated point from the nondominated frontier is another research direction that is worth exploring. For example, a natural question is that whether there is any point in the nondominated frontier that is better than others in terms of fairness or even freedom? Nevertheless, a simple and reasonable choice can be a point that has the minimum Euclidean distance from the ideal point of the nondominated frontier since it is expected to be attractive for each building in terms of its total operational cost.

We also note that Constraints (3.3)-(3.11) have similar characteristics to the constraints of the classical lot-sizing problem with constant capacity. So, exploring this connection may result in computational advantages since it may be possible to customize (and employ) the techniques developed for the lot-sizing problem. Another future research direction can be incorporating data uncertainty, such as the electricity price and demand, into mathematical optimization model by using stochastic or robust optimization techniques. Finally, increasing the complexity of the energy system by incorporating more buildings and/or other energy resources, for example renewable energy, requires further research.

Chapter 4: A Robust Bi-objective Optimization Approach for Operating a Shared Energy Storage under Price Uncertainty

This chapter was previously published as [56]: Dai, R., Charkhgard, H., & Rigterink, F. (2020). A robust biobjective optimization approach for operating a shared energy storage under price uncertainty. International Transactions in Operational Research. In this study, we extend our proposed contract balance strategy for energy storage sharing to handle energy price uncertainty. Robust optimization is applied to this strategy to ensure the robustness of the solution to balance the conflict between fairness and efficiency. We also adopt the binary formulation based piecewise McCormick relaxation to significantly improve computational efficiency.

4.1 Uncertainty in Energy Storage Sharing

In our previous paper [47], a contract balance strategy for Energy Storage (ES) sharing is proposed to bridge this research gap that the existing studies for ES sharing often give priority to maximize cost savings for the entire system and hence the fairness for each user in the sharing system is not emphasized. The proposed strategy is demonstrated to achieve the tradeoff between fairness and efficiency for ES sharing in the presence of two users. This paper extends the contract balance strategy to handle the price uncertainty through Robust optimization.

While balancing fairness and efficiency is promising, the contract balance strategy is only studied under the deterministic setting (and only for two users). Evidently, in practice, it is inevitable that energy systems experience uncertainty in terms of energy generation, load, and price. The mainstream methods to operate energy systems under uncertainty

are divided into two categories: stochastic optimization and robust optimization. Stochastic optimization relies on the distribution of uncertain parameters or probability of each possible scenario to handle the uncertainty in the energy system [84, 85, 86]. Robust optimization ensures the robustness of the energy systems under uncertainty by modeling the set-based uncertainty [87, 88, 89].

Overall, all sources of uncertainty are important. However, the issue of price uncertainty is becoming even more important because real-time pricing has been increasingly adopted by utility companies as one of the means to perform their DR programs. Since forecasting the real-time price for long time horizons is difficult, numerous papers have been published on the topic of handling real-time price uncertainty. The work in [90] compares the stochastic and robust approaches for DR management for residential appliances under uncertain real-time prices. The authors in [91] develop a multistage stochastic model to optimize forward generation thresholds for operating a pumped-storage plant under uncertain real-time price and a novel heuristic approach is proposed to facilitate solving this large-scale multistage stochastic optimization problem. In [92], a stochastic model is proposed to maximize the energy arbitrage for operating the ES under uncertain day-ahead and real-time prices.

In light of the above, this paper intends to address the problem of operating a shared ES for two users/buildings under electricity price uncertainty. We propose a robust optimization based sharing strategy that takes into account fair ES sharing under uncertain real-time price and nominal energy load. This sharing strategy is a robust extension of our previously proposed contract balance strategy due to its capability of balancing the fairness and efficiency for ES sharing. Adopting robust optimization to handle the price uncertainty gives us two benefits. First, modeling set-based uncertainty robust optimization is more applicable than the traditional approaches seizing upon probability distributions. Second, the robust counterpart to a deterministic problem formulated as a min-max problem is usually transferred into a tractable form which decreases the complexity of solving it. Hence,

based on the robust formulation of a *mixed integer linear program* (MILP) proposed by [93], we formulate our robust contract balance strategy as a bi-objective mixed integer bilinear programming model. We also develop a novel distance-based measurement to evaluate the performance of robust and nominal solutions since bi-objective optimization always returns a set of efficient solutions instead of a unique solution. By conducting a comprehensive computational study, we demonstrate the effectiveness of our robust contract balance strategy to ensure the robustness and profitability of the solution under price uncertainty. In addition, we employ the Nash bargaining solution [94] to guide the solution selection from the set of efficient solutions of this bi-objective problem for practical purposes. Experimental results illustrate that Nash bargaining solutions can achieve the balance distribution of ES sharing benefits to all users which strengthens their cooperation to share ES.

Another contribution of this work is that we propose a binary formulation based on piecewise McCormick relaxations to translate our bilinear formulation of the robust contract balance strategy into a *bi-objective mixed integer linear program* (BOMILP) to facilitate its solution. McCormick relaxation is an approach to approximate a bilinear term by replacing it with its McCormick envelope proposed in [80]. In order to increase the accuracy of the approximation, McCormick relaxation is formulated in a piecewise way by partitioning the domain of variables in the bilinear term [95, 81]. Our proposed binary fromulation for piecewise McCormick relaxations is a time-efficient formulation. It is worth mentioning that our binary formulation reduces the runtime by approximately 80% compared to the traditional formulation for piecewise McCormick relaxations, whilst the qualitative difference in the results between both formulations is negligible.

4.2 Robust Optimization

4.2.1 Essential Concepts for BOMILP

In this section, we introduce some necessary notations and concepts related to BOMILP to facilitate presentation and discussion of the remaining sections. A BOMILP can be stated

as follows:

$$\min_{x \in \mathcal{X}} \{z_1(x), z_2(x)\}, \tag{4.1}$$

where x represents an n-dimensional vector, $\mathcal{X} := \left\{x \in \mathbb{R}^n_+ : Ax \leq b; \quad x_j \in \mathbb{Z} \text{ for } \forall j \in \{1, \ldots, n_1\}\right\}$ is the *feasible set in the decision space*, and $z_p(x) = c_p x$ for each $p \in \mathcal{M} := \{1, 2\}$ represents a linear objective function. The image $\mathcal{Y}$ of $\mathcal{X}$ under vector-valued function $z = \{z_1, z_2\}$ represents the *feasible set in the objective/criterion space*, i.e., $\mathcal{Y} := z(\mathcal{X}) := \{y \in \mathbb{R}^2 : y = z(x) \text{ for some } x \in \mathcal{X}\}$. It is assumed that $\mathcal{X}$ is *bounded*, and all coefficients/parameters are real-valued, i.e., $A \in \mathbb{R}^{m \times n}$ and $c_p \in \mathbb{R}^n$ for all $p \in \mathcal{M}$.

Definition 17. A feasible solution $x' \in \mathcal{X}$ is called *efficient* if there is no other $x \in \mathcal{X}$ such that $z_p(x) \leq z_p(x')$ for $p \in \mathcal{M}$ and $z(x) \neq z(x')$. If x' is efficient, then $z(x')$ is called a *nondominated point*. The set of all efficient solutions $x' \in \mathcal{X}$ is denoted by $\mathcal{X}_E$. The set of all nondominated points $z(x') \in \mathcal{Y}$ for some $x' \in \mathcal{X}_E$ is denoted by $\mathcal{Y}_N$, and referred to as the *nondominated frontier*.

Definition 18. The point $z^I \in \mathbb{R}^2$ is the *ideal point* if $z^I_p = \min_{(x,y) \in \mathcal{X}_E} z_p(x, y)$ for all $p \in \mathcal{M}$.

If the objectives are conflicting, i.e., $|\mathcal{Y}_N| > 1$, then the ideal point should be an *utopia* point in the criterion space, i.e., there is no corresponding feasible solution for it in the decision space. Hence, bi-objective optimization is concerned with finding *some* and possibly *all* nondominated points. The nondominated frontiers of the BOMILPs may contain single points, segments, and half-open (or open) segments. Figure 4.1 is an illustration of the nondominated frontier of a BOMILP, where the ideal point is denoted by the square. In this study, we employ the *Triangle Splitting Method* (TSM) developed by [79] to solve BOMILPs. TSM is proven to be effective in generating an exact representation of the nondominated frontier of a BOMILP.

Once we obtained the entire nondominated frontier, we still need to select a non-dominated point and its corresponding efficient solution from this frontier to implement. This process can be accomplished by *Optimizing Over the Efficient Set* (OOES) [96]. The

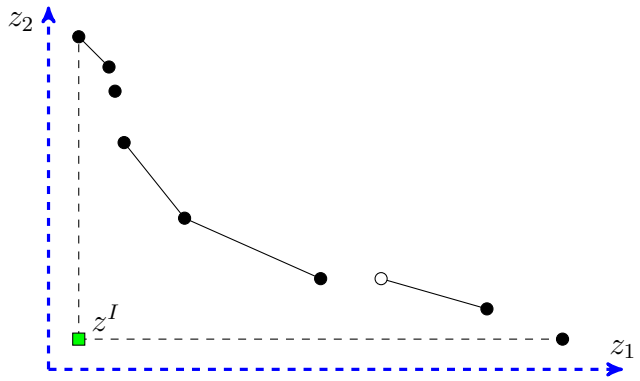

Figure 4.1 – The nondominated frontier and ideal point of a BOMILP

problem of OOES can be formulated as follows:

$$\min_{x \in \mathcal{X}_E} f(x) \quad \text{or} \quad \max_{x \in \mathcal{X}_E} f(x), \tag{4.2}$$

where $f(x)$ can be a linear or nonlinear function.

4.2.2 Robust Single-objective Optimization

Robust optimization is a fundamental method to handle data uncertainty in an optimization problem. The idea of robust optimization is to hedge against the perturbation of the presupposed coefficients in the mathematical model. It is free from the exact distribution of the uncertain data or the probability of each possible scenario, which makes it outperform stochastic optimization in some real-world problems. Overall, robust optimization is a conservative approach to guarantee the robustness of the solution under uncertainty. We employ the robust optimization approach developed by [93] in this work, since their method can transfer the robust counterpart of a MILP model into an equivalent formulation without min-max terms. We next give the description of their method.

Let x and c be both n-dimensional vectors, A be an $m \times n$ matrix, and b be an m-dimensional vector. Also, let $N = \{1, 2, \ldots, n\}$ and $M = \{1, 2, \ldots, m\}$. The nominal

formulation for a MILP is given as

$$
\begin{aligned}
\text{(MIP)} \qquad & \min\ c^T x \\
& \text{s.t. } Ax \leq b \\
& \qquad x \geq 0 \\
& \qquad x_j \in \mathbb{Z} \qquad \forall j \in \{1, \ldots, n_1\}.
\end{aligned}
$$

where x is a vector of n variables in which the first n_1 of them are integers and the rest of them are real-valued. We denote the above model by "(MIP)".

Robust optimization does not rely on the distribution of uncertain parameters by modeling set-based data uncertainty. Let $i \in M$ and $j \in N$. In order to model the uncertainty of each entry a_{ij} in matrix A, we make a_{ij} a random variable assuming values in $[a_{ij} - \hat{a}_{ij}, a_{ij} + \hat{a}_{ij}]$ where $\hat{a}_{ij} \geq 0$. Similarly, we make each entry c_j a random variable assuming values in $[c_j, c_j + \hat{c}_j]$ where $\hat{c}_j \geq 0$. Note that we limit ourselves to the possibility of the value of c_j increasing, since for minimization problems, this will result in a worse objective value.

One of the highlights of Bertsimas and Sim's approach is that they allow the decision makers to adjust the level of conservatism. This level is measured by the number Γ_i where $i \in M \cup \{0\}$. Γ_i for each $i \in M$ assumes values in $[0, |J_i|]$ where $J_i = \{j : \hat{a}_{ij} > 0\}$, and Γ_0 assumes values in $[0, |J_0|]$ where $J_0 = \{j : \hat{c}_j > 0\}$. We separate J_i for each $i \in M \cup \{0\}$ into two sets, S_i and $\{t_i\}$, i.e., $J_i = S_i \cup \{t_i\}$ and $S_i \cap \{t_i\} = \emptyset$. If $j \in S_i$, a_{ij} can increase or decrease by at most $\hat{a}_{ij}$, and c_j can increase by at most $\hat{c}_j$. If $j \in \{t_i\}$, a_{ij} can increase or decrease by at most $(\Gamma_i - \lfloor \Gamma_i \rfloor)\hat{a}_{ij}$, and c_j can increase by at most $(\Gamma_0 - \lfloor \Gamma_0 \rfloor)\hat{c}_j$.

With the above preliminaries, the robust counterpart for (MIP) can be formulated as

$$
\begin{aligned}
\text{(RC)} \qquad \min\ & c^T x + \max_{\{S_0 \cup \{t_0\} | S_0 \subseteq J_0, |S_0| \leq |\lfloor \Gamma_0 \rfloor|, t_0 \in J_0 \setminus S_0\}} \left\{ \sum_{j \in S_0} \hat{c}_j x_j + (\Gamma_0 - \lfloor \Gamma_0 \rfloor) \hat{c}_{t_0} x_{t_0} \right\} \\
\text{s.t.}\ & \sum_j a_{ij} x_j + \max_{\{S_i \cup \{t_i\} | S_i \subseteq J_i, |S_i| \leq |\lfloor \Gamma_i \rfloor|, t_i \in J_i \setminus S_i\}} \left\{ \sum_{j \in S_i} \hat{a}_{ij} x_j \right. \\
& \qquad \left. + (\Gamma_i - \lfloor \Gamma_i \rfloor) \hat{a}_{it_i} x_{t_i} \right\} \leq b_i \qquad \forall i \in M \\
& x \geq 0 \\
& x_j \in \mathbb{Z} \qquad \forall j \in \{1, \ldots, n_1\},
\end{aligned}
$$

and we denote this formulation as "(RC)". Obviously, solving (RC) is challenging due to its min-max structure. Based on Bertsimas and Sim's approach, (RC) can be transformed to an equivalent MILP formulation which we denote as "(RE)" and is given as follows:

$$
\begin{aligned}
\text{(RE)} \qquad \min\ & c^T x + \theta_0 \Gamma_0 + \sum\nolimits_{j \in J_0} \beta_{0j} \\
\text{s.t.}\ & \sum_{j \in N} a_{ij} x_j + \theta_i \Gamma_i + \sum_{j \in J_i} \beta_{ij} \leq b_i && \forall i \in M \\
& \theta_0 + \beta_{0j} \geq \hat{c}_j x_j && \forall j \in J_0 \\
& \theta_i + \beta_{ij} \geq \hat{a}_{ij} x_j && \forall i \in M, \forall j \in J_i \\
& \theta_i \geq 0 && \forall i \in M \cup \{0\} \\
& \beta_{ij} \geq 0 && \forall i \in M \cup \{0\}, \forall j \in J_i \\
& x \geq 0 \\
& x_j \in \mathbb{Z} && \forall j \in \{1, \ldots, n_1\}.
\end{aligned}
$$

4.2.3 Robust Bi-objective Optimization

In this study, the process of applying robust optimization to a bi-objective optimization problem is similar to the one described in Section 4.2.2. So, in this section, rather than

showing the robust mathematical model corresponding to bi-objective optimization, we explain how the robustness impacts the nondominated frontier of a bi-objective optimization model. We present Figure 4.2 to facilitate the understanding of such an impact.

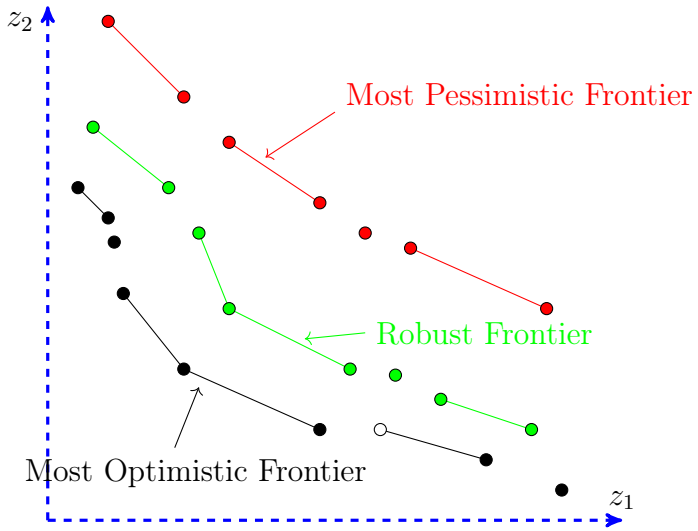

Figure 4.2 – Explanation to the frontiers of robust bi-objective optimization

Note that, as mentioned in Section 4.2.2, in robust single-objective optimization, there is a parameter indicating the level of conservatism of a decision maker (denoted by Γ). The parameter shows how many uncertain parameters in the mathematical model take their worst, i.e., maximum, values, from the view point of the decision maker. The model then automatically decides which uncertain parameters should take their worst values to create the maximum negative impact on the model (in terms of shrinking its feasible set and/or increasing its objective value). In other words, based on the level of conservatism of a decision maker, the model will automatically create the worst case scenario to generate a solution. In the context of bi-objective optimization, the same process will be done but the only difference is that there are two decision makers and each one has their own beliefs/perceptions about dealing with uncertainty. So, for each decision maker, there is a parameter indicating its level of conservatism. With this in mind, in Figure 4.2, “Most Optimistic Frontier" shows the nondominated frontier of the bi-objective optimization model when using the nominal data, i.e., no uncertain parameter is allowed to take its worst value from the view point of

both decision makers. “Most Pessimistic Frontier" shows the nondominated frontier of the bi-objective optimization model when all uncertain parameters must take their worst values from the view point of both decision makers. Evidently, “Robust Frontier" lies between the most optimistic and pessimistic frontiers depending on which level of conservatism is selected for each decision maker. Overall, we observe that the influence of robustness in bi-objective optimization is the (maximum) upward move of the nondominated frontier with respect to the level of conservatism of decision makers.

4.3 Robust Bi-objective Optimization for Energy Storage Sharing

The purpose of this paper is to develop a fair sharing strategy to handle uncertainty in the ES sharing system. As is well-known, ES is capable of cost savings for an energy system by providing the energy arbitrage. The energy arbitrage can be further boosted if allowing multiple users to share an ES and exchange the energy they stored. One concern when sharing ES is the fairness between all users. In our previous paper [47], we proposed a contract balance strategy which is validated to achieve the fair energy distribution when maximizing the energy arbitrage for an ES sharing system. In that model, we assumed all parameters such as electricity price and demand of buildings to be nominal. We explain the difficulty of the energy storage sharing problem and the idea of our contract balance strategy as follows.

The energy storage sharing problem is a resource sharing problem, in which the buildings cooperate to create more energy arbitrage and compete for higher allocation of the cooperative benefits. The buildings exchange their energy stored in the storage to create more energy arbitrage. This exchange should be assured to be fair to consolidate the cooperation of the buildings. Our contract balance strategy establishes a compensation mechanism to ensure a payoff for the building selling its stored energy. Additionally, the buildings will compete with each other to achieve a higher allocation for the energy arbitrage. The contract balance strategy studies the competition by modeling the problem as a multi-objective optimization

based formulation. Our previous work has demonstrated that this strategy can guarantee the fairness and efficiency for energy storage sharing, and the obtained efficient set can provide a complete perspective of the competition among the buildings.

However, it is inevitable that electricity price (if real-time pricing is applied) or energy demand may deviate from our prediction in practice. Hence, our optimal solution obtained under deterministic assumptions may be infeasible due to the parameters' perturbation or an increase in the operational costs outside of our tolerance, i.e., the operational costs of this solution are higher than without using ES. This is why we are motivated to develop the robust optimization based contract balance strategy for handling the uncertainty in the ES sharing system. In order to better illustrate our proposed strategy, we still consider (in this paper) the typical ES system with two buildings sharing one ES (as [47] did in their paper).

We select robust optimization to handle the energy price uncertainty for the ES sharing problem because of the following reasons. 1) Robust optimization can ensure the fair exchange of stored energy with respect to the level of conservatism of players (i.e., buildings) to avoid the buildings quit the ES sharing. 2) Robust optimization does not assume any prior knowledge on the distribution of the uncertain data. Note that *Conditional Value at Risk* (CVaR) can also optimize the average loss over a specific time period of worse scenarios beyond the confidence level. However, CVaR still needs prior knowledge on the distribution to calculate the confidence interval, but it is challenging to generate the distribution of uncertain energy price in practice. Robust optimization can overcome this challenge by adopting a simple assumption on the uncertain price such as set-based uncertain price. 3) Robust optimization has computational advantages. Specifically, robust optimization technique that we have employed is based on the work of [93] that does not change the computational complexity class of a problem, i.e., if a problem is easy it remains easy.

Before discussing the robust contract balance strategy for handling the uncertainty in the ES sharing system, we note that only the uncertainty of electricity price is considered in this work. The following two reasons apply: first, the energy arbitrage is sensitive to the

electricity price. This is because the energy arbitrage benefits from charging at off-peak price and discharging at peak price to satisfy the energy demand instead of electricity purchases from the market. Second, the contract balance strategy validates the fair energy sharing largely depending on the electricity price. In this strategy, we compute the average price of the stored electricity for each building and use it to compute the payoff for the building purchasing stored electricity from the other buildings.

4.3.1 Deterministic Formulation for the Contract Balance Strategy

In order to facilitate the illustration of the robust contract balance strategy for handling price uncertainty, we first review the nominal version of this strategy presented in [47]. Overall, the underlying idea of the contract balance strategy is that users can freely use stored energy but they have to pay other users if they discharge more energy from the storage than what they charge into it (during the entire planning horizon). In fact, the assumption is that each user will never pay for the energy that other users have used. For example, suppose that an energy storage is shared by user X and Y. User X discharges 9 kWh extra energy from the storage during the entire planning horizon. The extra energy indicates the difference between the total energy used by user X and charged by this user. Additionally, the extra energy measures the energy used by user X but charged by user Y. Suppose further that at the end of the planning horizon, it turns out that the cost of the 9 kWh extra energy paid by user Y is \$4. Hence under this contract, user X should pay \$4 to user Y at the end of the planning horizon.

In light of the above, we now present the nominal formulation. Note that in this formulation we still retain the bilinear terms. The parameters and decision variables used in the nominal formulation for the contract balance strategy are listed in the Nomenclature. The assumptions that ES is shared by two buildings and the power grid capacity is unlimited applies throughout. The standard formulation for the contract balance strategy is expressed

Table 4.1 – Decision variables and parameters for contract balance strategy

Decision Variables	
b_t^i	Energy purchased by building $i \in \mathcal{N}$ at time $t \in \mathcal{T}$ to charge the ES. Note that $b_t^i \times \eta^c$ is the real amount of energy stored in the ES.
d_t^i	Energy discharged from the ES for building $i \in \mathcal{N}$ at time $t \in \mathcal{T}$. Note that d_t^i/η^d is the real amount of energy extracted from the ES.
e_t^i	Energy purchased by building $i \in \mathcal{N}$ at time $t \in \mathcal{T}$ to satisfy the energy load.
m_t	Energy available in the ES at the end of time period $t \in \mathcal{T}$.
s_t^c/s_t^d	A binary variable that is 1 if the ES is at charging/discharging state at time $t \in \mathcal{T}$, and 0 otherwise.
z^i	Operational cost of building $i \in \mathcal{N}$.
g^i	Difference between the total energy charged into the ES by building $i \in \mathcal{N}$ and the total stored energy used by this building.
$\bar{r}^i$	Average price of the total energy charge into the ES by building $i \in \mathcal{N}$.
v^i	The compensation that building $i \in \mathcal{N}$ should receive for exchanging the stored energy.
w_t^i	The regulated cost of the energy charged to the ES by building $i \in \mathcal{N}$ at time $t \in \mathcal{T}$.
Parameters	
$\bar{B}/\underline{B}$	The maximum/minimum amount of energy that can be stored in the ES at each time period.
$\bar{C}/\underline{C}$	The maximum/minimum amount of energy that can be charged into the ES at a given time period if the storage is at charging state.
$\bar{D}/\underline{D}$	The maximum/minimum amount of energy that can be discharged from the ES at a given time period if the storage is at discharging state.
η^c/η^d	The charging/discharging efficiency coefficient of the ES i.e., $\eta^c, \eta^d \in (0, 1]$.
$\mathcal{N}$	The index set of buildings, i.e., $\mathcal{N} := \{1, 2\}$.
$\mathcal{T}$	The index set of time periods of equal length.
L_t^i	The electricity (load) demand of building $i \in \mathcal{N}$ at time $t \in \mathcal{T}$.
r_t^i	The price for building $i \in \mathcal{N}$ to purchase energy from power grid at time $t \in \mathcal{T}$.
$\hat{r}_t^i$	The maximum deviation from the nominal price r_t^i for building $i \in \mathcal{N}$ at time $t \in \mathcal{T}$.

as follows and we denote this formulation as "(D1)".

$$
\begin{aligned}
\text{(D1)} \quad & \min \sum_{t\in\mathcal{T}} r_t^1(e_t^1+b_t^1) - \max\{\bar{r}^1 g^1, 0\} + \max\{\bar{r}^2 g^2, 0\} && && (4.3)\\
& \min \sum_{t\in\mathcal{T}} r_t^2(e_t^2+b_t^2) - \max\{\bar{r}^2 g^2, 0\} + \max\{\bar{r}^1 g^1, 0\} && && (4.4)\\
& \text{s.t. } e_t^i + d_t^i = L_t^i && \forall i\in\mathcal{N}, \forall t\in\mathcal{T} && (4.5)\\
& s_t^c + s_t^d \le 1 && \forall t\in\mathcal{T} && (4.6)\\
& \underline{C} s_t^c \le \sum_{i\in\mathcal{N}} b_t^i \eta^c \le \bar{C} s_t^c && \forall t\in\mathcal{T} && (4.7)\\
& \underline{D} s_t^d \le \sum_{i\in\mathcal{N}} \frac{d_t^i}{\eta^d} \le \bar{D} s_t^d && \forall t\in\mathcal{T} && (4.8)\\
& \sum_{i\in\mathcal{N}} b_t^i \eta^c - \sum_{i\in\mathcal{N}} \frac{d_t^i}{\eta^d} = m_t - m_{t-1} && \forall t\in\mathcal{T} && (4.9)\\
& \underline{B} \le m_t \le \bar{B} && \forall t\in\mathcal{T} && (4.10)\\
& m_0 = m_{|T|} = \underline{B} && && (4.11)\\
& e_t^i, b_t^i, d_t^i, m_t \ge 0 && \forall i\in\mathcal{N},\ t\in\mathcal{T} && (4.12)\\
& s_t^c, s_t^d \in \{0,1\} && \forall t\in\mathcal{T} && (4.13)\\
& g^1, g^2 \in \mathbb{R} && && (4.14)\\
& \bar{r}^1, \bar{r}^2 \ge 0, && && (4.15)
\end{aligned}
$$

where g^i is introduced to measure the amount of energy exchanged between two buildings and $\bar{r}^i$ indicates the average price of building i charging energy to the storage during the entire planning horizon. These two decision variables can be computed by imposing the following constraints:

$$
\begin{aligned}
& g^i = \sum_{t\in\mathcal{T}} \left(b_t^i - \frac{d_t^i}{\eta^c \eta^d} \right) && \forall i\in\mathcal{N} && (4.16)\\
& \sum_{t\in\mathcal{T}} r_t^i b_t^i = \sum_{t\in\mathcal{T}} \bar{r}^i b_t^i && \forall i\in\mathcal{N}. && (4.17)
\end{aligned}
$$

Overall, objective functions (4.3)–(4.4) indicate the operational costs for both buildings, constraint (4.5) assures the energy demand is satisfied, and constraints (4.6)–(4.10) control the operation of ES. Note that no buildings can sell energy to the grid (e.g., d_t^i discharge is limited by the load L_t^i). Specifically, constraint (4.6) ensures that the state of the electrical energy storage cannot be charging and discharging at the same time. Constraints (4.7) and (4.8) ensure that the amount of energy charged and/or discharged from the electrical energy storage is within the allowed range during any time period. Constraint (4.9) imposes the energy conservation in the electrical energy storage during any time period. Finally, constraint (4.10) ensures that the amount of energy available at the electrical energy storage is within the allowed range during any time period. Finally, for simplicity, we assume that $m_0 = m_{|T|} = \underline{B}$ and so we impose it as constraint (4.11).

Note that there are max functions in the objective functions (4.3) and (4.4). We can translate these objective functions into an equivalent form without the max functions by introducing two non-negative variables, $\hat{g}^1$ and $\hat{g}^2$, and one binary variable, $\bar{y}$. Then we reformulate the model (D1) for the contract balance strategy as follows and we denote this formulation as "(D2)":

$$\text{(D2)} \qquad \min \sum_{t\in\mathcal{T}} r_t^1(e_t^1 + b_t^1) - \bar{r}^1\hat{g}^1 + \bar{r}^2\hat{g}^2 \tag{4.18}$$

$$\min \sum_{t\in\mathcal{T}} r_t^2(e_t^2 + b_t^2) - \bar{r}^2\hat{g}^2 + \bar{r}^1\hat{g}^1 \tag{4.19}$$

$$\text{s.t. } (4.5)\text{–}(4.17)$$

$$g^1 \leq \hat{g}^1 \tag{4.20}$$

$$\hat{g}^1 \leq \bar{G}\bar{y} \tag{4.21}$$

$$\hat{g}^1 \leq g^1 + \bar{G}(1-\bar{y}) \tag{4.22}$$

$$g^2 \leq \hat{g}^2 \tag{4.23}$$

$$\hat{g}^2 \leq \bar{G}(1-\bar{y}) \tag{4.24}$$

$$\hat{g}^2 \leq g^2 + \bar{G}\bar{y} \tag{4.25}$$

$$\hat{g}^1, \hat{g}^2 \geq 0 \tag{4.26}$$

$$\bar{y} \in \{0,1\}, \tag{4.27}$$

where $\bar{G}$ is an adequate upper bound of g^1 and g^2, e.g. $\frac{1}{2}|\mathcal{T}|\max\{\bar{C}/\eta^c, \bar{D}/\eta^c\}$.

4.3.2 Uncertainty in the Equality Constraints

As is well-known, the idea of handling uncertainty of robustness optimization is to capture the solution that can provide a backup to maintain the feasibility for worse scenarios, i.e., we need to modify the solution not to bind the inequality constraints under uncertainty. Obviously, we cannot provide a solution that successfully hedges against any parameter perturbation in the equality constraints due to uncertainty.

Unfortunately, we have equality constraint (4.17) with uncertain parameters in our contract balance strategy. Constraint (4.17) restricts that the average price $\bar{r}^i$ should be equal to the weighted average electricity price based on the amount of energy charged during each time period. Obviously, a slight variation on the electricity price r_t^i will violate this constraint, i.e., our obtained average price lacks resilience. In order to handle this particular uncertainty, we change the equality constraint to an inequality constraint:

$$\sum_{t\in\mathcal{T}} r_t^i b_t^i \leq \sum_{t\in\mathcal{T}} \bar{r}^i b_t^i \qquad \forall i \in \mathcal{N}. \tag{4.28}$$

Here, we allow the “average" price (more accurately, exchange price) $\bar{r}^i$ to be larger than the weighted average price. This transformation has two benefits. First, we enable the solution of $\bar{r}^i$ to provide backup, which allows us to obtain a feasible solution working well in all possible scenarios for the price uncertainty. Besides, allowing the exchange price $\bar{r}^i$ to be greater than the average electricity price is meaningful in real-world practice. In order to incentivize the building to store extra energy for selling to other buildings, it is necessary to guarantee that selling stored energy to other buildings is profitable, which requires the exchange price to be greater than the cost, the average price.

When we replace the equality constraint (4.17) with inequality constraint (4.28), however, another issue arises. The objective functions of our contract balance strategy are shown as (4.3) and (4.4). Since we allow $\bar{r}^i$ to be anything but no less than the average price, then if $\hat{g}^1$ is positive, we can keep increasing the value of $\bar{r}^1$ to reduce the operational cost of the first building and simultaneously the cost of the second building is increased to infinity. Hence, there will exist long tails on both sides of the nondominated frontier which is impractical. The building will participate in the cooperation to share ES only if the operational cost can be reduced by the energy arbitrage. Based on this requirement, we are able to provide an upper bound to the operational cost of both buildings as follows:

$$\sum_{t\in\mathcal{T}} r_t^1(e_t^1 + b_t^1) - \bar{r}^1\hat{g}^1 + \bar{r}^2\hat{g}^2 \leq \sum_{t\in\mathcal{T}} r_t^1 L_t^1 \tag{4.29}$$

$$\sum_{t\in\mathcal{T}} r_t^2(e_t^2 + b_t^2) - \bar{r}^2\hat{g}^2 + \bar{r}^1\hat{g}^1 \leq \sum_{t\in\mathcal{T}} r_t^2 L_t^2. \tag{4.30}$$

We assume that the power grid is unlimited, which means the buildings can satisfy their electricity demand without ES. Then the right hand sides of constraints (4.29) and (4.30) indicate the operational cost that the building completely purchases electricity from the power grid to fulfill its electricity load without using ES. Thus, we establish a restriction to avoid $\bar{r}^i$ increasing to an irrational value. We give the formulation for this revised contract balance strategy as follows. To facilitate the illustration of linearizing the bilinear terms, we

use equations (4.33) and (4.34) to represent the bilinear terms in the following formulation which we denote as "(D3)".

$$\text{(D3)} \qquad \min\ z_1 := \sum_{t\in\mathcal{T}} r_t^1(e_t^1 + b_t^1) - v^1 + v^2 \tag{4.31}$$

$$\min\ z_2 := \sum_{t\in\mathcal{T}} r_t^2(e_t^2 + b_t^2) - v^2 + v^1 \tag{4.32}$$

$$\text{s.t. } (4.5)\text{–}(4.16),\ (4.20)\text{–}(4.30)$$

$$v^i = \bar{r}^i \hat{g}^i \qquad \forall i \in \mathcal{N} \tag{4.33}$$

$$w_t^i = \bar{r}^i b_t^i \qquad \forall i \in \mathcal{N} \tag{4.34}$$

$$\sum_{t\in\mathcal{T}} r_t^i b_t^i \le \sum_{t\in\mathcal{T}} w_t^i \qquad \forall i \in \mathcal{N}, \tag{4.35}$$

where v^i is introduced to quantify the payoff for exchanging stored energy and w_t^i represents the regulated cost for charging energy from building $i \in \mathcal{N}$ in time period $t \in \mathcal{T}$. Here, introducing variables v^i and w^i is to facilitate the explanation of using piecewise McCormick relaxation to linearize the bilinear terms in our contract balance strategy.

4.3.3 Formulation for the Robust Contract Balance Strategy

In order to handle the energy price uncertainty for ES sharing, we employ robust optimization to generate the solution that works well with respect to the level of conservatism of players. The formulation for the robust contract balance strategy is established based on the process described in Section 4.2.2. Assume that r_t^i takes values in $[r_t^i, r_t^i + \hat{r}_t^i]$, where $\hat{r}_t^i$ represents the maximum deviation from the nominal price coefficient r_t^i for both objective functions and constraints. This assumption indicates that any increase of the nominal price result in higher operational costs for the buildings.

Assume that the robustness budget, i.e., the level of conservatism, for building i is Γ^i. This in the context of robust optimization implies that exactly $\lfloor \Gamma^i \rfloor$ number of energy prices increase by $\hat{r}_t^i$ and one energy price increases by at most $(\Gamma^i - \lfloor \Gamma^i \rfloor)\hat{r}_t^i$. However, the

main question is which ones? As mentioned in Section 4.2.3, such selection will be done by the robust model automatically. Specifically, the model attempts to create the worst possible scenario, i.e., increasing objective values as much as possible, by selecting the prices that should increase. In other words, the robust model attempts to shift the nondominated frontier for both buildings up as much as possible. In light of these descriptions, the robust counterpart formulation for (D3) is "(R1)".

(R1)

$$\min\ \hat{z}_1 := z_1 + \max_{\{S^1\cup\{t_1\}|S^1\subseteq\mathcal{T},|S^1|\le\lfloor\Gamma^1\rfloor,t_1\in\mathcal{T}\setminus S^1\}}\left\{\sum_{t\in S^1}\hat{r}_t^1(e_t^1+b_t^1)+(\Gamma^1-\lfloor\Gamma^1\rfloor)\hat{r}_{t_1}^1(e_{t_1}^1+b_{t_1}^1)\right\} \tag{4.36}$$

$$\min\ \hat{z}_2 := z_2 + \max_{\{S^2\cup\{t_2\}|S^2\subseteq\mathcal{T},|S^2|\le\lfloor\Gamma^2\rfloor,t_2\in\mathcal{T}\setminus S^2\}}\left\{\sum_{t\in S^2}\hat{r}_t^2(e_t^2+b_t^2)+(\Gamma^2-\lfloor\Gamma^2\rfloor)\hat{r}_{t_2}^1(e_{t_2}^2+b_{t_2}^2)\right\} \tag{4.37}$$

s.t. (4.5)–(4.16), (4.20)–(4.27), (4.33), (4.34)

$$\sum_{t\in\mathcal{T}} r_t^i b_t^i + \max_{\{S^i\cup\{t_i\}|S^i\subseteq\mathcal{T},|S^i|\le\lfloor\Gamma^i\rfloor,t_i\in\mathcal{T}\setminus S^i\}}\left\{\sum_{t\in S^i}\hat{r}_t^i b_t^i+(\Gamma^i-\lfloor\Gamma^i\rfloor)\hat{r}_{t_i}^i b_{t_i}^i\right\} \le \sum_{t\in\mathcal{T}} w_t^i, \qquad \forall i\in\mathcal{N} \tag{4.38}$$

$$z_i + \max_{\{S^i\cup\{t_i\}|S^i\subseteq\mathcal{T},|S^i|\le\lfloor\Gamma^i\rfloor,t_i\in\mathcal{T}\setminus S^i\}}\left\{\sum_{t\in S^i}\hat{r}_t^i(e_t^i+b_t^i)+(\Gamma^i-\lfloor\Gamma^i\rfloor)\hat{r}_{t_i}^i(e_{t_i}^i+b_{t_i}^i)\right\} \le \sum_{t\in\mathcal{T}} r_t^i L_t^i + \max_{\{S^i\cup\{t_i\}|S^i\subseteq\mathcal{T},|S^i|=\lfloor\Gamma^i\rfloor,t_i\in\mathcal{T}\setminus S^i\}}\left\{\sum_{t\in S^i}\hat{r}_t^i L_t^i+(\Gamma^i-\lfloor\Gamma^i\rfloor)\hat{r}_{t_i}^i L_{t_i}^i\right\}, \qquad \forall i\in\mathcal{N}, \tag{4.39}$$

where Γ^i takes values in the interval $[0,|\mathcal{T}|]$. The parameter Γ^i restricts the maximal number of the uncertain prices in the objective functions and the constraints that are allowed to change. It is an indicator to the budget that each building in the ES sharing system reserves to protect themselves against the energy price uncertainty. Since we assume that the buildings can adopt different energy price plans, they can independently decide their

uncertain budget Γ^i based on their knowledge to the uncertain prices and their specific risk preferences. Additionally, in practice the uncertain price is the real-time price. Real-time price, as a demand response program of the utility company, is decided by the energy supply and demand in energy market. The variations of real-time energy price of time t does not directly influence on the price of time t+1. Hence, the uncertainty budget Γ^i is not subject to the time series of energy price.

Objectives (4.36) and (4.37) contain two parts: the deterministic operational costs, i.e., the objectives of model (D3), and the maximal increments of the operational costs caused by the price uncertainty. These objectives guarantee the robustness of the minimal operational costs of both buildings by minimizing the maximal increments of the costs. Note that in objectives (4.36) and (4.37), z_i is a function that is defined in (D3). Therefore the compensation v^i is in z_i and it will be affected by the price uncertainty as it contains the average price $\bar{r}^i$. Specifically, the robustness of the compensation v^i is achieved by constraint (4.38). Constraint (4.38) is the robust counterpart of constraint (4.35). The left hand side of Constraint (4.38) is the maximal cost for the building charging the ES. The right hand side of Constraint (4.38) is the cost for charging the ES computed based on the exchange price. Hence, constraint (4.38) can maintain the exchange price for the stored energy exchange to be larger than the average price under the price uncertainty.

Constraint (4.39) is the robust counterpart of constraints (4.29) and (4.30) to remove the irrational part of the nondominated frontier. The left hand side of constraint (4.39) is the objective value $\hat{z}_i$. The right hand side of constraint (4.39) is the maximum cost that the building can achieve if completely using the power grid to satisfy its load under fixed Γ^i. For each $i \in \mathcal{N}$, let

$$z_i^P := \sum_{t\in\mathcal{T}} r_t^i L_t^i + \max_{\{S^i\cup\{t^i\}|S^i\subseteq\mathcal{T},|S^i|=\lfloor\Gamma^i\rfloor,t^i\in\mathcal{T}\setminus S^i\}} \left\{ \sum_{t\in S^i} \hat{r}_t^i L_t^i + (\Gamma^i - \lfloor\Gamma^i\rfloor) L_t^i \right\}.$$

Obviously, z_i^P is constant for this robust counterpart formulation and can be computed easily in advance if r_t^i, $\hat{r}_t^i$ and Γ^i are given. Note that the purpose of constraint (4.39) is to cut

the nondominated frontier at the rational point. In constraint (4.39), the operational costs of each building should be no larger than a rational amount, i.e., the operational cost each building can achieve if they completely purchase electricity from the power grid to fulfill their demand. If $\hat{z}_i \leq z_i^P$, then some optimistic decision makers are willing to participate in the ES sharing for cost saving purposes. Of course, some pessimistic decision makers would cooperate only if $\hat{z}_i \leq \lambda z_i^P$ where λ assumes values in $(0, 1)$. Overall, if $\hat{z}_i > z_i^P$, no decision maker would share ES, since at that exchange price, they will always experience a higher operational cost than not using ES for all possible scenarios. z_i^P is the threshold at which the maximum exchange price can be achieved for the buildings sharing ES and exchanging the stored energy.

Equivalently for transforming (RC) to (RE), we can present the linear transformation of (R1) as follows and we denote this formulation as "(R2)".

$$
\begin{aligned}
\text{(R2)} \qquad & \min \ \bar{z}_1 := z_1 + \theta_0^1 \Gamma^1 + \sum_{t \in \mathcal{T}} \beta_{0t}^1 && && (4.40)\\
& \min \ \bar{z}_2 := z_2 + \theta_0^2 \Gamma^2 + \sum_{t \in \mathcal{T}} \beta_{0t}^2 && && (4.41)\\
& \text{s.t. } (4.5)\text{–}(4.16),\ (4.20)\text{–}(4.27),\ (4.33),\ (4.34) \\
& \quad \theta_0^i + \beta_{0t}^i \geq \hat{r}_t^i (e_t^i + b_t^i) && \forall i \in \mathcal{N}, \forall t \in \mathcal{T} && (4.42)\\
& \quad \sum_{t \in \mathcal{T}} r_t^i b_t^i + \theta_1^i \Gamma^i + \sum_{t \in \mathcal{T}} \beta_{1t}^i \leq \sum_{t \in \mathcal{T}} w_t^i && \forall i \in \mathcal{N} && (4.43)\\
& \quad \theta_1^i + \beta_{1t}^i \geq \hat{r}_t^i b_t^i && \forall i \in \mathcal{N}, \forall t \in \mathcal{T} && (4.44)\\
& \quad z_i + \theta_0^i \Gamma^i + \sum_{t \in \mathcal{T}} \beta_{0t}^i \leq z_i^P && \forall i \in \mathcal{N} && (4.45)\\
& \quad \theta_0^i, \theta_1^i, \beta_{0t}^i, \beta_{1t}^i \geq 0 && \forall i \in \mathcal{N}, \forall t \in \mathcal{T}. && (4.46)
\end{aligned}
$$

Compared to the deterministic model (D3), model (R2) has $2 \times |\mathcal{N}| \times (|\mathcal{T}| + 1)$ more number of variables and $2 \times |\mathcal{N}| \times (|\mathcal{T}| + 0.5)$ more number of constraints. This implies that the size complexity of the robust model (R2) is greater than the deterministic model (D3). However,

since all the constraints introduced are linear, an algorithm that can solve (D3) can be applied to solve (R2).

4.4 Linearization Technique for the Bilinear Terms

In this section, we introduce an approximation technique based on the so-called McCormick relaxation (see for instance [80, 81]) to linearize the bilinear terms in our robust contract balance strategy. As is well-known, the McCormick relaxation is capable of linearizing a bilinear term with two bounded continuous variables using the so-called McCormick envelopes. However, the solution of the McCormick relaxation is an approximation of the original bilinear term, and the quality of this approximation is domain-dependent. Hence, we adopt a piecewise approach to the McCormick relaxation to capture a high-quality approximation of the bilinear term. The piecewise McCormick relaxation is done by partitioning the domain of a variable in the bilinear term into several sequential intervals and applying McCormick relaxations to the bilinear terms formed in every interval.

The common approach to execute the piecewise McCormick relaxation is unary formulation based. This unary formulation introduces a set of binary variables to indicate which partition of the bilinear terms is activated. For example, if the 4^{th} binary variable in the set is equal to 1, it indicates the value of the partitioned variable in the bilinear term should be chosen in the 4^{th} partition of its range and all the other binary variables in the set should be equal to 0. The issue for the unary formulation is that when we increase the partition numbers for high quality approximations, the formulation becomes computationally intractable.

To counter this defect of the unary formulation and improve the computational efficiency for large partition numbers, we introduce a binary formulation based piecewise McCormick relaxation to linearize the bilinear terms constructed by two continuous variables. The binary formulation employs an integer variable to indicate the index of the activated partition of the bilinear term and the value of this integer variable is represented by the bi-

nary numeral system. For example, if the 4^{th} partition is activated, then this integer variable is represented as $1 \times 2^2 + 0 \times 2^1 + 0 \times 2^0$. In the following, we present the details of these two versions of piecewise McCormick relaxations.

4.4.1 Mathematical Models for Piecewise McCormick Relaxations

For bounded continuous variables $x \in [\underline{X}, \bar{X}]$ and $y \in [\underline{Y}, \bar{Y}]$, and a variable w representing the product of x and y, consider the following bilinear set

$$\mathbf{P}(w) := \Big\{(x, y, w) \in \mathbb{R}_+ \times \mathbb{R}_+ \times \mathbb{R}_+ : w = xy; \underline{X} \leq x \leq \bar{X}; \underline{Y} \leq y \leq \bar{Y}\Big\},$$

where w in the notation $\mathbf{P}(w)$ indicates that this set is constructed for the bilinear term xy.

The unary formulation based piecewise McCormick relaxation is expressed as follows. Assume that we separate variable y into M pieces. Then

$$\begin{aligned}\mathbf{M}(w) :=\Big\{&(x, \tilde{x}, y, \tilde{y}, z, w) \in \mathbb{R}_+ \times \mathbb{R}_+^M \times \mathbb{R}_+ \times \mathbb{R}_+^M \times \{0,1\}^M \times \mathbb{R}_+ : x = \sum_{i=1}^{M} \tilde{x}_i; \quad y = \sum_{i=1}^{M} \tilde{y}_i; \\ &w \geq \sum_{i=1}^{M} (\underline{Y}_i \tilde{x}_i + \underline{X} \tilde{y}_i - \underline{Y}_i \underline{X} z_i); \quad w \geq \sum_{i=1}^{M} (\bar{Y}_i \tilde{x}_i + \bar{X} \tilde{y}_i - \bar{Y}_i \bar{X} z_i); \quad w \leq \sum_{i=1}^{M} (\bar{Y}_i \tilde{x}_i + \\ &\underline{X} \tilde{y}_i - \bar{Y}_i \underline{X} z_i); \quad w \leq \sum_{i=1}^{M} (\underline{Y}_i \tilde{x}_i + \bar{X} \tilde{y}_i - \underline{Y}_i \bar{X} z_i); \ \sum_{i=1}^{M} z_i = 1; \quad \underline{X} z_i \leq \tilde{x}_i \leq \bar{X} z_i, \\ &\forall i \in \{1, \ldots, M\}; \quad \underline{Y}_i z_i \leq \tilde{y}_i \leq \bar{Y}_i z_i, \quad \forall i \in \{1, \ldots, M\}\Big\}.\end{aligned}$$

where $\underline{Y}_i$ and $\bar{Y}_i$ are the lower and upper bounds for y_i if the i-th piece is activated. Apply the following formula to compute $\underline{Y}_i$ and $\bar{Y}_i$:

$$\begin{aligned}\underline{Y}_i &:= \underline{Y} + \frac{(\bar{Y} - \underline{Y})(i-1)}{M}, \\ \bar{Y}_i &:= \underline{Y} + \frac{(\bar{Y} - \underline{Y})i}{M}.\end{aligned}$$

Based on Section 5.2.2 in the thesis of [97], if the bilinear term is constructed by a continuous and an integer variable, we can conduct a binary expansion on its piecewise McCormick relaxation. Assume y is the integer variable and in the range $[0, \bar{Y}]$. Then the binary expansion formulation is given as follows:

$$\begin{aligned}\mathbf{B}(w) :=\Bigg\{&(x, y, w, z, u) \in \mathbb{R}_+ \times \mathbb{Z}_+ \times \mathbb{R}_+ \times \{0,1\}^K \times \mathbb{R}_+^K : w = \sum_{k=1}^{K} 2^{k-1} u_k; \quad \sum_{k=1}^{K} 2^{k-1} z_k \leq \bar{Y}; \\ &u_k \geq \underline{X} z_k, \quad \forall k \in \{1, \ldots, K\}; \quad u_k \geq x + \bar{X} z_k - \bar{X}, \quad \forall k \in \{1, \ldots, K\}; \quad u_k \leq x + \\ &\underline{X} z_k - \underline{X}, \quad \forall k \in \{1, \ldots, K\}; \quad u_k \leq \bar{X} z_k, \quad \forall k \in \{1, \ldots, K\}\Bigg\},\end{aligned}$$

where $K = \lfloor \log_2 \bar{Y} \rfloor + 1$.

Since the binary expansion for piecewise McCormick relaxations only applies to mixed integer bilinear terms, we transfer $\mathbf{P}(w)$ into the following form:

$$\begin{aligned}\mathbf{I}(w) :=\Bigg\{&(x, p, q, w) \in \mathbb{R}_+ \times \mathbb{Z}_+ \times \mathbb{R}_+ \times \mathbb{R}_+ : w = x\underline{Y} + Dxp + xq; \underline{X} \leq x \leq \bar{X}; p \leq M - 1; \\ &q \leq D\Bigg\},\end{aligned}$$

where M is the number of pieces we want to separate the variable y into, and $D = (\bar{Y} - \underline{Y})/M$ is the length of each piece on the y-axis. We employ the binary expansion formulation $\mathbf{B}$ to handle the mixed integer bilinear term xp, and the standard McCormick relaxation to relax xq. Hence, the binary formulation based piecewise McCormick relaxation for $\mathbf{I}(w)$ is given

by the following formulation:

$$\begin{aligned}\mathbf{C}(w) :=\Big\{ & (x,q,z,w,u,v) \in \mathbb{R}_+ \times \mathbb{R}_+ \times \{0,1\}^K \times \mathbb{R}_+ \times \mathbb{R}_+^K \times \mathbb{R}_+ : w = \underline{Y}x + D\sum_{k=1}^{K} 2^{k-1}u_k \\ & + v; \sum_{k=1}^{K} 2^{k-1}z_k \leq M-1; \quad v \geq \underline{X}q; \quad v \geq Dx + \bar{X}q - D\bar{X}; \quad v \leq Dx + \underline{X}q - D\underline{X}; \\ & v \leq \bar{X}q; \quad u_k \geq \underline{X}z_k, \quad \forall k \in \{1,\ldots,K\}; \quad u_k \geq x + \bar{X}z_k - \bar{X}, \quad \forall k \in \{1,\ldots,K\}; \\ & u_k \leq x + \underline{X}z_k - \underline{X}, \quad \forall k \in \{1,\ldots,K\}; \quad u_k \leq \bar{X}z_k, \quad \forall k \in \{1,\ldots,K\}\Big\},\end{aligned}$$

where $K = \lceil \log_2 M \rceil$.

4.4.2 Piecewise McCormick Relaxation for the Robust Formulation

In this section, we adopt the binary formulation based piecewise McCormick relaxation $\mathbf{C}(w)$ to handle the bilinear terms in the robust formulation (R2) for the robust contract balance strategy.

Before giving a detailed formulation of this relaxation, we first define the domains of the variables participating in the bilinear terms as follows:

- $b_t^i \in [\underline{A}, \bar{A}]$ for all $i \in \mathcal{N}$ and $t \in \mathcal{T}$. If $s_t^c = 0$, then $b_t^i = 0$, and if $s_t^c = 1$, then $b_t^i \in [\bar{C}/\eta^c, \bar{C}/\eta^c]$. To ensure the feasibility, we determine the complete domain of b_t^i as $[\underline{A}, \bar{A}]$ where $\underline{A} = 0$ and $\bar{A} = \bar{C}/\eta^c$.

- $\bar{r}^i \in [\underline{R}^i, \bar{R}^i]$ for all $i \in \mathcal{N}$ where $\underline{R}^i := \min\{r_t^i : t \in \mathcal{T}\}$ and $\bar{R}^i := \max\{r_t^i + \hat{r}_t^i : t \in \mathcal{T}\}$. Since $\bar{r}^i$ occurs in each bilinear term, we conduct the partitioning on the domain of $\bar{r}^i$. Furthermore, based on the comparison of piecewise numbers in [47], we equally separate the domain of $\bar{r}^i$ into 32 pieces, i.e $M = 32$.

- $\hat{g}^i \in [\underline{G}, \bar{G}]$ for all $i \in \mathcal{N}$ where $\underline{G} := 0$ and $\bar{G} := \frac{1}{2}|\mathcal{T}| \max\{\bar{C}/\eta^c, \bar{D}/\eta^c\}$. The upper bound can be obtained by assuming that one building only charges the electrical ES

and the other only discharges. So, given that the storage cannot be at both charging and discharging states at the same time, the result follows.

Furthermore, we introduce the following variables to facilitate the binary formulation based piecewise McCormick relaxation for the robust formulation (R2):

- We select the variable $\bar{r}^i$ for all $i \in \mathcal{N}$ for partitioning due to its co-occurrence in all of the bilinear terms. Assume we partition $\bar{r}^i$ into M pieces. Then we can rewrite $\bar{r}^i$ in a mixed integer form by the following formulation $\mathbf{I}(w)$: $\bar{r}^i = \underline{R}^i + D^i p^i + q^i$, where $D^i = (\bar{R}^i - \underline{R}^i)/M$, $p^i \in \{o \in \mathbb{Z}_+ : o \leq M-1\}$, and $q^i \in \{s \in \mathbb{R}_+ : s \leq D^i\}$.

- We introduce binary variables y^i_k for all $i \in \mathcal{N}$ and $k \in \{1, \ldots, K\}$ to express the integer variable p^i in the binary numeral system, i.e., $p^i = \sum_{k=1}^{K} 2^{k-1} y^i_k$, where $K = \lceil \log_2(M-1) \rceil$.

- Based on formulation $\mathbf{C}(w)$, we introduce continuous variables h^i_k and f^i to represent $v^i = \underline{R}^i \hat{g}^i + D^i \sum_{k=1}^{K} 2^{k-1} h^i_k + f^i$ for all $i \in \mathcal{N}$, and continuous variables u^i_{tk} and l^i_t to represent $w^i_t = \underline{R}^i b^i_t + D^i \sum_{k=1}^{K} 2^{k-1} u^i_{tk} + l^i_t$ for all $i \in \mathcal{N}$ and $t \in \mathcal{T}$.

Hence, the binary formulation based piecewise McCormick relaxation for the robust model (R2) can be expressed as follows and we denote this formulation as "(R3)":

$$\text{(R3)} \qquad \min \ \bar{z}_1 = z_1 + \theta^1 \Gamma^1 + \sum_{t \in \mathcal{T}} \beta^1_{0t} \tag{4.47}$$

$$\min \ \bar{z}_2 = z_2 + \theta^2 \Gamma^2 + \sum_{t \in \mathcal{T}} \beta^2_{0t} \tag{4.48}$$

$$\text{s.t. } (4.5)\text{–}(4.16),\ (4.20)\text{–}(4.27),\ (4.42)\text{–}(4.46)$$

$$(\hat{g}^i, q^i, y^i, v^i, h^i, f^i) \in \mathbf{C}(v^i) \qquad \forall i \in \mathcal{N} \tag{4.49}$$

$$(b^i_t, q^i, y^i, w^i_t, u^i_t, l^i_t) \in \mathbf{C}(w^i_t) \qquad \forall i \in \mathcal{N},\ t \in \mathcal{T}, \tag{4.50}$$

where $\mathbf{C}(v^i)$ denotes the set representing the binary formulation based piecewise McCormick relaxation for $v^i = \bar{r}^i \hat{g}^i$, and $\mathbf{C}(w^i_t)$ for $w^i_t = \bar{r}^i b^i_t$.

4.5 Computational Study

Case studies are presented in this section to demonstrate that 1) the binary formulation can significantly improve the computational efficiency of piecewise McCormick relaxations without quality loss when compared to the unary formulation, 2) the robust solution derived from our robust contract balance strategy can provide remarkable benefits in contrast to the deterministic solution in terms of price uncertainty handling for the ES sharing problem, and 3) it is capable of optimizing on the nondominated frontier to obtain a solution with balanced cooperation benefits distribution.

We implement all formulations and the solution algorithm TSM in C++ with CPLEX 12.7 as the single-objective MILP solver. All computational experiments have been carried out on a Dell PowerEdge R630 with two Intel Xeon E5-2650 2.2 GHz 12-Core Processors (30MB), 128GB RAM, the RedHat Enterprise Linux 6.8 operating system, and using a single thread.

In the experiments, we select one day as our planning horizon, and one hour as the length of each time period. Thus, we have 24 time periods in the planning horizon, i.e., $|\mathcal{T}| = 24$. Note that the uncertainty in energy price arises by the real-time pricing in practice. Real-time pricing program, as one of efficient demand response programs implemented by utility companies, publishes the energy price on hourly basis. Utility companies also publish the so-called day-ahead prices that are predictions to the hourly real-time prices for the next day to guide the customers to plan their energy consumption. Hence, our selection of the planning horizon and the length of time period matches with the practice of energy price uncertainty. We assume that there is no recourse decision in the real-time, i.e., the buildings and their storage determine their plans one day ahead.

The dataset for testing our robust optimization based contract balance strategy contains six classes. Each class includes the same 20 instances and different values for Γ^i and $\hat{r}_t^i$. These 20 instances are generated by randomly drawing r_t^i and L_t^i for each $i \in \mathcal{N}$ and

$t \in \mathcal{T}$ as uniformly distributed integers from the interval $[1, 20]$. The capacity of the battery is set to $\bar{B} = 2 \times \max\{L_t^i : \forall i \in \mathcal{N}, \forall t \in \mathcal{T}\} = 40$ and $\underline{B} = 1$. Furthermore, we assume that $\bar{C} = \bar{D} = 0.2 \times \bar{B}$ and $\underline{C} = \underline{D} = 0.05 \times \bar{B}$. We form six different classes by changing the values of Γ^i and $\hat{r}_t^i$ in the robust formulation. Specifically, let $\Gamma^i = \mu \times |\mathcal{T}|$ where $\mu \in [0, 1]$ and $\hat{r}_t^i = \upsilon \times r_t^i$ where $\upsilon \in [0, \infty)$. For class A, we set $\mu = 0.3$ and $\upsilon = 0.3$, for class B, $\mu = 0.6$ and $\upsilon = 0.3$, for class C, $\mu = 0.3$ and $\upsilon = 0.6$, and for class D, $\mu = 0.6$ and $\upsilon = 0.6$. The values of υ are randomly chosen from the interval $[0, 0.6]$ in class E with $\mu = 0.3$, and in class F with $\mu = 0.6$.

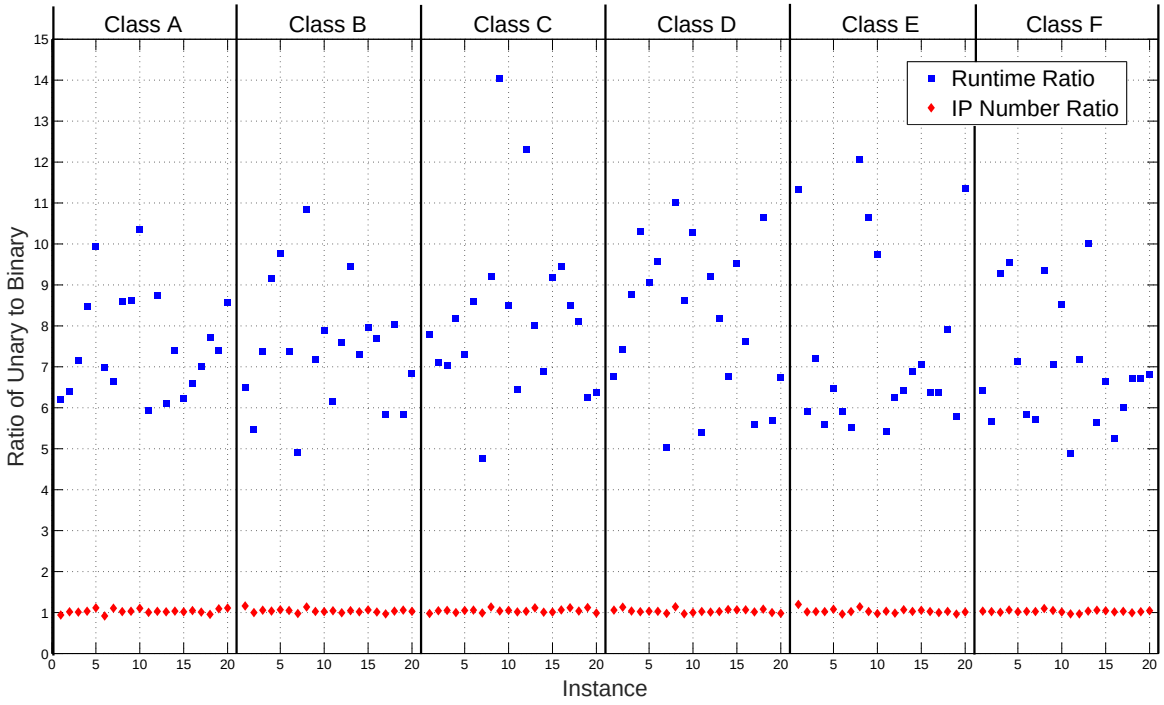

Figure 4.3 – Runtime and IP ratios of unary to binary formulation

4.5.1 Efficiency of Binary Formulation for Piecewise McCormick Relaxation

This section presents the comparison between the binary and unary formulation for the piecewise McCormick relaxation. We employ TSM to solve the bi-objective MILP to generate their exact nondominated frontier.

Table 4.2 – Runtime and IPs results for binary vs unary formulation

		Binary Formulation		Unary Formulation				Binary Formulation		Unary Formulation	
Class	Instance	Time(s)	IPs	Time(s)	IPs	Class	Instance	Time(s)	IPs	Time(s)	IPs
	1	42.1	131	261.5	123		1	40.8	144	265.2	167
	2	33.9	112	216.6	114		2	32.0	124	175.1	124
	3	78.6	182	561.8	184		3	79.4	178	585.8	188
	4	53.3	215	451.4	222		4	114.9	267	1051.6	277
	5	32.7	96	325.2	107		5	50.4	145	492.2	155
	6	37.1	144	258.7	132		6	35.3	117	260.6	123
	7	43.5	162	288.3	179		7	63.7	205	312.8	200
	8	11.0	85	94.5	87		8	10.6	89	114.6	101
	9	89.3	124	769.4	128		9	64.4	109	462.6	112
	10	137.0	232	1416.8	256		10	70.5	169	556.1	173
A	11	48.5	235	287.3	236	**B**	11	38.2	206	234.9	215
	12	182.7	205	1595.9	211		12	163.3	216	1240.0	215
	13	41.7	166	255.1	169		13	87.7	194	829.3	203
	14	146.8	318	1085.9	329		14	119.9	218	874.4	222
	15	36.0	113	224.0	115		15	38.3	125	304.3	133
	16	122.1	207	806.3	217		16	92.1	212	708.9	215
	17	17.5	83	122.8	84		17	27.6	89	160.6	86
	18	85.3	206	658.8	197		18	91.2	207	733.6	214
	19	29.2	142	216.5	155		19	28.1	170	164.2	180
	20	115.3	219	986.9	243		20	114.9	267	785.0	275
	Ave	**69.2**	**169**	**544.2**	**174**		**Ave**	**68.2**	**173**	**515.6**	**179**
	1	51.5	128	400.8	125		1	60.8	168	411.5	178
	2	66.9	188	476.2	196		2	31.5	114	233.5	129
	3	93.6	189	657.5	199		3	104.3	191	915.2	198
	4	31.4	149	257.1	149		4	59.8	189	615.8	193
	5	28.8	80	210.7	84		5	54.1	184	490.4	190
	6	35.0	133	301.0	141		6	49.7	136	476.0	140
	7	85.0	188	405.3	186		7	55.8	180	280.3	176
	8	12.7	74	116.8	84		8	18.3	107	201.9	122
	9	30.2	76	424.5	79		9	84.2	130	726.2	126
	10	63.1	170	535.8	179		10	96.0	174	987.7	174
C	11	37.5	195	241.7	198	**D**	11	35.4	195	190.8	200
	12	146.3	167	1800.3	172		12	157.5	189	1449.8	191
	13	20.6	95	164.9	106		13	73.0	167	597.5	171
	14	160.2	259	1101.8	261		14	150.1	230	1013.1	247
	15	29.2	84	268.0	85		15	50.7	151	483.7	161
	16	150.2	221	1418.8	235		16	126.7	214	964.8	228
	17	12.6	60	106.8	67		17	27.6	89	160.6	86
	18	76.1	194	616.7	201		18	39.1	144	309.6	148
	19	27.4	107	170.8	120		19	25.4	135	146.8	130
	20	71.6	159	457.4	157		20	136.5	209	920.4	205
	Ave	**61.5**	**146**	**506.6**	**151**		**Ave**	**74.3**	**168**	**607.3**	**174**
	1	43.1	147	488.0	176		1	75.2	204	483.8	211
	2	49.1	246	290.1	250		2	45.8	181	259.5	185
	3	98.8	184	711.5	188		3	70.7	179	655.6	180
	4	65.4	232	365.5	237		4	67.0	213	638.9	226
	5	20.3	75	131.1	81		5	37.4	110	267.1	112
	6	30.8	165	181.8	159		6	42.0	184	245.0	189
	7	77.9	186	429.6	190		7	103.5	278	591.9	285
	8	11.1	64	133.8	73		8	56.3	164	526.7	180
	9	39.4	83	419.8	85		9	33.8	122	238.5	128
	10	111.5	199	1087.2	194		10	96.1	230	819.1	233
E	11	32.9	192	177.9	198	**F**	11	41.0	149	200.9	144
	12	200.0	205	1250.3	202		12	159.6	213	1144.8	206
	13	71.8	158	460.1	169		13	129.5	259	1295.6	268
	14	107.4	267	739.0	274		14	136.7	230	772.5	243
	15	32.6	110	230.6	116		15	41.5	210	275.4	219
	16	116.4	211	742.2	216		16	94.7	185	497.1	188
	17	54.5	190	347.8	190		17	55.6	166	333.7	171
	18	39.1	144	309.6	148		18	111.4	244	748.1	243
	19	25.4	135	146.8	130		19	48.1	156	323.5	159
	20	123.6	240	1404.0	243		20	124.0	247	844.7	258
	Ave	**67.5**	**172**	**502.3**	**176**		**Ave**	**78.5**	**196**	**558.1**	**201**

Figure 4.3 presents the runtime ratio and IP number ratio of unary formulation to binary formulation. Note that the runtime indicates the time it takes the TSM to solve a bi-objective MILP and to generate its entire nondominated frontier, and IP number is the number of single objective IPs solved by TSM in this process. Let T_B be the runtime of the binary formulation and T_U of the unary one. The points in Figure 4.3 marked as *squares* denote the runtime ratio $R_T = T_U/T_B$. Let I_B be the IP number of the binary formulation and I_U of the unary one. The points in Figure 4.3 marked as *diamonds* denote the IP number ratio $R_I = I_U/I_B$. It is shown that the runtime ratio R_T ranges from 5 to 14, and its average is approximately 8. The results imply that our binary formulation is able to guarantee at least 80% runtime reduction, and on average 87.5% in runtime savings compared to the unary formulation. In addition, the IP number ratios are shown to be close to 1, which means the number of single objective IPs solved for both the binary and the unary formulation are almost the same. For more details about the comparison between binary and unary formulation for piecewise McCormick relaxation, see Table 4.2. Table 4.2 shows the details of the run time and IP numbers for both the binary and unary formulation based piecewise McCormick relaxations. In the table, "Time" indicates the run time when using TSM to solve the binary and unary formulation based piecewise McCormick relaxation of (R2), and "IPs" the number of single objective IPs solved. Additionally, "Ave" denotes the average run time and IP numbers of all instances in the given class. We can conclude that the reason why the binary formulation can significantly reduce the runtime compared to the unary formulation is that the runtime to solve a single objective IP is significantly decreased.

In addition, one may consider the difference between the solutions of binary and unary formulations. Figure 4.4 compares the nondominated frontiers of binary and unary formulations for one instance in six classes. The blue line represents the nondominated frontier for the binary formulation, and the dashed red line the nondominated frontier for the unary formulation. It is clear that the frontiers of both the binary and the unary formulation

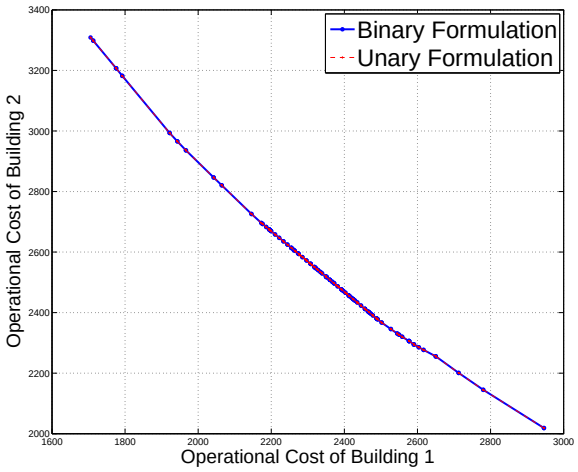

(a) Class A

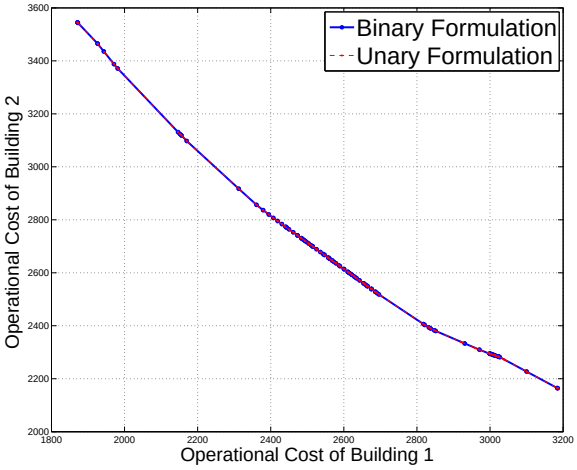

(b) Class B

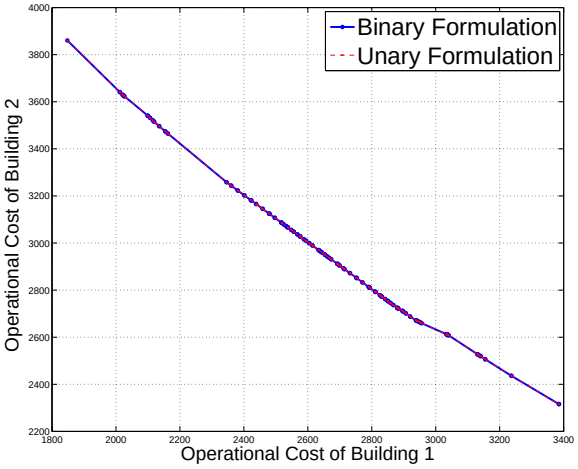

(c) Class C

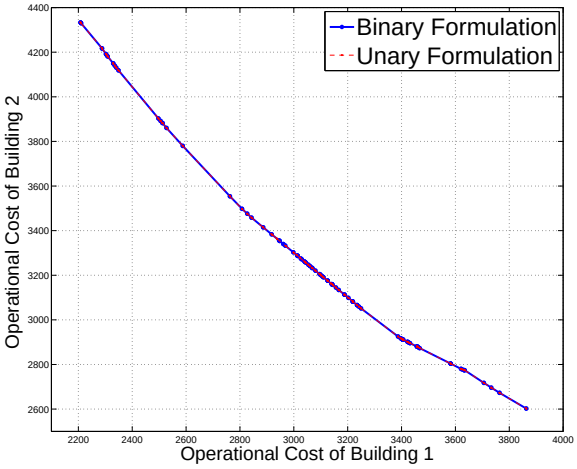

(d) Class D

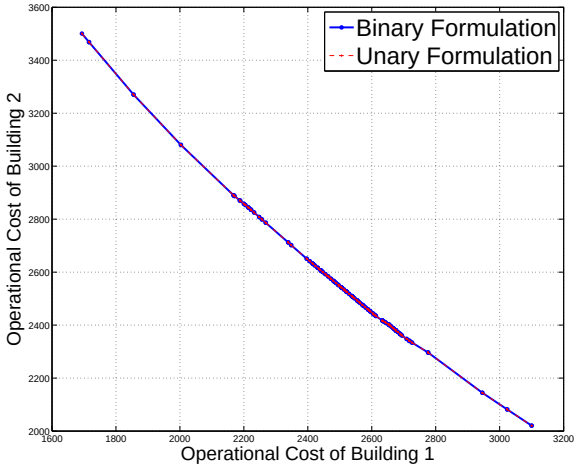

(e) Class E

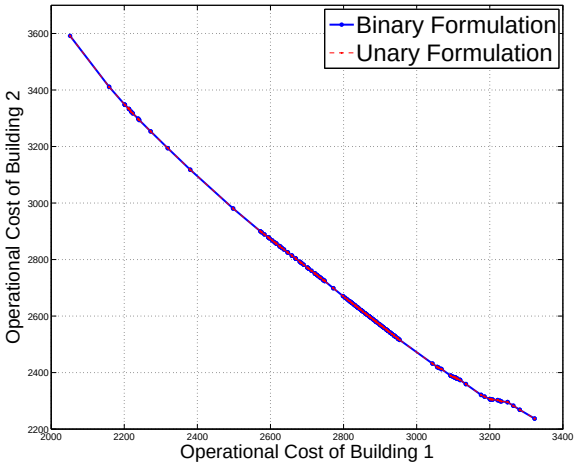

(f) Class F

Figure 4.4 – Nondominated frontiers for Binary and Unary formulations

overlap except for several endpoints on the frontier which differ. Furthermore, even though there exists some bending on the frontiers in Class F, the shapes of the frontiers of both the binary and the unary formulation are still almost identical. Hence, we have illustrated that both the binary and the unary formulation represent almost identical solutions, and their differences are negligible.

These experimental results confirm that directly solving the binary formulation for our robust contract balance strategy (R3) is more efficient than solving the unary formulation, and the solutions for both formulations are almost identical.

4.5.2 Effectiveness of the Robust Contract Balance Strategy

In order to validate the effectiveness of the robust optimization based contract balance strategy for managing the uncertain energy price, we compare the robust solution $x^r \in \mathcal{X}_E^R$ (where $\mathcal{X}_E^R$ is the efficient set for the robust model (R2)) with the deterministic solution $x^d \in \mathcal{X}_E^D$ (where $\mathcal{X}_E^D$ is the efficient set for the deterministic model (D3)). The deterministic solution x^d can be interpreted as the solution obtained by setting the mean of the uncertain prices as the prediction. Note that these efficient sets are captured by solving the binary formulation based piecewise McCormick relaxation of (R2) and (D3).

Since x^r and x^d are both Pareto-optimal for (R2) and (D3), respectively, the way we conduct this comparison is to evaluate the performance of x^r for (D3) and of x^d for (R2). Let "(RtoD)" denote the deterministic model obtained from fixing some of the decision variables of (D3) to the value of the corresponding variables in x^r, and let "(DtoR)" denote the robust model obtained from fixing some of the decision variables of (R2) to the value of the corresponding variables in x^d. Thus, the performance of x^r for (D3) and of x^d for (R2) can be represented by the results of (RtoD) and (DtoR), respectively. The fixed variables in both (RtoD) and (DtoR) include e_t^i, b_t^i, d_t^i, m_t, s_t^c, s_t^d, g^i, and $\hat{g}^i$. Obviously, models (RtoD) and (DtoR) are still bi-objective optimization problems. Note that we do not apply piecewise McCormick relaxations to these two formulations due to the fact that one of the variables

participating in the bilinear terms has been fixed, i.e., (RtoD) and (DtoR) are bi-objective MILPs and can directly be solved by TSM. Moreover, the frontier of (RtoD) or (DtoR) is a segment without any bending or discontinuity, because the sum of the operational costs of both buildings is fixed if the above variables are fixed.

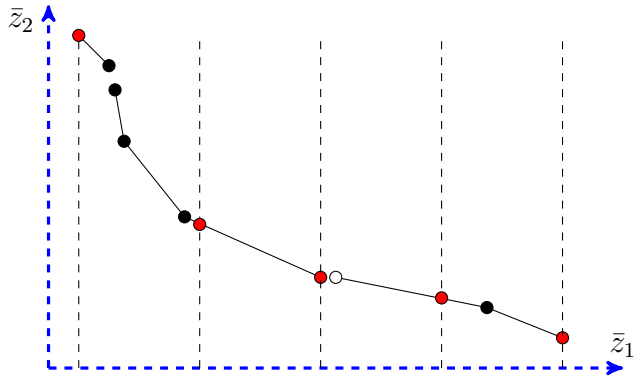

Figure 4.5 – The process to select a subset of $\mathcal{X}_E^R$ or $\mathcal{X}_E^D$

When using x^r and x^d to formulate (RtoD) and (DtoR), we cannot apply every solution in $\mathcal{X}_E^R$ and $\mathcal{X}_E^D$ since they are infinite sets. Our approach is to select a finite subset of $\mathcal{X}_E^R$ and $\mathcal{X}_E^D$ and apply all solutions in this subset. To achieve this, we select $I+1$ (where $I > 0$ is a user-defined parameter) points from the nondominated frontier of (D3) by vertically partitioning it into I pieces with equal length. The selected points are on the boundary of each partitions. Figure 4.5 presents an example to select a finite subset of points from a nondominated frontier with $I = 4$. In this figure, the red points are selected to construct the subset. After picking the points, we construct a set, denoted by $\mathcal{X}^D$, that contains an efficient solution corresponding to each of the points. Obviously, $\mathcal{X}^D \subseteq \mathcal{X}_E^D$ is finite and this enables us to formulate (DtoR) for all $x^d \in \mathcal{X}^D$. Similarly, we select $I+1$ points from the nondominated frontier of (R2) by vertically partitioning it into I equal segments with respect to the $\bar{z}^1$-axis. After picking the points, we construct a set, denoted by $\mathcal{X}^R$, that contains an efficient solution corresponding to each of the points. Obviously, $\mathcal{X}^R \subseteq \mathcal{X}_E^R$ is finite and this enables us to formulate (RtoD) for all $x^r \in \mathcal{X}^R$. In summary, with the efficient solutions in $\mathcal{X}^R$ and $\mathcal{X}^D$, we obtain finite (RtoD) and (DtoR) models.

Figure 4.6 shows a comparison between the nondominated frontiers of (R2), (D3), and some (RtoD) and (DtoR) models for one instance in six classes. For the (RtoD) and (DtoR) models we set $I = 5$ and then we obtain six (RtoD) and six (DtoR) models. In the legend, "Robust Frontier" implies the frontiers of (R2), "Deterministic Frontier" the frontiers of (D3), "Robust to Deterministic" the frontiers of (RtoD), and "Deterministic to Robust" the frontiers of (DtoR).

First, we can see in Figure 4.6 that the frontiers of (DtoR) are always dominated by the frontier of (R2), which means the deterministic solution always increases the operational cost of both buildings in contrast to the robust solution when a certain level of robustness should be maintained under the price uncertainty. This is the first advantage of the robust solution x^r: it guarantees the best outcome for robust model (R2). Additionally, as can be seen in Figure 4.6, the frontiers of (RtoD) are intuitively very close to the frontier of (D3). This implies that for the most optimistic scenario, i.e., the nominal scenario, operating the energy system following the robust solution can still achieve almost the same performance as the deterministic solution. We also find that the gap between the frontiers of (DtoR) and the frontiers of (R2) is significant. It indicates that the deterministic solution will result in a notable benefit loss in contrast to the robust solution when a certain robustness is being sought to handle price uncertainty. The gap between the frontiers of (DtoR) and (R2) is enlarged as well with an increased value of $\hat{r}^i$ when comparing Figure 4.6(a) with 4.6(c) and 4.6(b) with 4.6(d). Thus, the second advantage of the robust solution x^r is uncovered: the performance of implementing x^r for deterministic model (D3) is better than implementing x^d for robust model (R2).

In light of the above observations, we compare the distance between the frontiers of (RtoD) and (D3), which is denoted as "RtoD Distance", with the distance between the frontiers of (DtoR) and (R2), which is denoted as "DtoR Distance", to interpret the benefit of the robust solution. Since the frontiers of the above models are not parallel, we cannot use

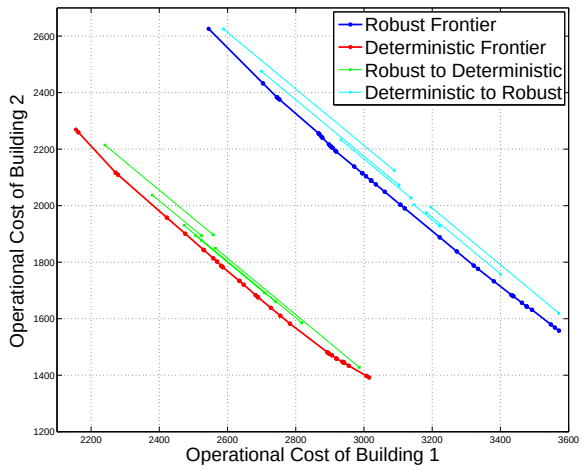

(a) Class A

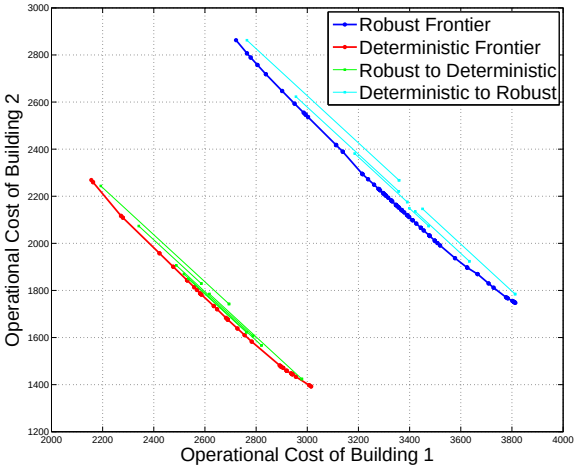

(b) Class B

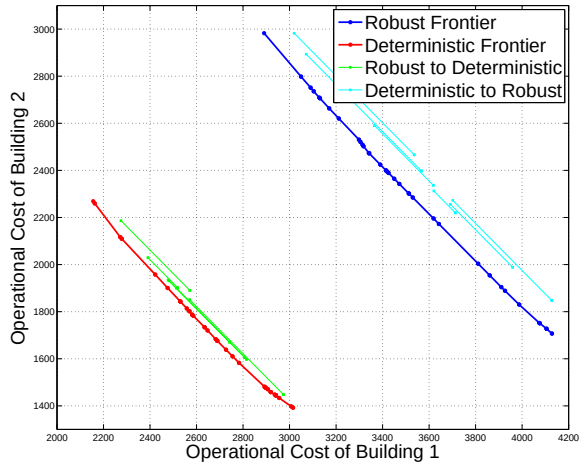

(c) Class C

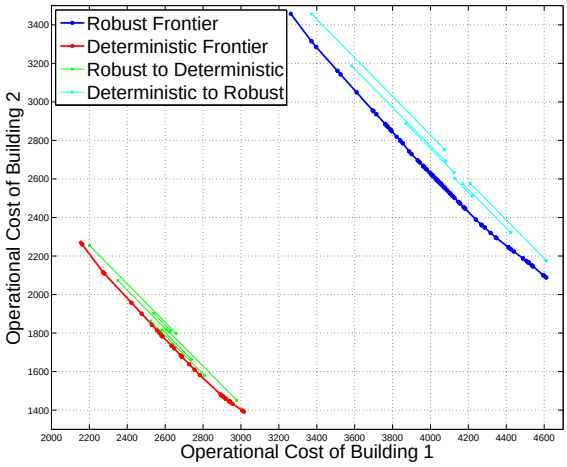

(d) Class D

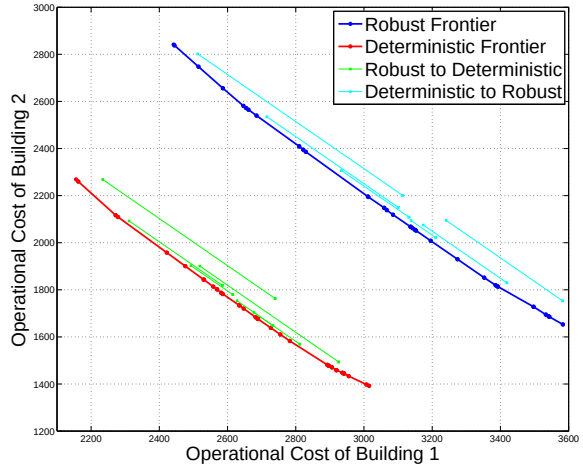

(e) Class E

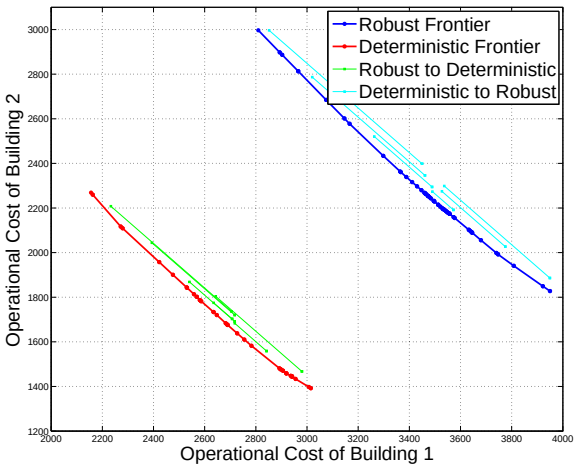

(f) Class F

Figure 4.6 – Frontiers for deterministic, robust, (RtoD), and (DtoR) models

the line-line distance to compute the DtoR Distance and RtoD Distance. Thus, we compute the distances with the following procedure.

For the RtoD Distance, we first select a set of points on the nondominated frontier of (D3) by vertically cutting the frontier where the intervals between each two adjacent cuts are identical in length. Similarly, we select a set of points on the frontier for each (RtoD) model. We compute the distances of a point y_n on the frontier of (RtoD) to all points selected on the frontier of (D3), and refer to the minimum of these distances as the distance of y_n to the frontier of (D3). Then the RtoD Distance can be represented by the average of the distances of all selected points on the frontiers for all (RtoD) models to the frontier of (D3). In detail, we set $|\mathcal{X}^R| = 101$ ($I = 100$), then 101 points are selected from the frontier of (R2) and 101 (RtoD) models are generated. We also select 101 points on the frontier for each (RtoD) model, which provide $101 \times 101 = 10201$ points selected from all frontiers of the (RtoD) models. Then the RtoD Distance is calculated by taking the average of the distances of these 10201 points to the frontier of (D3). The DtoR Distance is evaluated analogously.

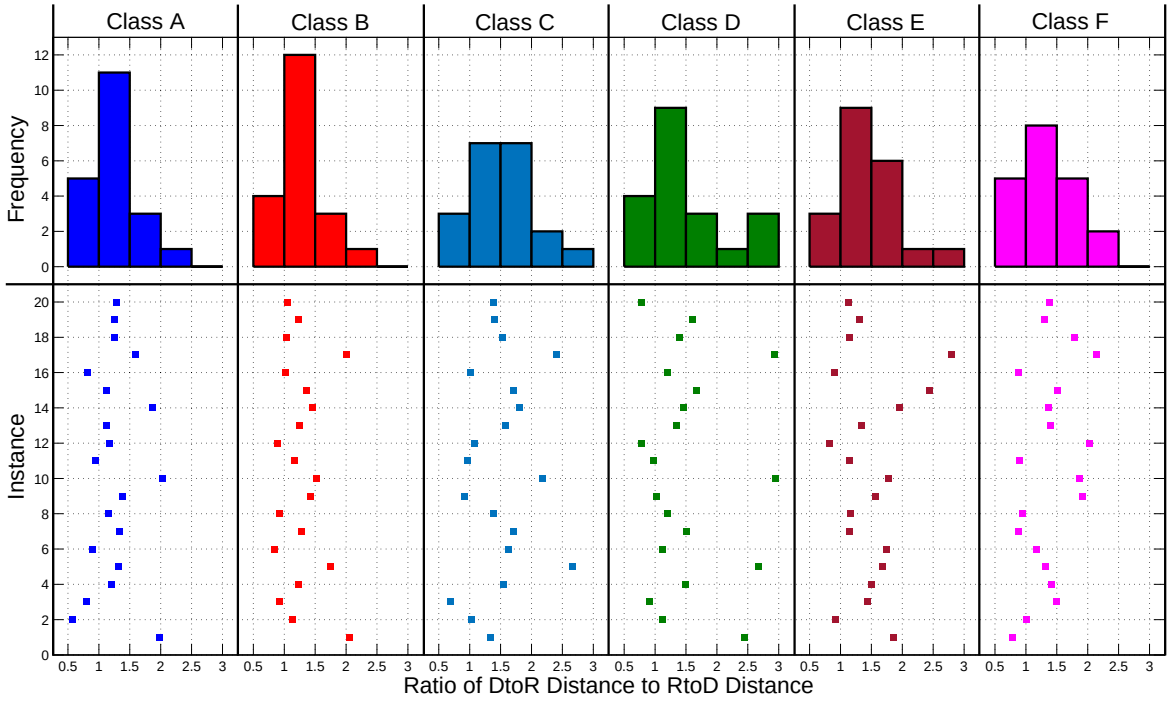

Figure 4.7 – Ratios of DtoR Distance to RtoD Distance for the test instances

If the RtoD Distance is less than the DtoR Distance, i.e., the ratio of DtoR Distance to RtoD Distance is greater than 1, it validates the second advantage of the robust solution: solving the deterministic model in a robust setting is subject to larger benefit losses than solving the robust model in a deterministic setting. Figure 4.7 presents the ratios of DtoR Distance to RtoD Distance for all instances in six classes. The horizontal axis represents the ratio of DtoR Distance to RtoD Distance and its scales are repeated for the six classes. The vertical axis has two parts: the upper part denotes the frequency of the ratios being located in a given interval, and the lower part the index of instances. The histograms show the number of instances whose ratios belong to each of the following intervals: $[0.5, 1]$, $(1, 1.5]$, $(1.5, 2]$, $(2, 2.5]$, and $(2.5, 3]$. The scatter plot indicates the exact ratio for each instance in the six classes. As can be seen in Figure 4.7, approximately 80% of instances have a ratio of DtoR Distance to RtoD Distance greater than 1. This demonstrates the aforementioned second advantage of a robust solution for most instances. Comparing classes C and D with A and B, we find that when υ is increased from 0.3 to 0.6, i.e., the range of energy price variation is extended, the ratios of DtoR Distance to RtoD Distance are generally enlarged. This implies that if the perturbation of energy price is intensified, the benefits of a robust solution are further emphasized.

In summary, the experimental results justify the two advantages of robust solutions compared to deterministic solutions. Robust solutions carry out the best performance with a certain robustness of solutions guaranteed if there exists a perturbation of electricity price and its benefit loss is negligible when the prices show no difference compared to the predictions. In contrast, the deterministic solutions result in a clear benefit deterioration when compared to the robust solutions.

4.5.3 Unique Robust Solution from the Nondominated Set

This section explores how to select a desirable point on the nondominated frontier to compute its corresponding efficient solution in practice. We have illustrated the effectiveness

of the robust solution generated by our robust contract balance strategy in the last section and we have shown that there exist infinite robust solutions in the efficient set $\mathcal{X}_E^R$ obtained by solving (R2). However, this begs the question how to select a unique robust solution from $\mathcal{X}_E^R$ in practice. One effective technique to select a solution from the efficient set is OOES (4.2).

We present two versions of the objective functions for OOES. One is to select the solution of the nondominated point with the minimal distance to the ideal point. The ideal point based OOES is formulated as

$$\min_{x^r \in \mathcal{X}_E^R} \|\bar{z}(x^r) - \bar{z}^I\|^2,$$

where $\bar{z}(x^r) = (\bar{z}_1(x^r), \bar{z}_2(x^r))$ and $\bar{z}^I$ is the ideal point for (R2). Since the ideal point $\bar{z}^I$ represents the best outcome for both buildings, the point with minimal distance to $\bar{z}^I$ can be described as the point that achieves the best tradeoff for both buildings seeking their individual best outcomes. The other one follows the Nash bargaining problem [94, 98]. Here we investigate the benefits for both buildings to participate in the collaboration for ES sharing, so the disagreement point is naturally determined by assuming both buildings entirely use the electricity purchased from the power grid to satisfy their demands, that is to say point (z_1^P, z_2^P). The Nash bargaining problem based OOES is formulated as

$$\max_{x^r \in \mathcal{X}_E^R} (z_1^P - \bar{z}_1(x^r))(z_2^P - \bar{z}_2(x^r)).$$

In order to maintain the collaboration for both buildings sharing ES and exchanging stored energy, it is necessary for the efficient solution to balance the distribution for the benefits of the cooperation. Here, the benefits are the operational cost savings for each building in contrast to the noncooperative outcome, which is quantified by $z_i^P - \bar{z}_i(x^r)$ for each $i \in \mathcal{N}$. We introduce the ratio of unbalanced benefits to the total cost savings for an efficient solution to examine the level of the collaborative benefits distribution to enhance

the coalition for energy storage sharing. The ratio for efficient solution x^r can be computed by

$$\frac{|(z_1^P - \bar{z}_1(x^r)) - (z_2^P - \bar{z}_2(x^r))|}{(z_1^P - \bar{z}_1(x^r)) + (z_2^P - \bar{z}_2(x^r))}.$$

Clearly, this ratio ranges between 0 and 1 and the smaller values correspond to a more balanced benefit distribution to enhance the coalition. If the ratio is 0 then a completely balanced benefit distribution for both buildings is achieved.

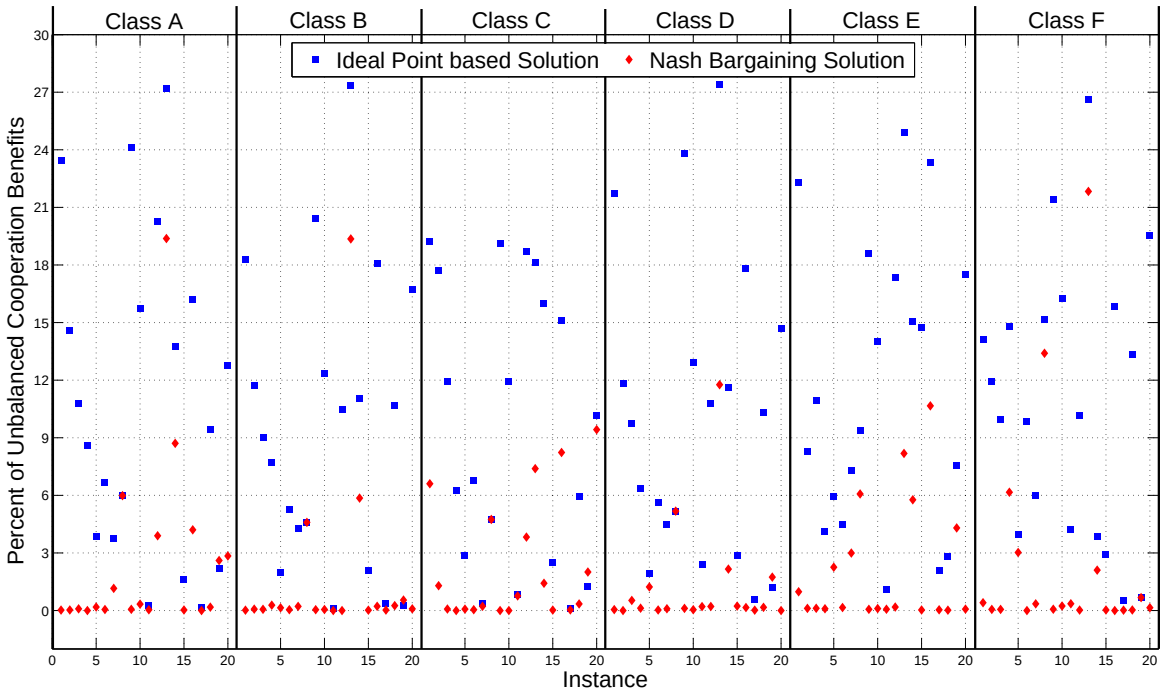

Figure 4.8 – Ratios of unbalanced benefits for two types of OOES

Figure 4.8 shows the ratios of unbalanced benefits to the total cost savings for both types of OOES for all instances in the six classes. The horizontal axis denotes the index of the instances in each class, and the vertical axis represents the ratios in percentages. The blue squares denote the ratios of the solutions obtained from the ideal point based OOES, and the red diamonds denote the Nash bargaining problem based OOES. First, Figure 4.8 shows that most ratios of Nash bargaining solution are 0 or very close to 0. This implies that Nash bargaining solutions are almost always able to accomplish an equal benefits distribution

for both buildings. Comparing the ratios of ideal point based solutions and Nash bargaining solutions in Figure 4.8, we find that Nash bargaining solutions almost always provide the smaller ratio and for some of the instances their gaps are greater than 15%.

Given the above findings, we can conclude that adopting the Nash bargaining solutions selected from the efficient set to practice our robust contract balance strategy enables us to achieve the desirable fair distribution for the cooperative benefits and enhance the solidity of the cooperation between both buildings.

4.6 Conclusion

In this paper, we presented a robust optimization based sharing strategy to handle the energy price uncertainty for ES sharing. This robust sharing strategy was developed based on our previously proposed contract balance strategy due to its property to achieve the balance of fairness and efficiency for the ES sharing. The robust contract balance strategy is formulated as a bi-objective mixed integer bilinear model by applying the set-described price uncertainty. Moreover, in order to handle the bilinear terms in the model, we propose a novel binary formulation based piecewise McCormick relaxation to linearize the bilinear terms. A computational study demonstrates that our robust sharing strategy is able to ensure the robustness and to minimize the operational costs for the ES sharing system under price uncertainty. It is also worth mentioning that the binary formulation for piecewise McCormick relaxations is capable of reducing the runtime by approximately 80% when compared to the unary formulation, and the solutions of both formulations are almost identical. In addition, due to the infinitely many efficient solutions for the bi-objective model, we employ the Nash bargaining solution to guide the unique solution selection from the efficient set. We validated that the Nash bargaining solutions almost equally distribute the ES sharing benefits to both buildings, which enhances the cooperation of all buildings to share ES.

In future studies, we will develop a branch-and-bound algorithm to generate the Nash bargaining solutions for the ES sharing problem without capturing the entire nondominated

frontiers, i.e., modeling our robust contract balance strategy as a bi-objective framework will no longer be a must. Our future study is motivated by the following: first, generating the exact nondominated frontiers for a bi-objective MILP is of significant computational complexity. Second, if we consider ES sharing by more than two users/buildings, to the best of our knowledge, there is no algorithm that generates the exact frontiers for a BOMILP with more than two objectives.

Chapter 5: A Game-theoretical Approach for Balancing Multi-prosumer Energy Trading through a Shared Energy Storage

This chapter was previously submitted as: Dai, R., Charkhgard, H., & Feizollahi, M. J. (2020). A Game-theoretical Approach for Balancing Multi-prosumer Energy Trading through a Shared Energy Storage", preprint. In this study, we apply the game-theoretical approach to develop the sharing strategy to manage an energy storage sharing system with multiple (more than two) prosumers to share this storage. This strategy is formulated as a Nash Bargaining problem and will return the solution to maximize the product of the cost savings of each prosumer. In contrast to the contract balance strategy developed based on Multi-objective optimization, this strategy will return exactly one solution and can handle the energy storage sharing system with many participants. The proposed sharing strategy applies Nash Bargaining solution and backward pricing mechanism to ensure that the economic benefit is maximized, the stored energy exchange among the prosumers is fair, and the cooperative benefits from the energy storage sharing are fairly distributed.

5.1 Overview

5.1.1 Contributions of the Game Theory-based Sharing Strategy

Motivated by the challenge of applying *Energy Storage* (ES) for energy trading or sharing and the limits of distributed ES system, this work focuses on an energy trading system with an ES shared by multiple prosumers under dynamic energy prices. The prosumers cooperate with each other to share the ES. In this system, the prosumers do not install any energy generation units or renewable energy sources. They produce energy by discharging the energy already stored in the ES which is purchased from power grid by the prosumers

and charged in previous time windows. We emphasize that the energy trading relies on the shared ES in this system. Since the energy trading between the prosumers is realized by selling the stored energy to other prosumers or purchasing the energy stored by other prosumers. To operate this ES sharing system, we develop a *balanced sharing strategy* (BSS) based on the cooperative game framework to minimize the cost of the prosumers and balance their conflict through a backward pricing mechanism. Both *Capacity Sharing* (CS), i.e., the capacity of ES is traded to other prosumers who will temporarily own and use the capacity, and *Stored Energy Sharing* (SES), i.e., the energy in ES stored by a prosumer is traded to other prosumers, for the proposed ES sharing system are implemented by the proposed strategy. The backward pricing mechanism evaluates the price and corresponding compensation for the prosumers trading their stored energy at the end of planning horizon to ensure the fairness for the energy trading.

Note that cooperative game theory has been applied to solving different types of energy trading problems for maximizing and fairly distributing the cooperative benefits simultaneously [18, 99, 12]. Hence, the BSS can ensure the benefits from the cooperation of sharing ES to be maximized and well-distributed. The proposed BSS for ES sharing is formulated as a Nash bargaining problem [94] with mixed integer nonlinear constraints. Several linearization techniques are employed to handle the nonlinear constraints. The Nash bargaining model is transferred to an equivalent *Second Order Conic Program* (SOCP) and solved by an enhanced algorithm. The experimental results demonstrate the efficiency of our solution techniques. Also the proposed ES sharing framework is validated to be effective on maximizing the cooperative benefits and balancing the conflict between prosumers for stored energy trading.

Overall, in contrast to the current frameworks for operating ES in an energy trading or sharing system, the main contributions of this work are generalized as follows:

- The BSS determines both CS and SES. In this strategy, the economic benefits of the prosumers are maximized by assigning them sufficient freedom to share the capacity and trade the stored energy through the shared ES with other prosumers.

- The backward pricing mechanism determines the compensations for energy trading at the end of planning horizon. This mechanism can guarantee the fairness for stored energy trading with respect to the freedom of prosumers. To the best of our knowledge, this mechanism is the first backward pricing strategy for handling the energy trading through ES sharing. Compared with operating ES as an independent operator, the backward pricing can skip the tough step for predetermining the energy trading price and protect the prosumers against the price discrimination.

- The Nash bargaining Solution (NBS) based cooperative game framework can ensure the cooperative benefits from ES sharing to be fairly distributed. An enhancement is proposed to advance the approach for solving the Nash bargaining problem, which is illustrated to dramatically reduce the computational time.

5.1.2 Nash Bargaining Solution

The bargaining problem represents a cooperative game in which all players agree to create a grand coalition instead of competing with each other, i.e., to get a higher payoff. The kernel of the bargaining problem is to decide how to allocate the benefits created by the cooperation of the players. One solution to the bargaining problem was proposed by Nash, known as NBS, which is able to address both efficiency and fairness in the cooperative game. We now consider a bargaining problem with two players to explain NBS.

The basic component of the bargaining problem is the achievable utility under the combination of the actions of all players. Here, we denote the achievable utility values by $\boldsymbol{y} = (y_1, y_2)$ for the bargaining problem with two players. $\mathcal{Y}$ is defined as a 2-dimensional feasible set in the payoff space containing all possible achievable utility values for the players.

Obtaining an NBS depends on the disagreement point denoted by $\boldsymbol{q} := (q_1, q_2)$ in the payoff space. This point represents the payoffs that the players will receive if they do not cooperate. Hence, the NBS to the bargaining problem is the point $\boldsymbol{y}^* = (\boldsymbol{y}_1^*, \boldsymbol{y}_2^*)$ obtained by solving the following optimization problem:

$$\boldsymbol{y}^* \in \arg\max \Big\{ (y_1 - q_1)(y_2 - q_2) : \boldsymbol{y} \in \mathcal{Y},\ y_1 \geq q_1,\ y_2 \geq q_2 \Big\}.$$

The idea of NBS is to find the point $\boldsymbol{y}^*$ on the Pareto frontier of $\mathcal{Y}$ to capture the largest area of the rectangle created by this point and the disagreement point $\boldsymbol{q}$. Figure 5.1 shows the idea of NBS for the cooperative game with two players.

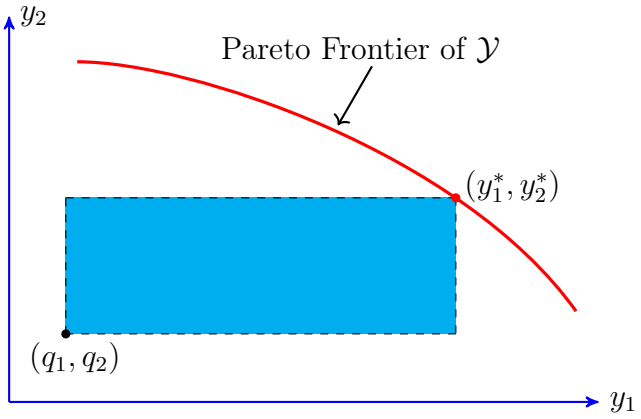

Figure 5.1 – The explanation of NBS for two players

Nash's result can also be extended to bargaining problems with N players ($N > 2$) in a straightforward manner. Namely, let $\mathcal{Y}$ be the N-dimensional feasible set in the payoff space. Hence for a disagreement point $\boldsymbol{q} = (q_1, \cdots, q_N)$, the optimal solution $\boldsymbol{y}^* = (y_1^*, \cdots, y_N^*)$ to the bargaining problem is given by a point satisfying:

$$\boldsymbol{y}^* \in \arg\max \Big\{ \prod_{i=1}^{N} (y_i - q_i) : \boldsymbol{y} \in \mathcal{Y},\ y_i \geq q_i\ \forall i \in \{1, \cdots, N\} \Big\}.$$

In the ES sharing problem, the payoff is the operational cost of each prosumer. Also, the disagreement point represents the operational cost of a prosumer if the prosumer rejects to share ES. It means that the prosumer is disconnected with the shared ES and the energy

load is totally satisfied by the energy purchased from power grid. Hence, the prosumers are degraded to a pure energy consumer. To follow the maximization formulation of NBS, we consider to maximize the cost saving for each prosumer in contrast to the disagreement point.

5.2 Game Theory-based Sharing Strategy for Energy Storage Sharing

In this section, we first describe the topology of the energy sharing system constructed by multiple prosumers and an shared ES. We then emphasize the conflict between efficiency and fairness for operating the shared ES for energy sharing. To address the dilemma of ES sharing, we propose a BSS based on the NBS to achieve the maximal efficiency for the integrated ES sharing system with the fair energy trading between multiple prosumers.

5.2.1 Topology of an Energy Storage Sharing System

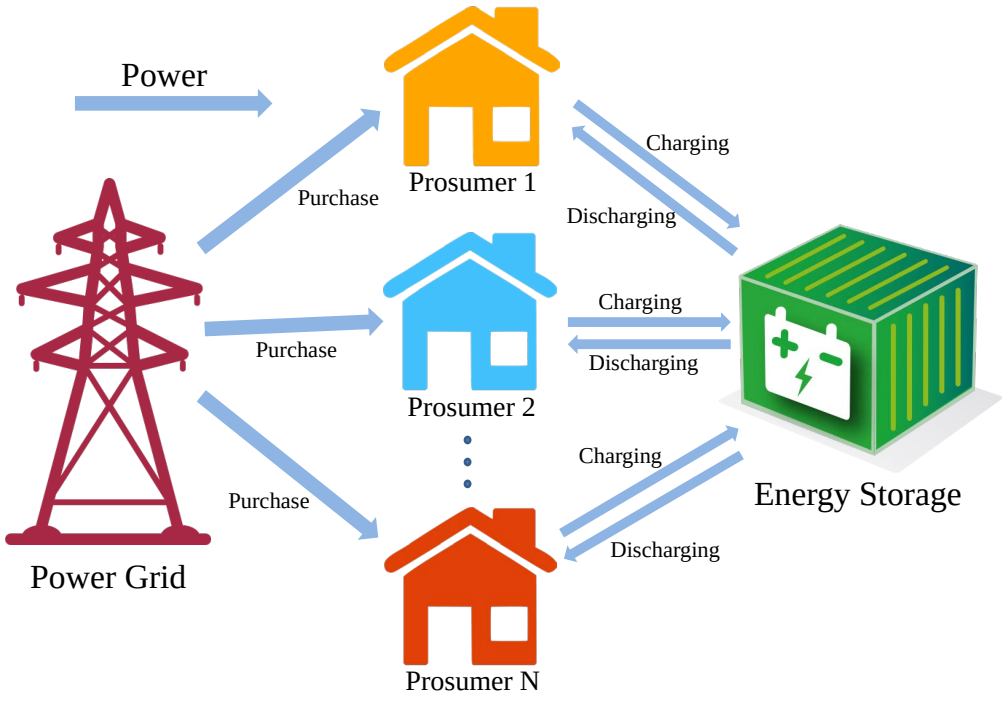

Figure 5.2 – The structure of energy storage sharing

Figure 5.2 presents the topology of an integrated energy system with multiple prosumers sharing an ES. Note that prosumers here can be different types of energy consumers with energy generation and/or storage units such as commercial or residential buildings and communities. In contrast to the generic energy system constructed by multiple interconnected prosumers [100], the ES sharing system excludes the energy generation units from the prosumers. The prosumers can still perform energy producing and trading by discharging the energy already stored in the ES.

The ES sharing system in Figure 5.2 contains three components: prosumers with energy load, power grid for almost unlimited energy supply, and an ES. The energy purchased by the prosumers from power grid can be used to satisfy their energy demands or stored in ES for future use. Discharging the ES is a complementary source for the energy consumption of prosumers. The prosumers should decide the amount of energy to purchase for the consumption of prosumers and charging the ES. They also need to decide the amount of energy discharged from ES to supplement the energy consumption. Note that the ES is forbidden to be charged and discharged simultaneously due to the energy loss and technical restrictions. The objectives of the prosumers are minimizing their operational cost, i.e., maximizing the energy arbitrage generated by using the shared ES.

Here ES sharing contains both CS and SES. We allocate the decisions for operating the energy system into several decision time windows. The length of each time window is equal. Thus, the process of CS and SES for the ES sharing system can be described as follows. In each time window, the prosumers cooperate to decide the amount of energy to charge the ES if it is at charging state or extract from ES if at discharging state. No specified limit to the capacity of the shared ES is allocated to any prosumer. The energy charged by different prosumers is mixed once it is imported into the ES. Note that after mixing, the ownership of the stored energy expires. At one of future time windows, if the ES is at the discharging state, all prosumers will be coordinated to use the energy in the storage which is not subjected to the origin of the stored energy.

5.2.2 Efficiency and Fairness in Energy Storage Sharing

ES is acknowledged to produce energy arbitrage to the prosumers if dynamic energy price applies. This arbitrage can be further boosted when the ES is shared by multiple prosumers, particularly if these prosumers hold different energy profiles and preferences or have access to different energy price plans from utilities. This benefit is originated from that ES sharing provides an opportunity for each prosumer to trade their stored energy. However, when operating a shared ES, the conflict of efficiency and fairness, i.e., the efficiency and fairness cannot be optimized simultaneously, appeals an effective sharing strategy.

Efficiency in ES sharing is the measurement for the reduction of the operational cost for each prosumer. To pursue the efficiency, the ES sharing system needs to minimize the operational cost for each prosumer. The minimal cost can be realized by allowing the prosumers trade their stored energy freely, i.e., efficiency refers to the freedom of the prosumers using the energy in the shared ES to minimize their operation cost. Hence, we formulate the objective of our BSS based on minimizing the operational cost.

Fairness in ES sharing is achieved by meeting two qualifications. First, since the prosumers discharge energy in the shared ES not based on its ownership, it leads to an unrestricted exchange of the stored energy among prosumers. For example, if the energy price of a prosumer is lower than others, this prosumer will always charge ES and export the stored energy to other prosumers to minimize their operational costs. Thus, this prosumer is the only provider of the stored energy. This stored energy is free to other prosumers due to the unrestricted exchange. However, in order to maintain the cohesion of the cooperation to share ES, the fair exchange should be guaranteed. The first qualification of fairness is to regulate the stored energy exchange among prosumers. It should ensure the provider of the stored energy not to lose when other prosumers using this energy. The fairness of energy trading in our BSS is assured by a backward compensation mechanism proposed in our previous paper [47], in which a prosumer will be paid based on the cost of the energy that is charged by this prosumer and used by other prosumers.

The other qualification of fairness in ES sharing is the allocation of the benefits created by the cooperation of ES sharing. When discharging the ES, the discharged energy should be coordinated to distribute to each prosumer. Every prosumer has the opportunity to use the discharged energy to reduce the operational cost. The benefit each prosumer can obtain depends on the decision for distributing the discharged energy to each prosumer. Obviously, this sharing problem is related to the distribution of cooperative benefits from ES sharing, which can be referred to as a bargaining problem or cooperative game. As known, NBS is a solution to the resource sharing problems in which the surplus generated by the cooperation of multiple players is maximized and fairly allocated. The cooperative benefits are distributed based on the power/weight of the players in NBS [101]. Hence, we apply NBS to achieve the balanced benefits distribution for ES sharing. The detailed mathematical model for our BSS is presented in the following subsection.

5.2.3 Mathematical Model of the Balanced Sharing Strategy

In this subsection, we illustrate the mathematical model of the BSS to address the efficiency and fairness for ES sharing. The BSS is formulated as a Nash bargaining problem, i.e., the objective function is the multiplication of the cost savings. A backward pricing mechanism based on the average charging price is employed in this strategy to ensure the fairness of the stored energy trading. Table 5.1 and 5.2 explain the parameters and decision variables used in our BSS. The decision variables z_i and φ_i are introduced to create the

Table 5.1 – Parameters in the balanced sharing strategy

$\mathcal{T}$	The index set of time windows of equal length, i.e., $\mathcal{T} := \{1, 2, \ldots, T\}$.
$\mathcal{N}$	The index set of prosumers, i.e., $\mathcal{N} := \{1, 2, \ldots, N\}$.
r_t^i	The price for prosumer $i \in \mathcal{N}$ to purchase energy from power grid at time $t \in \mathcal{T}$.
L_t^i	The energy (load) demand of prosumer $i \in \mathcal{N}$ at time $t \in \mathcal{T}$.
$\bar{E}$	The capacity of the power grid or the transmission line limit.
$\bar{B}/\underline{B}$	The maximum/minimum amount of energy that can be stored in the ES at each time window.
$\bar{C}/\underline{C}$	The maximum/minimum amount of energy that can be charged into the ES at a given time window if the storage is at charging state.
$\bar{D}/\underline{D}$	The maximum/minimum amount of energy that can be discharged from the ES at a given time window if the storage is at discharging state.
η^c/η^d	The charging/discharging efficiency coefficient of the ES, i.e., $\eta^c/\eta^d \in (0, 1)$.

objective function of the BSS following Nash bargaining problem. The decision variables g^i,

Table 5.2 – Decision variables in the balanced sharing strategy

e_t^i	Energy purchased by prosumer $i \in \mathcal{N}$ at time $t \in \mathcal{T}$ to satisfy the energy load, i.e., $e_t^i \geq 0$.
b_t^i	Energy purchased by prosumer $i \in \mathcal{N}$ at time $t \in \mathcal{T}$ to charge the ES, i.e., $b_t^i \geq 0$. Note that $b_t^i \times \eta^c$ is the real amount of energy stored in the ES.
d_t^i	Energy discharged from the ES for prosumer $i \in \mathcal{N}$ at time $t \in \mathcal{T}$, i.e., $d_t^i \geq 0$. Note that d_t^i/η^d is the real amount of energy extracted from the ES.
m_t	Energy available in the ES at the end of time window $t \in \mathcal{T}$, i.e., $m_t \geq 0$.
s_t^c/s_t^d	A binary variable that is 1 if the ES is at charging/discharging state at time $t \in \mathcal{T}$, and 0 otherwise.
z_i	Operational cost of prosumer $i \in \mathcal{N}$, i.e., $z_i \geq 0$.
φ_i	Cost saving of prosumer $i \in \mathcal{N}$ in contrast to the disagreement point, i.e., $\varphi_i \geq 0$.
g^i	Difference between the total energy charged into the ES by prosumer $i \in \mathcal{N}$ and the total stored energy used by this prosumer, i.e., g^i is unrestricted in sign.
$\bar{r}^i$	Average price of the total energy charged into the ES by prosumer $i \in \mathcal{N}$, i.e., $\bar{r}^i \geq 0$.
$\hat{r}$	Average price of the total energy charged into the ES by all prosumers, i.e., $\hat{r} \geq 0$.

$\bar{r}^i$ and $\hat{r}$ are introduced to evaluate the compensation for the prosumer trading the stored energy to other prosumers. Hence, the mathematical model of the BSS for ES sharing is formulated as follows, and is denoted by "(BS)".

$$\text{(BS)} \quad \max \prod_{i=1}^{N} \varphi_i \tag{5.1}$$

$$\text{s.t. } \varphi_i = \sum_{t \in \mathcal{T}} r_t^i L_t^i - z_i \qquad \forall i \in \mathcal{N} \tag{5.2}$$

$$z_i = \sum_{t \in \mathcal{T}} r_t^i (e_t^i + b_t^i) - \bar{r}^i \max\{g^i, 0\} - \hat{r} \min\{g^i, 0\} \qquad \forall i \in \mathcal{N} \tag{5.3}$$

$$\sum_{i \in \mathcal{N}} (e_t^i + b_t^i) \leq \bar{E} \qquad \forall t \in \mathcal{T} \tag{5.4}$$

$$e_t^i + d_t^i = L_t^i \qquad \forall i \in \mathcal{N}, \forall t \in \mathcal{T} \tag{5.5}$$

$$s_t^c + s_t^d \leq 1 \qquad \forall t \in \mathcal{T} \tag{5.6}$$

$$\underline{C} s_t^c \leq \sum_{i \in \mathcal{N}} b_t^i \eta^c \leq \bar{C} s_t^c \qquad \forall t \in \mathcal{T} \tag{5.7}$$

$$\underline{D} s_t^d \leq \sum_{i \in \mathcal{N}} \frac{d_t^i}{\eta^d} \leq \bar{D} s_t^d \qquad \forall t \in \mathcal{T} \tag{5.8}$$

$$\sum_{i \in \mathcal{N}} b_t^i \eta^c - \sum_{i \in \mathcal{N}} \frac{d_t^i}{\eta^d} = m_t - m_{t-1} \qquad \forall t \in \mathcal{T} \tag{5.9}$$

$$\underline{B} \leq m_t \leq \bar{B} \qquad \forall t \in \mathcal{T} \tag{5.10}$$

$$g^i = \sum_{t \in \mathcal{T}} (b_t^i - \frac{d_t^i}{\eta^c \eta^d}) \qquad \forall i \in \mathcal{N} \tag{5.11}$$

$$\sum_{t\in\mathcal{T}} r_t^i b_t^i = \sum_{t\in\mathcal{T}} \bar{r}^i b_t^i \qquad \forall i \in \mathcal{N} \tag{5.12}$$

$$-\hat{r}\sum_{i\in\mathcal{N}} \min\{g^i, 0\} = \sum_{i\in\mathcal{N}} \bar{r}^i \max\{g^i, 0\} \tag{5.13}$$

Constraints (5.2) define the cost savings for each prosumer if they cooperates. The cost saving of a prosumer is computed based on the difference between the operational cost if cooperating and the cost in the disagreement point. Here, the disagreement point represents the operational cost if the prosumer disconnects from the ES and fulfills its energy load totally relying on power grid. Due to the assumption of deterministic energy demand, the operational cost of prosumer i in the disagreement point is $\sum_{t\in\mathcal{T}} r_t^i L_t^i$.

The operational costs of prosumers for ES sharing are determined by constraints (5.3). The operational cost contains two parts: the cost for purchasing the energy from power grid and the compensation for trading the stored energy. The compensation is formulated by a maximum and minimum function for providing the stored energy to other prosumers and receiving the stored energy from others, respectively. It is calculated based on the amount of the stored energy for trading and the average price for charging ES.

The variable g^i captures the net amount of the stored energy traded by prosumer i in the entire planning horizon, and is computed by constraints (5.11). If g^i is positive, prosumer i sells the stored energy to other prosumers at its average charging rate, and receives the compensation to reduce the operational cost. Hence, the value of maximum function is positive and the minimum function is zero. If g^i is negative, prosumer i uses the energy stored by other prosumers and is forced to pay for this energy at the overall average charging rate of all prosumers. Hence, the value of maximum function is zero and the minimum function is negative.

The compensation for prosumer i selling the stored energy is computed based on the average price $\bar{r}^i$ which is determined by constraints (5.12). If a prosumer sells the stored energy, this prosumer can request the compensation based on the amount of the stored

energy sold, g^i with positive value, and the average price for charging ES, $\bar{r}^i$. Note that this prosumer will not restrict which prosumer to pay for the compensation and only focuses on receiving the requested compensation at the end of the planning horizon. If a prosumer obtains the energy stored by other prosumers, this prosumer should pay for the energy based on the amount of this energy, g^i with negative value, and the overall average charging price, $\hat{r}$. Also, this prosumer is only required to submit the payment for the purchase of the stored energy at the end of the planning horizon and free from allocating the payment to the suppliers. Hence, the BSS creates an aggregator to coordinate the compensation for trading the stored energy. This aggregator should ensure the total compensations of the prosumers selling their stored energy are exactly covered by the prosumers using this exchanged energy, which is represented by constraint (5.13). Besides, the aggregator needs to coordinate the compensations to be received by the prosumers selling their stored energy and to be paid by the prosumers using the transactive stored energy.

In addition, constraints (5.4) restrict the total energy purchased from power grid to be lower than its capacity or the transmission line limit. Constraints (5.5) ensure the energy demand of each prosumer is satisfied. Constraints (5.6)-(5.10) are created for controlling the state of ES and maintaining the energy conservation for ES. Note that m_0 indicates the amount of energy stored in the ES at the start of the first time window. We assume that $m_0 = m_T$, which means all the energy charged by the prosumers should be exhausted before the end of the planning horizon.

Overall, our BSS achieves the fairness for the stored energy trading by evaluating the compensations for the prosumers providing their stored energy to other prosumers. Note that these compensations are computed at the end of planning horizon only depending on the total energy for charging and discharging of each prosumer. Hence, we avoid the complexity for investigating the details of allocating the stored energy among multiple prosumers. Furthermore, the NBS based sharing strategy guarantees that our strategy maximizes the energy arbitrage for ES sharing and addresses the fairness for distributing the arbitrage to

each prosumer. Hence, the proposed strategy leads to tremendous advances in efficiency for ES sharing with two types of fairness guaranteed.

5.3 Linearization for the Constraints

There are some nonlinear terms in model (BS), such as the multiplicative objective function, i.e., maximizing the product of multiple variables, maximum and minimum functions, and bilinear terms, i.e., the product of two variables. In this section, we focus on linearizing the nonlinear terms in the constraints (except the multiplicative objective function) in model (BS). We first linearize the maximum and minimum functions in constraints (5.3) and (5.13). This procedure can be accomplished by introducing a series of binary variables to formulate the max and min conditions. The obtained linearized model is equivalent to the original model. Then we apply binary formulation based Piecewise McCormick Relaxation (PMR) to linearize the bilinear terms in constraints (5.3), (5.12) and (5.13) by replacing the bilinear terms with the high-quality linear approximations.

5.3.1 Linearizing Maximum and Minimum Functions

In order to omit the maximum and minimum functions in constraints (5.3) and (5.13), we introduce non-negative continuous variables $\bar{g}^i$ and $\hat{g}^i$, and binary variables $\bar{y}^i$ for all $i \in \mathcal{N}$. The equivalent model without maximum and minimum functions for model (BS) is formulated as follows, and denoted by "(SE)".

$$
\begin{aligned}
\text{(SE)} \qquad & \max \prod_{i=1}^{N} \varphi_i \\
& \text{s.t. } (5.2), (5.4) - (5.12) \\
& z_i = \sum_{t \in \mathcal{T}} r_t^i (e_t^i + b_t^i) - \bar{r}^i \bar{g}^i + \hat{r} \hat{g}^i && \forall i \in \mathcal{N} && (5.14) \\
& \hat{r} \sum_{i \in \mathcal{N}} \hat{g}^i = \sum_{i \in \mathcal{N}} \bar{r}^i \bar{g}^i && && (5.15) \\
& g^i \leq \bar{g}^i && \forall i \in \mathcal{N} && (5.16)
\end{aligned}
$$

$$\bar{g}^i \leq \bar{G}\bar{y}^i \qquad \forall i \in \mathcal{N} \qquad (5.17)$$

$$\bar{g}^i \leq g^i + \bar{G}(1 - \bar{y}^i) \qquad \forall i \in \mathcal{N} \qquad (5.18)$$

$$-g^i \leq \hat{g}^i \qquad \forall i \in \mathcal{N} \qquad (5.19)$$

$$\hat{g}^i \leq \bar{G}(1 - \bar{y}^i) \qquad \forall i \in \mathcal{N} \qquad (5.20)$$

$$\hat{g}^i \leq -g^i + \bar{G}\bar{y}^i \qquad \forall i \in \mathcal{N} \qquad (5.21)$$

where $\bar{G}$ is an adequate upper bound for all $\bar{g}^i$ and $\hat{g}^i$. Constraints (5.16)-(5.21) can guarantee that if $g^i > 0$, $\bar{g}^i = g^i$ and $\hat{g}^i = 0$, and if $g^i < 0$, $\bar{g}^i = 0$ and $\hat{g}^i = -g^i$, which yield the same results as the maximum and minimum functions.

5.3.2 Linearizing the Bilinear Terms

In this subsection, we apply a binary formulation based PMR to linearize the bilinear terms in our BSS. Note that the bilinear terms exist in the non-convex quadratic equality constraints of model (SE), which cannot be solved by the commercial solvers like CPLEX currently. As is well-known, the McCormick Relaxation is capable of linearizing a bilinear term including two bounded continuous variables using the so-called McCormick envelopes. However, McCormick Relaxation actually replaces the original bilinear term with a linear approximation. The quality of this approximation is domain-dependent. Hence, we apply a piecewise way to the McCormick Relaxation to capture a high-quality approximation to the bilinear term. The PMR is done by partitioning the domain of a variable in the bilinear term into several sequential intervals and applying McCormick Relaxations to the bilinear terms in each interval.

The common approach to execute the PMR is unary formulation based. This unary formulation introduces a set of binary variables to indicate the activated partition of the bilinear terms. Furthermore, we have proposed a binary formulation for PMR in our previous study [56], which is demonstrated to be able to save 80% of run time in contrast to the unary formulation. The binary formulation employs an integer variable to indicate the index of the

activated partition of the bilinear term and the value of this integer variable is represented by the binary numeral system.

We now explain the binary formulation for PMR. For bounded continuous variables $x \in [\underline{X}, \bar{X}]$ and $y \in [\underline{Y}, \bar{Y}]$, and a variable w representing the product of x and y, consider the following bilinear set

$$\mathbf{P}(w) := \Big\{(x, y, w) \in \mathbb{R}_+ \times \mathbb{R}_+ \times \mathbb{R}_+ : w = xy; \underline{X} \leq x \leq \bar{X}; \underline{Y} \leq y \leq \bar{Y}\Big\},$$

where w in the notation $\mathbf{P}(w)$ indicates that this set is constructed for the bilinear term $w = xy$. In order to execute the binary formulation based PRM, we transfer $\mathbf{P}(w)$ into the following form:

$$\begin{aligned}\mathbf{I}(w) :=&\Big\{(x, p, q, w) \in \mathbb{R}_+ \times \mathbb{Z}_+ \times \mathbb{R}_+ \times \mathbb{R}_+ : w = x\underline{Y} + Dxp + xq; \underline{X} \leq x \leq \bar{X}; p \leq M - 1;\\ & q \leq D\Big\},\end{aligned}$$

where M is the number of pieces we want to divide the variable y into, and $D = (\bar{Y} - \underline{Y})/M$ is the length of each piece on the y-axis. Obviously, we derive $\mathbf{I}(w)$ by replacing y with $\underline{Y} + Dp + q$ in $\mathbf{P}(w)$. Given the mixed integer bilinear term xp and continuous bilinear term xq in $\mathbf{I}(w)$, the binary formulation based PMR for $\mathbf{I}(w)$ is given by the following formulation:

$$\begin{aligned}\mathbf{C}(w) :=&\Big\{(x, q, z, w, u, v) \in \mathbb{R}_+ \times \mathbb{R}_+ \times \{0,1\}^K \times \mathbb{R}_+ \times \mathbb{R}_+^K \times \mathbb{R}_+ : w = \underline{Y}x + D\sum_{k=1}^{K} 2^{k-1}u_k\\ &+ v; \sum_{k=1}^{K} 2^{k-1}z_k \leq M - 1; \quad v \geq \underline{X}q; \quad v \geq Dx + \bar{X}q - D\bar{X}; \quad v \leq Dx + \underline{X}q - D\underline{X};\\ &v \leq \bar{X}q; \quad u_k \geq \underline{X}z_k, \quad \forall k \in \{1, \ldots, K\}; \quad u_k \geq x + \bar{X}z_k - \bar{X}, \quad \forall k \in \{1, \ldots, K\};\\ &u_k \leq x + \underline{X}z_k - \underline{X}, \quad \forall k \in \{1, \ldots, K\}; \quad u_k \leq \bar{X}z_k, \quad \forall k \in \{1, \ldots, K\}\Big\},\end{aligned}$$

where xp is replaced by a linear binary expansion $\sum_{k=1}^{K} 2^{k-1}u_k$, xq is represented by a variable v, and the value of K is decided by $K = \lceil \log_2 M \rceil$.

We note that the bilinear terms in the constraints of (SE) include $\bar{r}^i\bar{g}^i$, $\hat{r}\hat{g}^i$ and $\bar{r}^i b_t^i$ for all $i \in \mathcal{N}$ and $t \in \mathcal{T}$. Before applying PMR to linearize these bilinear terms, we first conduct the preprocessing for the bilinear terms to indicate the domain of all variables and the variables selected for partitioning:

- $b_t^i \in [\underline{A}, \bar{A}]$ for all $i \in \mathcal{N}$ and $t \in \mathcal{T}$. Since if $s_t^c = 0$, then $b_t^i = 0$, and if $s_t^c = 1$, then $b_t^i \in [\frac{\underline{C}}{\eta^c}, \frac{\bar{C}}{\eta^c}]$. We set the complete range of b_t^i as $[\underline{A}, \bar{A}]$, where $\underline{A} = 0$, and $\bar{A} = \frac{\bar{C}}{\eta^c}$.

- $\bar{r}^i \in [\underline{R}^i, \bar{R}^i]$ for all $i \in \mathcal{N}$ where $\underline{R}^i := \min\{r_t^i : t \in \mathcal{T}\}$ and $\bar{R}^i := \max\{r_t^i : t \in \mathcal{T}\}$. $\hat{r} \in [\underline{R}, \bar{R}]$ where $\underline{R} := \min\{\underline{R}^i : i \in \mathcal{N}\}$ and $\bar{R} := \max\{\bar{R}^i : i \in \mathcal{N}\}$.

- $\bar{g}^i, \hat{g}^i \in [\underline{G}, \bar{G}]$ for all $i \in \mathcal{N}$ and $j \in \mathcal{N}\backslash\{i\}$, where $\underline{G} := 0$ and $\bar{G} := \frac{|\mathcal{T}| \max\{\frac{\bar{C}}{\eta^c}, \frac{\bar{D}}{\eta^c}\}}{2}$. The latter, i.e., the upper bound, can be obtained by assuming an extreme scenario that one prosumer only charges the shared ES and the others only discharge. So, given that $m_0 = m_T$ and the storage cannot be at the charging and discharging states simultaneously, the result follows.

- Assume that we separate $\bar{r}^i$ into M pieces due to its co-occurrence in all of bilinear terms (except $\hat{r}\hat{g}^i$). Then we rewrite $\bar{r}^i$ as a mixed integer form: $\bar{r}^i = \underline{R}^i + D^i p^i + q^i$, where $D^i = (\bar{R}^i - \underline{R}^i)/M$, $p^i \in \{o \in \mathbb{Z}_+ : o \leq M-1\}$, and $q^i \in \{s \in \mathbb{R}_+ : s \leq D^i\}$. In addition, let $\mathcal{K} := \{k \in \mathbb{Z}_{++} : k \leq K\}$, where $K = \lceil \log_2 M \rceil$. Similarly to $\bar{r}^i$, we separate $\hat{r}$ into M pieces and rewrite $\hat{r}$ as a mixed integer form: $\hat{r} = \underline{R} + Dp + q$, where $D = (\bar{R} - \underline{R})/M$, $p \in \{o \in \mathbb{Z}_+ : o \leq M-1\}$, and $q \in \{s \in \mathbb{R}_+ : s \leq D\}$.

- We replace the bilinear terms with the linear variables such that $\bar{v}^i := \bar{r}^i\bar{g}^i$, $\hat{v}^i := \hat{r}\hat{g}^i$, and $w_t^i := \bar{r}^i b_t^i$ for all $i \in \mathcal{N}$ and $t \in \mathcal{T}$.

According to the above assumption, the binary formulation based PMR for (SE) can be given as follows, which is denoted by "(SM)".

$$
\begin{aligned}
\text{(SM)} \qquad & \max \prod_{i=1}^{N} \varphi_i \\
& \text{s.t. } (5.2), (3.3)-(5.11), (5.16)-(5.21) \\
& z_i = \sum_{t\in\mathcal{T}} r_t^i (e_t^i + b_t^i) - \bar{v}^i + \hat{v}^i && \forall i \in \mathcal{N} && (5.22) \\
& \sum_{i\in\mathcal{N}} \bar{v}^i = \sum_{i\in\mathcal{N}} \hat{v}^i && && (5.23) \\
& \sum_{t\in\mathcal{T}} r_t^i b_t^i = \sum_{t\in\mathcal{T}} w_t^i && \forall i \in \mathcal{N} && (5.24) \\
& (\bar{g}^i, q^i, y^i, \bar{v}^i, h^i, f^i) \in \mathbf{C}(\bar{v}^i) && \forall i \in \mathcal{N} && (5.25) \\
& (\hat{g}^i, q, y^i, \hat{v}^i, \hat{h}^i, \hat{f}^i) \in \mathbf{C}(\hat{v}^i) && \forall i \in \mathcal{N} && (5.26) \\
& (b_t^i, q^i, y^i, w_t^i, u_t^i, l_t^i) \in \mathbf{C}(w_t^i) && \forall i \in \mathcal{N},\ t \in \mathcal{T}, && (5.27)
\end{aligned}
$$

where $\mathbf{C}(\bar{v}^i)$ denotes the set of constraints realizing the binary formulation based PMR for $\bar{v}^i = \bar{r}^i \bar{g}^i$, $\mathbf{C}(\hat{v}^i)$ for $\hat{v}^i = \hat{r}\hat{g}^i$, and $\mathbf{C}(w_t^i)$ for $w_t^i = \bar{r}^i b_t^i$.

5.4 Solution to Nash Bargaining Problem

In the previous section, we have linearized all the nonlinear terms in the constraints for our BSS. The only remaining nonlinear terms is the multiplicative objective function for the Nash bargaining problem. Based on the definition of NBS, the objective function is formulated as the product of the cost savings of all prosumers through ES sharing. We explore the solution techniques to the multiplicative model for our BSS in this section.

We note that the multiplicative objective function is the product of multiple variables. This product can be reconstructed as the product of multiple bilinear terms. Hence, the binary formulation based PMR can be applied to approximate the optimal solution for the multiplicative model. Another approach is to transfer the multiplicative model into an

equivalent SOCP, which can be solved by the commercial solvers such as CPLEX. Furthermore, we propose an enhancement to improve the computational efficiency for solving the equivalent SOCP model by introducing the effective primal and dual bound.

5.4.1 Piecewise McCormick Relaxation Based Solution

We first extend the PMR to solve the multiplicative model with the product of more than two variables in its objective. The extension of PMR works as that we take the objective function $\Pi_{i=1}^{N}\varphi_i$ as the bilinear term constructed by the first variable φ_1 and the product of the rest variables, and we denote this product as ω_2 such that $\omega_2 = \Pi_{i=2}^{N}\varphi_i$. Then, we take ω_2 as the bilinear term with φ_2 and the product of the rest variables, $\omega_3 = \Pi_{i=3}^{N}\varphi_i$. By repeating this procedure, we can transfer the multiplicative objective function to a sequential bilinear terms. The model (SM) is represented by a bilinear terms based formulation as follows, and denoted by "(SB)"

$$
\begin{aligned}
\text{(SB)} \quad & \max\ \omega_1 \\
& \text{s.t. } (5.2), (3.3)-(5.11), (5.16)-(5.27) \\
& \omega_i = \varphi_i \omega_{i+1} && \forall i \in \{1,\dots,N-1\} && (5.28) \\
& \omega_N = \varphi_N && && (5.29)
\end{aligned}
$$

In order to apply PMR to (SB), we first indicate the lower bound and upper bound of φ_i and ω_i based on its construction. Let $\varphi_i \in [\underline{\varphi}_i, \bar{\varphi}_i]$, where $\underline{\varphi}_i = 0$ and $\bar{\varphi}_i = \sum_{t\in\mathcal{T}} r_t^i L_t^i$ due to the definition of cost savings for ES sharing. Let $\omega \in [\underline{\omega}_i, \bar{\omega}_i]$, where $\underline{\omega}_i = 0$ and $\bar{\omega}_i = \Pi_{k=i}^{N}\bar{\varphi}_k$ due to the construction of ω_i. We select variables φ_i in the bilinear terms of constraints (5.28) to conduct the partition. We partition φ_i into $\hat{M}$ pieces, and the mixed integer form of φ_i is $\varphi_i = \underline{\varphi}_i + \hat{D}^i\hat{p}^i + \hat{q}^i$, where $\hat{D}^i = (\bar{\varphi}_i - \underline{\varphi}_i)/\hat{M}$, $\hat{p}^i \in \{o \in \mathbb{Z}_+ : o \le \hat{M}-1\}$, and $\hat{q}^i \in \{s \in \mathbb{R}_+ : s \le \hat{D}^i\}$. In order to maintain the accuracy of PMR based solution to the Nash bargaining problem, we need to select a sufficient large number for $\hat{M}$.

5.4.2 SOCP-based Solution

The motivation to transfer the multiplicative model into an equivalent SOCP is the utilization of the commercial solvers. In order to apply the SOCP solver, we transfer model (SM) to the following equivalent SOCP formulation denoted by "(SP)" using the procedure explained in [98],

$$\begin{aligned}
(\text{SP}) \quad & \max \boldsymbol{\gamma} \\
& \text{s.t. } (5.2), (5.4)-(5.11), (5.16)-(5.27) \\
& 0 \le \boldsymbol{\gamma} \le \Gamma && (5.30) \\
& 0 \le \Gamma \le \sqrt{\tau_1^{k-1}\tau_2^{k-1}} && (5.31) \\
& 0 \le \tau_j^l \le \sqrt{\tau_{2j-1}^{l-1}\tau_{2j}^{l-1}} \qquad \forall j \in \{1,\dots,2^{k-l}\}, \forall l \in \{1,\dots,k-1\} && (5.32) \\
& 0 \le \tau_i^0 = \varphi_i \qquad \forall i \in \{1,\dots,N\} && (5.33) \\
& 0 \le \tau_j^0 = \Gamma \qquad \forall j \in \{N+1,\dots,2^k\}, && (5.34)
\end{aligned}$$

where k is the smallest integer value such that $2^k \ge N$. Then we can apply the mixed integer quadratic program module in the commercial solvers to solve the SOCP model (SP) of the proposed BSS for ES sharing.

5.4.3 Enhancement for SOCP Model

The enhancement for the SOCP model of the BSS for ES sharing is developed by introducing the tightened primal and dual bound for model (SM).To better illustrate the primal and dual bound, we first introduce three optimization models.

$$\begin{aligned}
(\text{SA}) \qquad & \max \sum_{i=1}^{N} \varphi_i \\
& \text{s.t. } (5.2), (5.4)-(5.11), (5.16)-(5.21), (5.22)-(5.27)
\end{aligned}$$

The only difference between model (SA) and (SM) is that the objective function is replaced by the summation of all φ_i. Thus, model (SA) is a *mixed integer linear program* (MILP).

$$\begin{aligned} \text{(RSA)} \qquad & \max \sum_{i=1}^{N} \varphi_i \\ & \text{s.t. } (5.2), (5.4)-(5.10), (5.22), (5.23) \end{aligned}$$

In model (RSA), all constraints for regulating the stored energy trading are removed. Obviously, (RSA) is a relaxed problem for model (SA).

$$\begin{aligned} \text{(ESA)} \quad & \max \sum_{i=1}^{N} \varphi_i \\ & \text{s.t. } (5.2), (5.4)-(5.11), (5.16)-(5.21), (5.22)-(5.27) \\ & \varphi_i = \varphi_{i+1} \qquad \forall i \in \{1, \ldots, N-1\}. \end{aligned} \tag{5.35}$$

Since model (ESA) is obtained by adding several equality constraints to (SA), the solution of (ESA) should be feasible to (SA) and (SM).

Proposition 19. Let U^* denote the optimal objective function value for problem (RSA), and let φ_i^* denote an optimal solution of φ_i for problem (ESA). If $U^* = \sum_i^N \varphi_i^*$, then φ_i^* is an optimal solution of φ_i for problem (SM).

Proof. First, we know that if $\sum_{i=1}^N x_i = C$ where $x_i \geq 0$ for all $i \in \{1, \ldots, N\}$ and C is a positive constant, the optimal solution for maximizing $\prod_{i=1}^{N} x_i$ must be $x_i = \frac{C}{N}$ for all $i \in \{1, \ldots, N\}$ and optimal objective function value is $(\frac{C}{N})^N$. Hence, if the optimal objective function value of (SA) is S^*, then $(\frac{S^*}{N})^N$ provides a dual bound for problem (SM). Due to (RSA) being the relaxation problem for (SA), U^* is a dual bound for (SA), and $(\frac{U^*}{N})^N$ should also be a dual bound for problem (SM). Besides, since φ_i^* is the optimal solution of φ_i for problem (ESA) and also feasible for problem (SM), $\prod_{i=1}^{N} \varphi_i^*$ provides a primal bound for problem (SM). According to constraints (5.35) and the condition $U^* = \sum_i^N \varphi_i^*$, we can derive

that $\prod_{i=1}^{N} \varphi_i^* = (\frac{U^*}{N})^N$, i.e., the primal and dual bound for (SM) are identical. It indicates that the feasible solution φ_i^* is optimal for problem (SM). □

According to Proposition 1, when solving the SOCP model (SP), we first solve two MILPs, (RSA) and (ESA). Note that solving these MILPs is much faster than solving the SOCP model (SP). If the solutions of model (RSA) and (ESA) satisfy Proposition 1, we can directly obtain the optimal solution for (SP) and skip the time-consuming procedure of solving the mixed integer SOCP. If the condition of Proposition 1 is not satisfied, we can still employ the results obtained by solving model (RSA) and (ESA) to enhance the algorithm for solving SOCP model (SP). In detail, $(\frac{U^*}{N})^N$ obtained by solving model (RSA) should be the dual bound for (SP). A cut based on this dual bound can be applied to (SP). The solution of model (ESA) must be feasible to (SP). This feasible solution can be fed to the SOCP solver to warm start the procedure for solving (SP).

5.5 Experimental Results

This section presents the experimental results for the proposed BSS for operating the ES shared by multiple prosumers. The experimental results contain three parts. First we compare the PMR and transferred SOCP based method for solving the multiplicative model of Nash bargaining problem. Then, we investigate the effectiveness of the proposed enhancement for solving the SOCP model. Finally, we explore the performance of our BSS for ES sharing in terms of efficiency and fairness compared to the reference strategies. We employ CPLEX 12.7 for solving MILPs and SOCPs in this computational study. All the formulations and algorithms are implemented in C++.

The data for testing the BSS for ES sharing are explained as follows. We assume that the length of each time window is one hour, and the entire planning horizon contains 24 time windows, i.e., $|\mathcal{T}| = 24$. We test our strategy for 9 scenarios in which the number of prosumers in the ES sharing system ranges from 2 to 10, i.e., $|\mathcal{N}| \in \{2, \ldots, 10\}$. There

are 100 instances in each scenario. These instances are generated randomly drawing r_t^i and L_t^i for each $i \in \mathcal{N}$ and $t \in \mathcal{T}$ as uniformly distributed integers from the interval $[1, 20]$. The capacity of the battery is set to $\bar{B} = |\mathcal{N}| \times \max\{L_t^i : \forall i \in \mathcal{N}, \forall t \in \mathcal{T}\} = |\mathcal{N}| \times 20$. The minimum of the energy to be stored in the ES is set to $\underline{B} = 1$. The initial amount of energy in ES is set to $m_0 = \underline{B} = 1$. Besides, we set the upper and lower bound for charging and discharging rate following the assumption that $\bar{C} = \bar{D} = 0.2 \times \bar{B}$ and $\underline{C} = \underline{D} = 0.05 \times \bar{B}$. The capacity of power grid is fixed to $\bar{E} = 300$. The number of pieces for PRM in the constraints is 32 ($M = 32$) based on our previous work [47].

5.5.1 Comparison between the Methods for Solving Nash Bargaining Problem

In this subsection, we compare the NBSs returned by PMR based method and transferred SOCP model to select the efficient method. The comparison results contain the difference between the returned NBSs of two methods to show the precision of these methods, and the run time for both methods to validate the efficient method for solving model (SM). Here we consider the instances with the ES shared by two and three prosumers.

The comparison results are summarized in Table 5.3. In Table 5.3, "ST(s)" denotes the run time (in second) using the SOCP model (SP) to return NBS, "MT(s)" run time using PMR based model (SB), and "Diff(%)" the difference of the objective values (the product of cost savings for all prosumers) between both models. The statistics in Table 5.3 contain the average, standard deviation, median, maximum and minimum for the corresponding results of 100 instances. Note that the number of pieces for partitioning the variables in the multiplicative objective functions is 1000, i.e., $\hat{M} = 1000$ in model (SB). Table 5.3 shows that the average differences between the products of cost savings obtained by model (SP) and (SB) are 0.039% for two prosumers and 0.259% for three prosumers. This negligible difference suggest that the SOCP model (SP) and PMR based model (SB) are both precise to capture the NBS for the BSS.

Table 5.3 – Comparison of the NBS obtained by using different methods

	2 Prosumers					3 Prosumers				
	Average	STD	Median	Max	Min	Average	STD	Median	Max	Min
ST(s)	0.58	0.29	0.54	1.26	0.08	1.41	0.56	1.34	3.08	0.54
MT(s)	2.78	1.57	2.31	8.17	1.21	46.76	34.95	40.40	273.63	10.96
Diff(%)	0.039	0.076	0.022	0.609	0.012	0.259	0.033	0.258	0.350	0.192

The comparison of run time reports that when the ES is shared by two prosumers, the transferred SOCP and PMR based method for solving model (SM) are with similar computational time. If the number of prosumers increases to three, model (SP) is significantly faster than model (SB). Due to this noticeable advantage of the SOCP model, we select the SOCP based method for solving model (SM) with more than two prosumers.

5.5.2 Effectiveness of the Enhancement for SOCP

This subsection illustrates the effectiveness of the enhancement for using the transferred SOCP method to solve model (SM). The enhancement starts with solving two mixed integer linear model (RSA) and (ESA). If the solutions of these models satisfy Proposition 1, then the NBS for model (SM) is obtained. Otherwise, we apply the optimal objective value of (RSA) as the dual bound for model (SP) and the solution of (ESA) to warm start the SOCP solver. Since this subsection focuses on the reduction of computational time through the proposed enhancement for model (SP), only run times are compared.

Figure 5.3 presents the box plots of the run times for solving SOCP model (SP) with 2 to 5 prosumers in the ES sharing system by applying different combinations for the enhancement. In the figures, model “SOCP" indicates that solve model (SP) without any enhancement. “Warm" represents that only the warm start by feeding optimal solution of model (ESA) to model (SP) is applied. “Dual" stands for that only the cut based on the dual bound obtained by solving model (RSA) is employed. “Both" denotes that dual bound and warm start for SOCP solver are both implemented. Figure 5.3a reports the run time results with less than 5 prosumers. The run time of model “SOCP" is better than applying

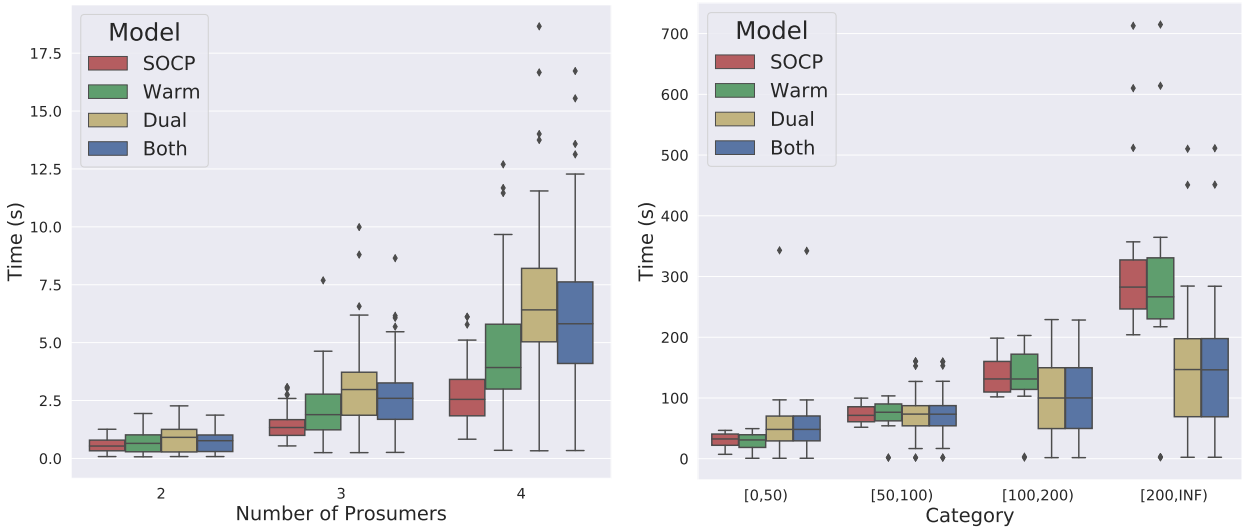

(a) Less than 5 prosumers

(b) Exactly 5 prosumers

Figure 5.3 – Run times for instances with at most 5 prosumers

the enhancement. However, since the run times for the instances with less than 5 prosumers are very small, the advantage of not using the enhancement is negligible.

Figure 5.3b reports run time results for solving model (SP) with 5 prosumers by dividing the results into 4 categories based on the run time of the model "SOCP". This figure shows that 1) when the run time for solving the instances with 5 prosumers is small (less than 50 seconds), the enhancement will slightly increase the run time, but 2) when the run time is large (more than 100 seconds), the enhancement can obviously decrease the computational time. Additionally, the results for the instances with 2 to 5 prosumers suggest to apply the enhancement with both warm start and dual bound.

Figures 5.4-5.6 present the results of run time and optimality gap for solving the instances with more than 5 prosumers by applying the enhancement with both dual bound and warm start. We first address that without using the enhancement, model (SP) with more than 5 prosumers cannot be solved within 3600 seconds (time limit for CPLEX solver). Even some instances require more than 5 hours to solve. Figure 5.4a presents the run times for solving the instances with more than 5 prosumers by applying the enhancement, in which the values of run times are reported as their binary logarithms for the better presentation

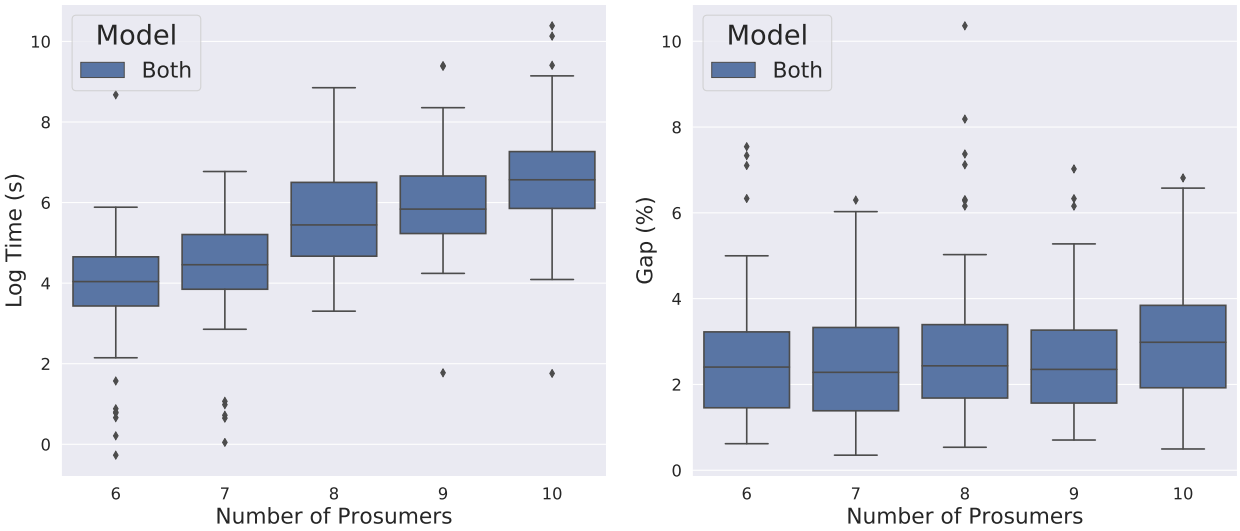

(a) Run times (b) Gaps

Figure 5.4 – Run times and dual bound gaps for instances with 5+ prosumers

of the box plot. We observe that when applying the enhancement, all instances are solvable under the time limit of 3600 seconds, and almost 90% of the instances are solved in less than 2^8 (=256) seconds. Figure 5.4b presents the gaps (in percent) between the dual bound obtained by solving model (RSA) and the optimal objective value of model (SP) to validate the quality of the dual bound.

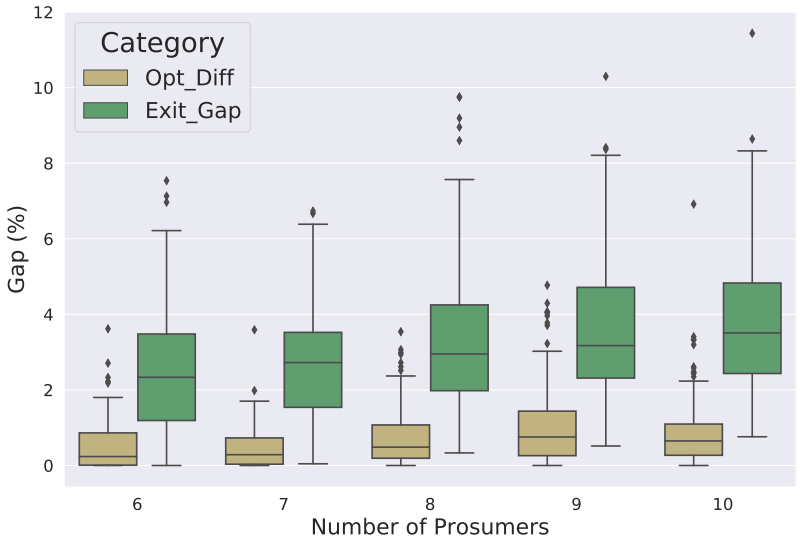

Figure 5.5 – Comparison of enhancement for instances with 5+ prosumer

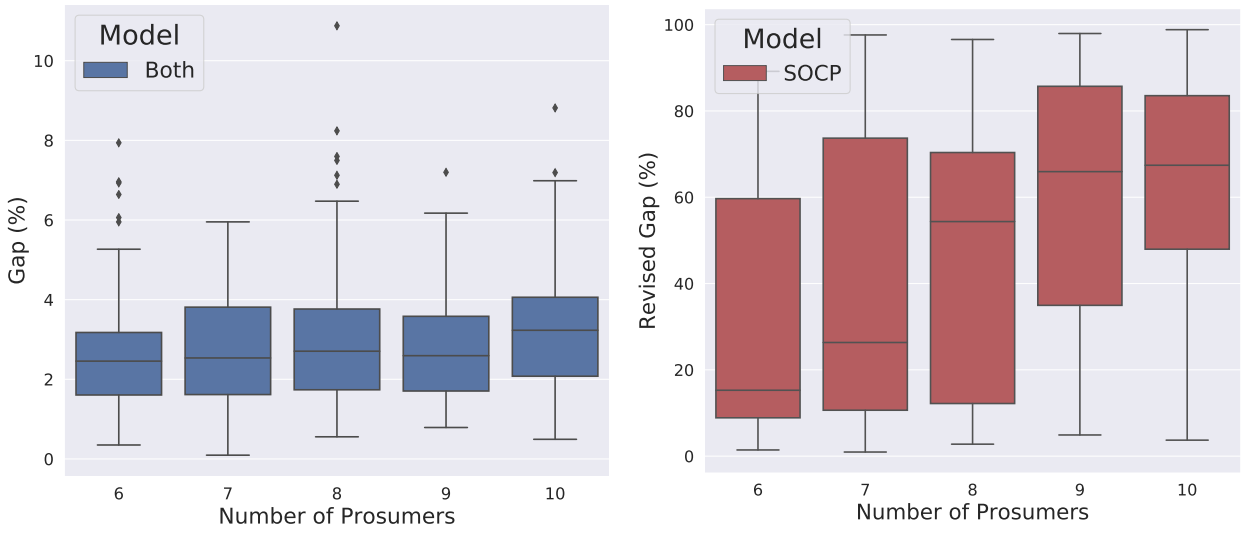

(a) Enhanced SOCP (b) SOCP

Figure 5.6 – Optimality gaps after first node for instances with 5+ prosumers

Figures 5.5 and 5.6 illustrate the reason why the enhancement can dramatically reduce the run time for CPLEX to solve SOCP model (SP). In Figure 5.5, “Opt_Diff" denotes the difference between the optimal objective values of using and not using the enhancement, and “Exit_Gap" the optimality gap for the solution without using the enhancement. Note that the optimal objective value and optimality gap for the model without the enhancement is captured when CPLEX is terminated due to the time limit being reached. Since the “Exit_Gap" is larger than the “Opt_Diff", we infer that when solving the SOCP model (SP) without the enhancement, the inefficient dual bound will hinder the convergence of the algorithm, even if the optimal solution already found.

Figure 5.6 reports the optimality gaps after CPLEX exploring the first node for the model using and not using the enhancement. Here, the “Revised Gap" in Figure 5.6b is introduced for better presenting the box plot, which is ratio of the difference between the dual/upper and primal/lower bound to the dual/upper bound. According to the definition of the “Revised Gap", let g^r denote the “Revised Gap", the real value of the optimality gap is computed by $\frac{g^r}{1-g^r}$. It is shown that when implementing the enhancement, the optimality gap after exploring the first node is significantly smaller than not applying the enhancement.

This observation also validates our previous inference that the inefficient dual bound slows down the convergence of the algorithm for solving SOCP.

We summarize the computational results for solving the instances of all scenarios with the enhancement in Table 5.4. The average, standard deviation, maximum and minimum of the run time for 9 scenarios are reported as "Average", "STD", "Max" and "Min", respectively. "Enhancement" indicates the ratio of the run time for solving the model (RSA) and (ESA) to the total run time. "Hold_Num" denotes the number of instances for each scenario that Proposition 1 is satisfied and the procedure to solve SOCP is skipped. Table 5.4 shows that the number of instances in which Proposition 1 holds is decreasing as the number of prosumers increases.

Table 5.4 – Computational results for solving model (SP) with enhancement

Prosumer_Num	Average	STD	Enhancement	Max	Min	Hold_Num
2	0.74	0.46	46.15%	1.87	0.48	35
3	2.60	1.51	42.59%	8.65	1.30	19
4	6.34	3.23	40.13%	16.73	2.79	8
5	99.17	86.56	7.41%	511.31	13.64	10
6	21.93	40.66	40.08%	408.71	4.43	7
7	28.87	22.52	37.07%	109.19	7.24	5
8	70.57	77.31	35.77%	461.69	9.88	0
9	89.90	103.69	34.01%	676.11	18.92	1
10	155.68	198.91	32.44%	1,339.40	17.03	1

We now draw the conclusion for the above results: 1) The proposed enhancement can dramatically reduce the computational time for solving SOCP model (SP) with at least 5 prosumers; 2) The remarkable performance of the enhancement originates from the high-quality dual bound to accelerate the convergence of the algorithm; 3) When solving the instances with less than 5 prosumers or some easy instances with 5 prosumers, the enhancement is ineffective, but the increase of run time is negligible.

5.5.3 Performance of the Balanced Sharing Strategy for ES Sharing

In this subsection, we investigate the performance of our proposed BSS for ES sharing in terms of efficiency and fairness. Note that the fairness examined in this section is the fair-

ness for the stored energy trading. Since NBS naturally ensures the cooperative benefits are fairly distributed, it is unnecessary to evaluate the fairness on the distribution of cooperative benefits. To better illustrate the advantage of the BSS, we compare it with two reference strategies, the efficiency-first strategy and the fairness-guaranteed strategy.

5.5.3.1 Explanation for Both Reference Strategies

The efficiency-first strategy allows the prosumers to use the energy stored in the ES with extreme freedom, i.e., the constraints to assure the fairness for trading the stored energy are totally omitted. The efficiency-first strategy is still formulated as a Nash bargaining problem, which is expressed as follows and denoted by "(EF)".

$$\begin{aligned} \text{(EF)} \qquad & \max \prod_{i=1}^{N} \varphi_i \\ & \text{s.t. } (5.2), (5.4) - (5.10), (5.22), (5.23). \end{aligned}$$

Actually the optimal objective value of model (EF) is equal to the dual bound we use in the enhancement which is derived from the optimal objective value of model (RSA).

The fairness-guaranteed strategy forces the prosumers not to trade their stored energy, i.e., g^i in constraints (5.11) is fixed to 0. It means that the total amount of energy charged to the ES by a prosumer is equal to the total amount of energy discharged by this prosumer for the entire planning horizon. Hence, the fairness for the stored energy trading is guaranteed due to the nonexistence of the transaction of stored energy. Note that the guaranteed fairness is for the stored energy trading and the fairness for the distribution of cooperative benefits is still assured by NBS. Thus, the fairness-guaranteed strategy is also formulated as a Nash bargaining problem, which is expressed as follows and denoted by "(FG)".

$$\begin{aligned} \text{(FG)} \qquad & \max \prod_{i=1}^{N} \varphi_i^f \\ & \text{s.t. } (5.4) - (5.10) \end{aligned}$$

$$\varphi_i^f = \sum_{t\in\mathcal{T}} r_t^i L_t^i - \sum_{t\in\mathcal{T}} r_t^i (e_t^i + b_t^i) \qquad \forall i \in \mathcal{N} \tag{5.36}$$

$$\sum_{t\in\mathcal{T}} (b_t^i - \frac{d_t^i}{\eta^c \eta^d}) = 0 \qquad \forall i \in \mathcal{N}. \tag{5.37}$$

Besides, we should address that the fairness-guaranteed strategy does not forbid a prosumer to approach the energy stored by other prosumers. This strategy just establishes a regulation for the prosumers sharing the stored energy in an absolute fair way.

According to the definition of both reference strategies, the efficiency-first strategy pursues the maximal cost savings for ES sharing by allowing the unfair stored energy trading, and the fairness-guaranteed strategy is of low efficiency for generating energy arbitrage due to the strict regulation of fairness. Hence, the efficiency-first strategy achieves the best performance on efficiency for ES sharing, and the fairness-guaranteed strategy the best on fairness. We illustrate the effectiveness of the BSS for ES sharing by comparing it with the reference strategies.

5.5.3.2 The Performance of the Balanced Sharing Strategy on Fairness

We investigate the performance of our BSS on fairness in this subsection. In order to conduct the comparison, we introduce a measurement to evaluate the fairness of a sharing strategy for ES sharing. This measurement is captured by the maximum of the ratios of the unbalanced compensation to the operational cost in the disagreement point $\sum_{t\in\mathcal{T}} r_t^i L_t^i$ for all prosumers. The unbalanced compensation is calculated by the difference between the operational cost z_i directly returned by the solution of model (SM) and the exact cost $\bar{z}_i$ computed based on the operational results. In detail, the operational results of a sharing strategy return the values of the variables e_t^i, b_t^i and d_t^i. With these values we can validate the exact compensations for stored energy trading by computing the exact amount $\sum_{t\in\mathcal{T}} (b_t^i - \frac{d_t^i}{\eta^c\eta^d})$ and the exact price $\frac{\sum_{t\in\mathcal{T}} r_t^i b_t^i}{\sum_{t\in\mathcal{T}} b_t^i}$ of the transactive stored energy for prosumer i. Then, we can obtain the exact operational cost $\bar{z}_i$ based on the cost for purchasing energy from power

grid and the above exact compensations for stored energy trading. Obviously, the value of the measurement is non-negative and the smaller value suggests a fairer performance of a sharing strategy. The fairness-guaranteed strategy hold the value 0 of the measurement due to the null compensations for stored energy trading.

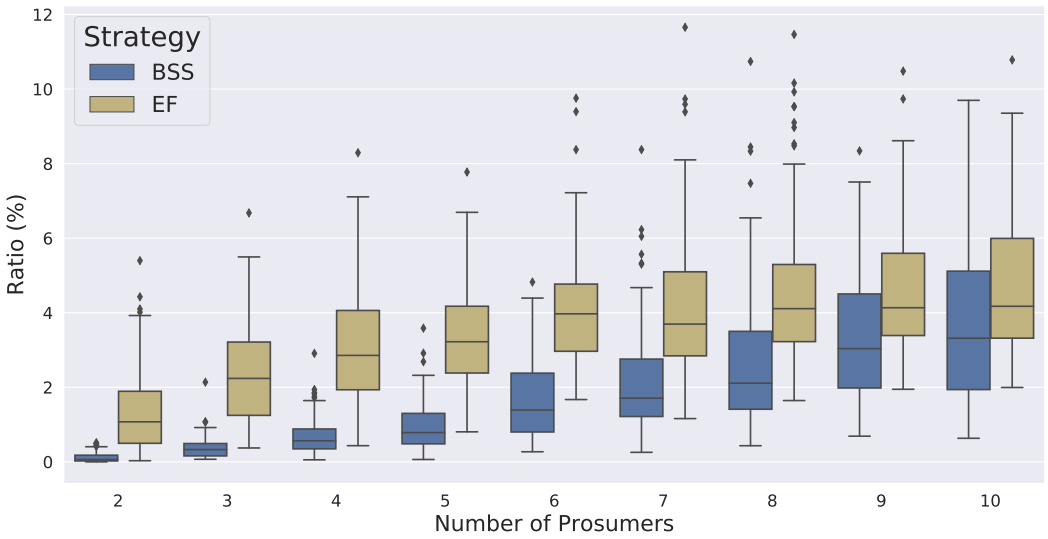

Figure 5.7 – Comparison of the performance of different strategies on fairness

Figure 5.7 graphically reports the values of the measurement of fairness for the instances with 2-9 prosumers sharing ES. In the legend, “BSS" indicates the proposed BSS and “EF" the efficiency-first strategy. Since the fairness-guaranteed strategy holds the value 0 of the measurement, we do not report the fairness results for the fairness-guaranteed strategy in Figure 5.7. It is shown that the performance of the BSS on fairness is very close to the best performance achieved by the fairness-guaranteed strategy. Our strategy manifests a dominant improvement on fairness in contrast to the efficiency-first strategy. As the number of prosumers increasing, our strategy obtain the worse performance on fairness. It indicates the difficulty to coordinate the fair stored energy transaction for an ES sharing system with more cooperators.

We further address that if the PMR can capture the accurate value of the bilinear terms, the BSS should capture the value 0 of the measurement due to $z_i = \bar{z}_i$. Since PMR

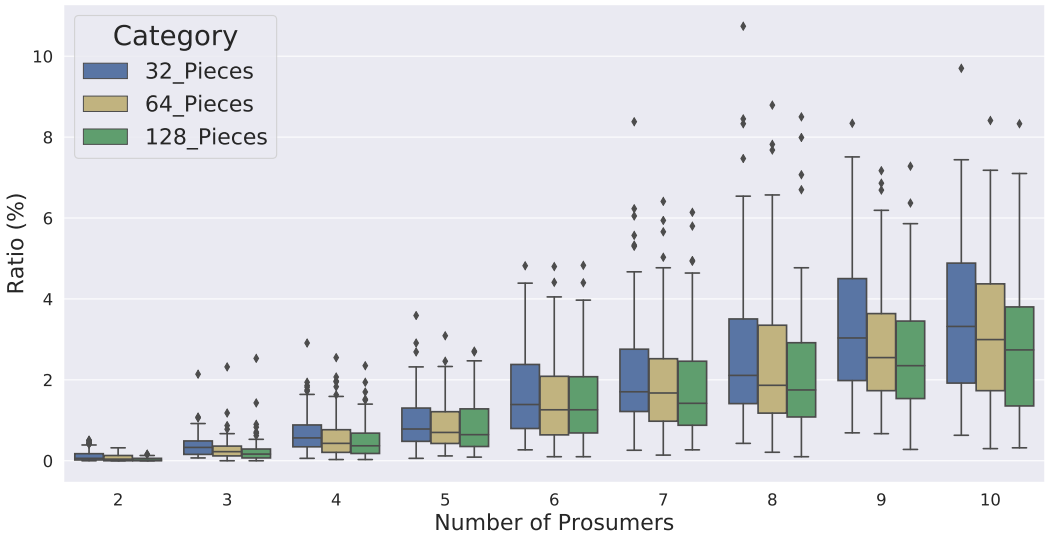

Figure 5.8 – Comparison of the BSS with different pieces of PMR for fairness

represents the bilinear terms with a high-quality approximation, the slight deviation from the accurate value leads to the imprecise pricing for the stored energy trading and further the unbalanced compensation. Increasing the number of pieces for PMR can advance the quality of the approximation to the bilinear terms. The performance of the BSS on fairness with different pieces ($M \in \{32, 64, 128\}$) for PMR is presented in Figure 5.8. It shows the improvement on the fairness for the BSS by increasing the number of pieces for PMR. In addition, the increase in pieces for PMR results in a loss of computational efficiency. To address the trade-off between the improvement of fairness and the loss of computational efficiency, we present the statistics on the run times for the instances with different pieces for PMR in Table 5.5. According to the results in Table 5.5, we conclude that increasing the pieces for PMR to an enormous value cannot gain the expected improvement on fairness for ES sharing with respect to the excessive loss of the computational efficiency.

5.5.3.3 The Performance of the Balanced Sharing Strategy on Efficiency

In this subsection, we illustrate the performance of the BSS in terms of efficiency compared with the reference strategies in Figure 5.9. Here, efficiency is measured by the optimal objective values of the sharing strategies, i.e., the maximal product of the cost

Table 5.5 – The statistics on the run times for PMR with different pieces

	32 Pieces		64 Pieces		128 Pieces	
Prosumer Num	Average	STD	Average	STD	Average	STD
2	0.74	0.46	1.41	0.82	1.64	0.89
3	2.60	1.51	5.08	2.82	5.31	3.10
4	6.34	3.23	13.26	7.17	13.14	7.09
5	99.17	86.56	248.21	235.30	532.65	432.94
6	21.93	40.66	48.42	187.91	47.21	35.58
7	28.87	22.52	46.04	37.64	76.64	84.95
8	70.57	77.31	134.25	200.44	189.01	274.71
9	89.90	103.69	174.44	416.51	221.14	280.39
10	155.68	198.91	260.53	319.32	406.21	566.54

savings of all prosumers. The label of y-axis in Figure 5.9 denotes the ratios of the optimal objective values of the balanced sharing and fairness-guaranteed strategy to the efficiency-first strategy, since the efficiency-first strategy returns the maximal product of the cost savings. The maximum of the ratio is 1 indicating the identical efficiency with the efficiency-first strategy. A larger ratio means the better performance of a sharing strategy on the efficiency. Besides, “FG" in the legend represents the fairness-guaranteed strategy.

According to Figure 5.9, we note that the performance of the BSS on efficiency is close to the best performance of the efficiency-first strategy for the scenarios with less than 5 prosumers. The gap between these two strategies is enlarged if the number of prosumers increases. However, due to the efficiency being measured by the product of cost saving, the gap between the cost savings for exact one prosumer should not be as large as the gap shown in Figure 5.9, especially for the ES sharing system with more prosumers. Additionally, the figure suggests that our strategy significantly outperforms the fairness-guaranteed strategy in terms of efficiency.

In summary, based on the above results we conclude that 1) the proposed BSS for ES sharing can accomplish an adequate balance between the efficiency and fairness by achieving a maximized cost saving for each prosumer under a fair mechanism for stored energy trading; 2) increasing the number of prosumers for ES sharing will lead to a more complex system in which optimizing the efficiency and assuring the fairness are more challenging; and 3)

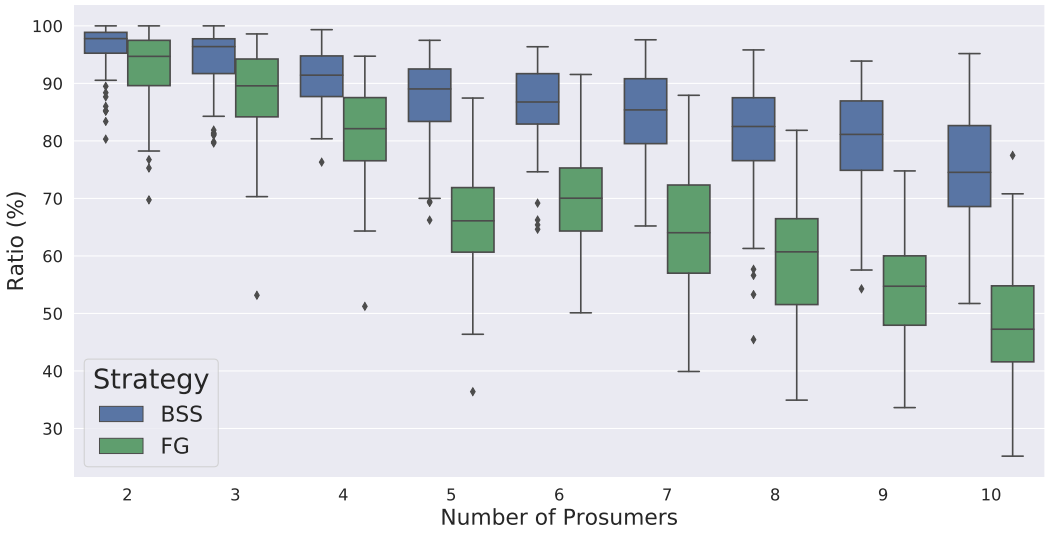

Figure 5.9 – Comparison of different pieces of PMR on efficiency performance

when increasing the number of pieces for PRM to advance the performance of fairness for ES sharing, it is necessary to evaluate the trade-off between the improvement of fairness and loss of computational efficiency.

5.6 Conclusion

In this paper, we explored the potential for applying ES in an energy trading and sharing system. We first presented an analysis by summarizing the architectures and corresponding operational strategies to utilize ES for energy trading and sharing in current research. According to the analysis, we proposed an ES sharing system in which the prosumers realize energy generation and trading by discharging the energy already stored in the shared ES. We then addressed the conflict between efficiency and fairness for operating this ES sharing system. An NBS based sharing strategy was developed to handle this conflict. This strategy implemented both CS and SES for ES sharing. The NBS based model ensures that the cost saving for each prosumer is maximized and the allocation of cooperative benefits is fair. We designed a backward pricing mechanism to maintain the fairness for the prosumers trading their stored energy. The proposed strategy was validated to successfully reduce the operational cost, coordinate the energy distribution and regulate the transaction

of stored energy for the prosumers. Additionally, we contributed on the algorithm to solve the Nash bargaining problem for the proposed strategy. The NBS was attained by solving an equivalent SOCP model of the Nash bargaining problem. We proposed a simple but powerful enhancement for the SOCP model by applying a high-quality dual bound. The experimental results illustrated the capability of the enhancement to dramatically reduce the computational time for capturing the NBS of the proposed strategy.

As future work, we are extending our proposed strategy to an ES sharing system where the prosumers will install energy generation units or renewable energy sources. We will also explore the decentralized framework for the ES sharing system to protect the privacy of the prosumers by developing an adequate distributed algorithm for this decentralized framework. In addition, we observe that almost all works on ES sharing focus on optimizing the economic benefits. This leaves a gap to study the potential of the shared ES or ES sharing system in terms of sustainable and environmental interests.

Chapter 6: Conclusions and Future Study

6.1 Conclusions

Energy Storage (ES) is an integral part of modern smart grids and energy systems. It plays a crucial role in improving the economic performance and resilience of these systems. With the increasing penetration of the ES technologies in energy systems, shared ES, i.e., the ES is built to serve multiple users, has become a promising way to apply ES in energy systems. This dissertation presents an integral knowledge framework for ES sharing in terms of system design, modeling, and optimization. The main challenge of ES sharing, the conflict between efficiency and fairness, has been addressed by the proposed balanced sharing strategy.

In Chapter 3, the balanced sharing strategy is proposed to manage the building clusters with and shared ES. Three ES sharing strategies are introduced, including extreme free, extreme fair, and contract balance strategies. By using bi-objective mixed integer programming techniques, we numerically showed that the contract balance strategy is almost as fair as the extreme fair strategy but it is significantly better than the extreme fair strategy, in terms of freedom.

In Chapter 4, the balanced sharing strategy is extended to handle energy price uncertainty in the ES sharing system. The robust sharing strategy is formulated as a bi-objective mixed integer bilinear model by applying the set-described price uncertainty. Moreover, in order to handle the bilinear terms in the model, we propose a novel binary formulation based piecewise McCormick relaxation to linearize the bilinear terms which are numerically demonstrated to save over 80% run time. The computational study also shows that our

robust sharing strategy is able to ensure the robustness and to minimize the operational costs for the ES sharing system under price uncertainty.

In Chapter 5, the balanced sharing strategy is remodeled using Nash Bargaining Solution to expand the efficacy of the strategy to operate the ES sharing system with many users. This model ensures that the cost saving for each prosumer is maximized and the allocation of cooperative benefits is fair due to the properties of Nash Bargaining Solution. The backward pricing mechanism is employed to maintain the fairness for the prosumers trading their stored energy. The proposed strategy was validated to successfully reduce the operational cost, coordinate the energy distribution, and regulate the transaction of stored energy for the prosumers.

6.2 Future Study

The dissertation has have demonstrated that ES sharing is a promising approach to expand the potential of ES in future energy systems. However, the review of the current study has enlightened a number of possible research gaps for the utilization of the shared ES.

First, we note that most papers have focused on economic or profit-making objectives when using shared ES in energy systems. However, ES can provide multiple benefits such as peak shaving, resiliency, and ancillary services. It is worth quantifying the extent to which these benefits can be obtained when the ES is shared. These benefits should be studied by extending the existing models or developing new ones. Considering the inevitable uncertainty in today's energy supply chain should be an important aspect of such models.

Another research gap in the literature can be identified based on the observation that ES can be realized through many energy technologies. The studies for ES sharing in the last decade only consider the battery as the technology to implement shared ES. However, some other existing ES technologies can be more suitable for the sharing framework due to their specific characteristics. For example, the mechanical ES is better suited for the sharing

model since they naturally require a huge space for operation, control, and maintenance. To the best of our knowledge, shared mechanical ES has not been studied in the literature. Interesting optimization models may be developed for operating mechanical shared ES.

Given the significant developments in electric vehicles and their ever-increasing role in the transportation sector, interesting research questions can be defined. For instance, the electric vehicles traveling between multiple locations (say building) can be viewed as the mobile ES which can be shared between users in these locations or between the electric vehicles themselves. Therefore, the efficient utilization of shared ES in the context of electric vehicles could be a promising direction for future research.

References

[1] Kyle Bradbury, Lincoln Pratson, and Dalia Patiño-Echeverri. Economic viability of energy storage systems based on price arbitrage potential in real-time US electricity markets. *Applied Energy*, 114:512–519, 2014.

[2] Pavithra Harsha and Munther Dahleh. Optimal management and sizing of energy storage under dynamic pricing for the efficient integration of renewable energy. *IEEE Transactions on Power Systems*, 30(3):1164–1181, 2015.

[3] Timm Weitzel and Christoph H Glock. Energy management for stationary electric energy storage systems: A systematic literature review. *European Journal of Operational Research*, 264(2):582–606, 2018.

[4] Olga Moraes Toledo, Delly Oliveira Filho, and Antônia Sônia Alves Cardoso Diniz. Distributed photovoltaic generation and energy storage systems: A review. *Renewable and Sustainable Energy Reviews*, 14(1):506–511, 2010.

[5] Haoran Zhao, Qiuwei Wu, Shuju Hu, Honghua Xu, and Claus Nygaard Rasmussen. Review of energy storage system for wind power integration support. *Applied Energy*, 137:545–553, 2015.

[6] Wim Van Ackooij, Jérôme De Boeck, Boris Detienne, Stefania Pan, and Michael Poss. Optimizing power generation in the presence of micro-grids. *European Journal of Operational Research*, 271(2):450–461, 2018.

[7] Guido Carpinelli, Gianni Celli, Susanna Mocci, Fabio Mottola, Fabrizio Pilo, and Daniela Proto. Optimal integration of distributed energy storage devices in smart grids. *IEEE Transactions on smart grid*, 4(2):985–995, 2013.

[8] Alaa Mohd, Egon Ortjohann, Andreas Schmelter, Nedzad Hamsic, and Danny Morton. Challenges in integrating distributed energy storage systems into future smart grid. In *IEEE international symposium on industrial electronics*, pages 1627–1632. IEEE, 2008.

[9] Thomas Morstyn, Branislav Hredzak, and Vassilios G Agelidis. Control strategies for microgrids with distributed energy storage systems: An overview. *IEEE Transactions on Smart Grid*, 9(4):3652–3666, 2016.

[10] Liuchen Chang, Wenping Zhang, Shuang Xu, and Katelin Spence. Review on distributed energy storage systems for utility applications. *CPSS Transactions on Power Electronics and Applications*, 2(4):267–276, 2017.

[11] Thomas Morstyn, Alexander Teytelboym, and Malcolm D McCulloch. Bilateral contract networks for peer-to-peer energy trading. *IEEE Transactions on Smart Grid*, 10(2):2026–2035, 2018.

[12] Jiayong Li, Chaorui Zhang, Zhao Xu, Jianhui Wang, Jian Zhao, and Ying-Jun Angela Zhang. Distributed transactive energy trading framework in distribution networks. *IEEE Transactions on Power Systems*, 33(6):7215–7227, 2018.

[13] Thomas Morstyn and Malcolm McCulloch. Multi-class energy management for peer-to-peer energy trading driven by prosumer preferences. *IEEE Transactions on Power Systems*, 34(5):4005–4014, 2019.

[14] Jianxiao Wang, Haiwang Zhong, Chenye Wu, Ershun Du, Qing Xia, and Chongqing Kang. Incentivizing distributed energy resource aggregation in energy and capacity markets: An energy sharing scheme and mechanism design. *Applied Energy*, 252:113471, 2019.

[15] Matthias Pilz and Luluwah Al-Fagih. Recent advances in local energy trading in the smart grid based on game-theoretic approaches. *IEEE Transactions on Smart Grid*, 10(2):1363–1371, 2017.

[16] Rehman Zafar, Anzar Mahmood, Sohail Razzaq, Wamiq Ali, Usman Naeem, and Khurram Shehzad. Prosumer based energy management and sharing in smart grid. *Renewable and Sustainable Energy Reviews*, 82:1675–1684, 2018.

[17] Juhar Abdella and Khaled Shuaib. Peer to peer distributed energy trading in smart grids: A survey. *Energies*, 11(6):1560, 2018.

[18] Hao Wang and Jianwei Huang. Incentivizing energy trading for interconnected microgrids. *IEEE Transactions on Smart Grid*, 9(4):2647–2657, 2016.

[19] Xiangyu Kong, Dehong Liu, Chengshan Wang, Fangyuan Sun, and Shupeng Li. Optimal operation strategy for interconnected microgrids in market environment considering uncertainty. *Applied Energy*, 275:115336, 2020.

[20] Su Nguyen, Wei Peng, Peter Sokolowski, Damminda Alahakoon, and Xinghuo Yu. Optimizing rooftop photovoltaic distributed generation with battery storage for peer-to-peer energy trading. *Applied Energy*, 228:2567–2580, 2018.

[21] Yunpeng Wang, Walid Saad, Zhu Han, H Vincent Poor, and Tamer Başar. A game-theoretic approach to energy trading in the smart grid. *IEEE Transactions on Smart Grid*, 5(3):1439–1450, 2014.

[22] Wayes Tushar, Bo Chai, Chau Yuen, Shisheng Huang, David B Smith, H Vincent Poor, and Zaiyue Yang. Energy storage sharing in smart grid: A modified auction-based approach. *IEEE Transactions on Smart Grid*, 7(3):1462–1475, 2016.

[23] Jingkun Liu, Ning Zhang, Chongqing Kang, Daniel Kirschen, and Qing Xia. Cloud energy storage for residential and small commercial consumers: A business case study. *Applied Energy*, 188:226–236, 2017.

[24] Dongwei Zhao, Hao Wang, Jianwei Huang, and Xiaojun Lin. Virtual energy storage sharing and capacity allocation. *IEEE Transactions on Smart Grid, Early Access*, 2019.

[25] Weifeng Zhong, Kan Xie, Yi Liu, Chao Yang, and Shengli Xie. Multi-resource allocation of shared energy storage: A distributed combinatorial auction approach. *IEEE Transactions on Smart Grid*, 2020.

[26] Wenyi Zhang, Wei Wei, Laijun Chen, Boshen Zheng, and Shengwei Mei. Service pricing and load dispatch of residential shared energy storage unit. *Energy*, page 117543, 2020.

[27] Dávid Zoltán Szabó, Peter Duck, and Paul Johnson. Optimal trading of imbalance options for power systems using an energy storage device. *European Journal of Operational Research, In Press*, 2018.

[28] Chathurika Prasadini Mediwaththe, Marnie Shaw, Saman Halgamuge, David Smith, and Paul Scott. An incentive-compatible energy trading framework for neighborhood area networks with shared energy storage. *IEEE Transactions on Sustainable Energy, Early Access*, 2019.

[29] Bizzat Hussain Zaidi, Dost Muhammad Saqib Bhatti, and Ihsan Ullah. Combinatorial auctions for energy storage sharing amongst the households. *Journal of Energy Storage*, 19:291–301, 2018.

[30] Eunsung Oh and Sung-Yong Son. Shared electrical energy storage service model and strategy for apartment-type factory buildings. *IEEE Access*, 7:130340–130351, 2019.

[31] Andreas Fleischhacker, Hans Auer, Georg Lettner, and Audun Botterud. Sharing solar pv and energy storage in apartment buildings: resource allocation and pricing. *IEEE Transactions on Smart Grid*, 2018.

[32] Simon C Müller and Isabell M Welpe. Sharing electricity storage at the community level: An empirical analysis of potential business models and barriers. *Energy policy*, 118:492–503, 2018.

[33] Dileep Kalathil, Chenye Wu, Kameshwar Poolla, and Pravin Varaiya. The sharing economy for the electricity storage. *IEEE Transactions on Smart Grid*, 10(1):556–567, 2017.

[34] P Lombardi and F Schwabe. Sharing economy as a new business model for energy storage systems. *Applied Energy*, 188:485–496, 2017.

[35] Hélène Le Cadre and David Mercier. Is energy storage an economic opportunity for the eco-neighborhood? *NETNOMICS: Economic Research and Electronic Networking*, 13(3):191–216, 2012.

[36] Pratyush Chakraborty, Enrique Baeyens, Kameshwar Poolla, Pramod P Khargonekar, and Pravin Varaiya. Sharing storage in a smart grid: A coalitional game approach. *IEEE Transactions on Smart Grid*, 2018.

[37] Xiaofeng Liu, Bingtuan Gao, Zhenyu Zhu, and Yi Tang. Non-cooperative and co-operative optimisation of battery energy storage system for energy management in multi-microgrid. *IET Generation, Transmission & Distribution*, 12(10):2369–2377, 2018.

[38] Xiaohe Yan, Chenghong Gu, Heather Wyman-Pain, and Furong Li. Capacity share optimization for multiservice energy storage management under portfolio theory. *IEEE Transactions on Industrial Electronics*, 66(2):1598–1607, 2018.

[39] Tom Brijs, Daniel Huppmann, Sauleh Siddiqui, and Ronnie Belmans. Auction-based allocation of shared electricity storage resources through physical storage rights. *Journal of Energy Storage*, 7:82–92, 2016.

[40] Zhimin Wang, Chenghong Gu, Furong Li, Philip Bale, and Hongbin Sun. Active demand response using shared energy storage for household energy management. *IEEE Transactions on Smart Grid*, 4(4):1888–1897, 2013.

[41] Weifeng Zhong, Kan Xie, Yi Liu, Chao Yang, Shengli Xie, and Yan Zhang. Online control and near-optimal algorithm for distributed energy storage sharing in smart grid. *IEEE Transactions on Smart Grid*, 2019.

[42] Katayoun Rahbar, Mohammad R Vedady Moghadam, Sanjib Kumar Panda, and Thomas Reindl. Shared energy storage management for renewable energy integration in smart grid. In *Innovative Smart Grid Technologies Conference (ISGT), 2016 IEEE Power & Energy Society*, pages 1–5. IEEE, 2016.

[43] Ryan T Elliott, Ricardo Fernandez-Blanco, Kelly Kozdras, Josh Kaplan, Brian Lockyear, Jason Zyskowski, and Daniel S Kirschen. Sharing energy storage between transmission and distribution. *IEEE Transactions on Power Systems*, 34(1):152–162, 2018.

[44] Philip Odonkor and Kemper Lewis. Control of shared energy storage assets within building clusters using reinforcement learning. In *ASME 2018 International Design Engineering Technical Conferences and Computers and Information in Engineering Conference*, 2018.

[45] Werner van Westering and Hans Hellendoorn. Low voltage power grid congestion reduction using a community battery: Design principles, control and experimental validation. *International Journal of Electrical Power & Energy Systems*, 114:105349, 2020.

[46] Rui Dai, Mengqi Hu, Dong Yang, and Yang Chen. A collaborative operation decision model for distributed building clusters. *Energy*, 84:759 – 773, 2015.

[47] Rui Dai and Hadi Charkhgard. Bi-objective mixed integer linear programming for managing building clusters with a shared electrical energy storage. *Computers & Operations Research*, 96:173–187, 2018.

[48] Ornella Pisacane, Marco Severini, Marco Fagiani, and Stefano Squartini. Collaborative energy management in a micro-grid by multi-objective mathematical programming. *Energy and Buildings*, 203:109432, 2019.

[49] Tom Terlouw, Tarek AlSkaif, Christian Bauer, and Wilfried van Sark. Multi-objective optimization of energy arbitrage in community energy storage systems using different battery technologies. *Applied Energy*, 239:356–372, 2019.

[50] Mohsen Rafiee Sandgani and Shahin Sirouspour. Coordinated optimal dispatch of energy storage in a network of grid-connected microgrids. *IEEE Transactions on Sustainable Energy*, 8(3):1166–1176, 2017.

[51] A.J. King and S.W. Wallace. Modeling with stochastic programming. Springer Series in Operations Research and Financial Engineering, chapter 1. Springer New York, 2012.

[52] Faeza Hafiz, Anderson Rodrigo de Queiroz, Poria Fajri, and Iqbal Husain. Energy management and optimal storage sizing for a shared community: A multi-stage stochastic programming approach. *Applied energy*, 236:42–54, 2019.

[53] Seyed Mohsen Hosseini, Raffaele Carli, and Mariagrazia Dotoli. Robust energy scheduling of interconnected smart homes with shared energy storage under quadratic pricing. In *2019 IEEE 15th International Conference on Automation Science and Engineering (CASE)*, pages 966–971. IEEE, 2019.

[54] Jiyun Yao and Parv Venkitasubramaniam. Privacy aware stochastic games for distributed end-user energy storage sharing. *IEEE Transactions on Signal and Information Processing over Networks*, 4(1):82–95, 2017.

[55] Islam Safak Bayram, Mohamed Abdallah, Ali Tajer, and Khalid A Qaraqe. A stochastic sizing approach for sharing-based energy storage applications. *IEEE Transactions on Smart Grid*, 8(3):1075–1084, 2015.

[56] Rui Dai, Hadi Charkhgard, and Fabian Rigterink. A robust biobjective optimization approach for operating a shared energy storage under price uncertainty. *International Transactions in Operational Research*, 2020.

[57] Mike B Roberts, Anna Bruce, and Iain MacGill. Impact of shared battery energy storage systems on photovoltaic self-consumption and electricity bills in apartment buildings. *Applied energy*, 245:78–95, 2019.

[58] Zhimin Wang, Chenghong Gu, and Furong Li. Flexible operation of shared energy storage at households to facilitate pv penetration. *Renewable energy*, 116:438–446, 2018.

[59] Chao Long, Jianzhong Wu, Yue Zhou, and Nick Jenkins. Aggregated battery control for peer-to-peer energy sharing in a community microgrid with pv battery systems. *Energy Procedia*, 145:522–527, 2018.

[60] Giuseppe Graber, Vito Calderaro, Vincenzo Galdi, and Antonio Piccolo. Battery second-life for dedicated and shared energy storage systems supporting ev charging stations. *Electronics*, 9(6):939, 2020.

[61] Shengyang Zhong, Jing Qiu, Lingling Sun, Yanli Liu, Chenxi Zhang, and Guibin Wang. Coordinated planning of distributed wt, shared bess and individual vess using a two-stage approach. *International Journal of Electrical Power & Energy Systems*, 114:105380, 2020.

[62] Moiz Syed, Paula Hansen, and Gregory M Morrison. Performance of a shared solar and battery storage system in an australian apartment building. *Energy and Buildings*, page 110321, 2020.

[63] Raffaele Carli, Mariagrazia Dotoli, Jan Jantzen, Michael Kristensen, and Sarah Ben Othman. Energy scheduling of a smart microgrid with shared photovoltaic panels and storage: The case of the ballen marina in samsø. *Energy*, 198:117188, 2020.

[64] Natashia Boland, Hadi Charkhgard, and Martin Savelsbergh. A criterion space search algorithm for biobjective integer programming: The balanced box method. *INFORMS Journal on Computing*, 27(4):735–754, 2015.

[65] V Chankong and Y Y Haimes. *Multiobjective Decision Making: Theory and Methodology*. Elsevier Science, New York, 1983.

[66] Rui Dai and Hadi Charkhgard. A two-stage approach for bi-objective integer linear programming. *Operations Research Letters*, 46(1):81–87, 2018.

[67] W H Hamacher, C R Pedersen, and S Ruzika. Finding representative systems for discrete bicriterion optimization problems. *Operations Research Letters*, 35:336–344, 2007.

[68] T K Ralphs, M J Saltzman, and M M Wiecek. An improved algorithm for solving biobjective integer programs. *Annals of Operations Research*, 147:43–70, 2006.

[69] K Dächert, J Gorski, and K Klamroth. An augmented weighted Tchebycheff method with adaptively chosen parameters for discrete bicriteria optimization problems. *Computers & Operations Research*, 39:2929–2943, 2012.

[70] L G Chalmet, L Lemonidis, and D J Elzinga. An algorithm for bi-criterion integer programming problem. *European Journal of Operational Research*, 25:292–300, 1986.

[71] Markus Leitner, Ivana Ljubić, Markus Sinnl, and Axel Werner. ILP heuristics and a new exact method for bi-objective 0/1 ILPs: Application to FTTx-network design. *Computers & Operations Research*, 72:128–146, 2016.

[72] Hui Wang and Peter Varman. Balancing fairness and efficiency in tiered storage systems with bottleneck-aware allocation. In *Proceedings of the 12th USENIX Conference on File and Storage Technologies (FAST '14)*, pages 229–242, Feb 2014.

[73] H Isermann. The enumeration of the set of all efficient solutions for a linear multiple objective program. *Operational Research Quarterly*, 28(3):711–725, 1977.

[74] P Belotti, B Soylu, and M M Wiecek. A branch-and-bound algorithm for biobjective mixed-integer programs. `http://www.optimization-online.org/DB_HTML/2013/01/3719.html`, 2013.

[75] Kerstin Dächert. *Adaptive Parametric Scalarizationsin Multicriteria Optimization*. The University of Wuppertal, PhD thesis, 2014.

[76] M Ehrgott. A discussion of scalarization technique for multiple objective integer programming. *Annals of Operations Research*, 147:343–360, 2006.

[77] Thomas Stidsen, Kim Allan Andersen, and Bernd Dammann. A branch and bound algorithm for a class of biobjective mixed integer programs. *Management Science*, 60(4):1009–1032, 2014.

[78] T. Vincent, F Seipp, S Ruzika, A Przybylski, and X Gandibleux. Multiple objective branch and bound for mixed 0-1 linear programming: Corrections and improvements for biobjective case. *Computers & Operations Research*, 40(1):498–509, 2013.

[79] Natashia Boland, Hadi Charkhgard, and Martin Savelsbergh. A criterion space search algorithm for biobjective mixed integer programming: The triangle splitting method. *INFORMS Journal on Computing*, 27(4):597–618, 2015.

[80] Garth P. McCormick. Computability of global solutions to factorable nonconvex programs: Part i — convex underestimating problems. *Mathematical Programming*, 10(1):147–175, 1976.

[81] Pedro M. Castro. Tightening piecewise mccormick relaxations for bilinear problems. *Computers & Chemical Engineering*, 72:300 – 311, 2015. A Tribute to Ignacio E. Grossmann.

[82] E. Zitzler, L. Thiele, M. Laumanns, C.M. Fonseca, and V. Grunert da Fonseca. Performance assessment of multiobjective optimizers: an analysis and review. *Evolutionary Computation, IEEE Transactions on*, 7(2):117–132, April 2003.

[83] E Zitzler, D Brockhoff, and L Thiele. The hypervolume indicator revisited: On the design of Pareto-compliant indicators via weighted integration. In S. Obayashi, K. Deb, C. Poloni, T. Hiroyasu, and T. Murata, editors, *Evolutionary Multi-Criterion Optimization*, volume 4403 of *Lecture Notes in Computer Science*, pages 862–876. 2007.

[84] Victor M Albornoz, Pablo Benario, and Manuel E Rojas. A two-stage stochastic integer programming model for a thermal power system expansion. *International Transactions in Operational Research*, 11(3):243–257, 2004.

[85] Takayuki Shiina and John R Birge. Stochastic unit commitment problem. *International Transactions in Operational Research*, 11(1):19–32, 2004.

[86] Mengqi Hu and Heejin Cho. A probability constrained multi-objective optimization model for CCHP system operation decision support. *Applied Energy*, 116:230–242, 2014.

[87] Marco Zugno, Juan Miguel Morales, and Henrik Madsen. Commitment and dispatch of heat and power units via affinely adjustable robust optimization. *Computers & Operations Research*, 75:191–201, 2016.

[88] Luhao Wang, Qiqiang Li, Ran Ding, Mingshun Sun, and Guirong Wang. Integrated scheduling of energy supply and demand in microgrids under uncertainty: A robust multi-objective optimization approach. *Energy*, 130:1–14, 2017.

[89] Bingying Zhang, Qiqiang Li, Luhao Wang, and Wei Feng. Robust optimization for energy transactions in multi-microgrids under uncertainty. *Applied Energy*, 217:346–360, 2018.

[90] Zhi Chen, Lei Wu, and Yong Fu. Real-time price-based demand response management for residential appliances via stochastic optimization and robust optimization. *IEEE Transactions on Smart Grid*, 3(4):1822–1831, 2012.

[91] Goran Vojvodic, Ahmad I Jarrah, and David P Morton. Forward thresholds for operation of pumped-storage stations in the real-time energy market. *European Journal of Operational Research*, 254(1):253–268, 2016.

[92] Dheepak Krishnamurthy, Canan Uckun, Zhi Zhou, Prakash R Thimmapuram, and Audun Botterud. Energy storage arbitrage under day-ahead and real-time price uncertainty. *IEEE Transactions on Power Systems*, 33(1):84–93, 2018.

[93] Dimitris Bertsimas and Melvyn Sim. Robust discrete optimization and network flows. *Mathematical Programming*, 98(1):49–71, 2003.

[94] John F Nash Jr. The bargaining problem. *Econometrica: Journal of the Econometric Society*, pages 155–162, 1950.

[95] Santiago Cerisola, Jesus M Latorre, and Andres Ramos. Stochastic dual dynamic programming applied to nonconvex hydrothermal models. *European Journal of Operational Research*, 218(3):687–697, 2012.

[96] Yoshitsugu Yamamoto. Optimization over the efficient set: overview. *Journal of Global Optimization*, 22(1-4):285–317, 2002.

[97] Fabian Rigterink. *Pooling problems: advances in theory and applications*. PhD thesis, University of Newcastle, 2017.

[98] Hadi Charkhgard, Martin Savelsbergh, and Masoud Talebian. A linear programming based algorithm to solve a class of optimization problems with a multi-linear objective function and affine constraints. *Computers & Operations Research*, 89:17 – 30, 2018.

[99] Songli Fan, Zhengshuo Li, Jianhui Wang, Longjian Piao, and Qian Ai. Cooperative economic scheduling for multiple energy hubs: A bargaining game theoretic perspective. *IEEE Access*, 6:27777–27789, 2018.

[100] Rosemarie Velik and Pascal Nicolay. Energy management in storage-augmented, grid-connected prosumer buildings and neighborhoods using a modified simulated annealing optimization. *Computers & Operations Research*, 66:248–257, 2016.

[101] Hadi Charkhgard, Kimia Keshanian, Rasul Esmaeilbeigi, and Parisa Charkhgard. The magic of nash social welfare in optimization: Do not sum, just multiply! *Optimization Online*, 2020.

Appendix A: Copyright Permissions

Chapter 2 was firstly published in *Operations Research Letters*, and is cited as [66] in References. Chapter 3 was firstly published in *Computers & Operations Research*, and is cited as [47] in References. Chapter 4 was firstly published in *International Transactions in Operational Research*, and is cited as [56] in References.

The permissions to reuse these three previous publications are attached here.

Appendix A1: Reprint Permission for Chapter 2

A two-stage approach for bi-objective integer linear programming

Author: Rui Dai,Hadi Charkhgard
Publication: Operations Research Letters
Publisher: Elsevier
Date: January 2018

Appendix A2: Reprint Permission for Chapter 3

Appendix A3: Reprint Permission for Chapter 4

Copyright Clearance Center RightsLink®

Home | Help | Email Support | Rui Dai

A robust biobjective optimization approach for operating a shared energy storage under price uncertainty

Author: Rui Dai, Hadi Charkhgard, Fabian Rigterink
Publication: International Transactions in Operational Research
Publisher: John Wiley and Sons
Date: Jun 8, 2020

Order Completed

Thank you for your order.

This Agreement between Rui Dai ("You") and John Wiley and Sons ("John Wiley and Sons") consists of your license details and the terms and conditions provided by John Wiley and Sons and Copyright Clearance Center.

Your confirmation email will contain your order number for future reference.

Printable Details

License Number	4930670840576
License date	Oct 16, 2020

Licensed Content

Licensed Content Publisher	John Wiley and Sons
Licensed Content Publication	International Transactions in Operational Research
Licensed Content Title	A robust biobjective optimization approach for operating a shared energy storage under price uncertainty
Licensed Content Author	Rui Dai, Hadi Charkhgard, Fabian Rigterink
Licensed Content Date	Jun 8, 2020
Licensed Content Volume	0
Licensed Content Issue	0
Licensed Content Pages	32

Order Details

Type of use	Dissertation/Thesis
Requestor type	Author of this Wiley article
Format	Print and electronic
Portion	Full article
Will you be translating?	No

About Your Work

Title	The Utilization of Shared Energy Storage in Energy Systems: Design, Modeling and Optimization
Institution name	University of South Florida
Expected presentation date	Nov 2020

Additional Data

Order reference number	56